PHARMACOKINETICS/PHARMACODYNAMICS OF VORICONAZOLE

By

YANJUN LI

A DISSERTATION PRESENTED TO THE GRADUATE SCHOOL
OF THE UNIVERSITY OF FLORIDA IN PARTIAL FULFILLMENT
OF THE REQUIREMENTS FOR THE DEGREE OF
DOCTOR OF PHILOSOPHY

UNIVERSITY OF FLORIDA

2008

To my beloved husband, daughters, and parents, for their love

ACKNOWLEDGMENTS

I express my deep appreciation and grateful thanks to Dr. Hartmut Derendorf for his intelligent guidance and generous support throughout my Ph.D. study. He gave me the opportunity of being part of his group exploring the opportunities in research area of pharmacokinetics and pharmacodynamics. The knowledge I learned from him benefits me and will be cherished in my entire lifetime.

Thanks go to Dr. Cornelius J. Clancy and Dr. Minh-Hong Nguyen for their broad knowledge in microbiology and infectious diseases, intelligent guidance and generous support in the lab space and equipment necessary for my experiments. It has really been a wonderful experience to learn knowledge in their laboratories. Without their help the pharmacodynamic studies would not have been performed. I thank Dr. Veronika Butterweck for her support and guidance during the animal studies and in my projects. I offer my grateful thanks to the members of my supervisory committee, Dr. Guenther Hochhaus and Dr. Kenneth Rand for their support and valuable advice.

I thank Stephan, Jian, Vipul, Sab for the study discussion and help. I thank the administrative people of the Department of Pharmaceutics, Mr. Marty Rhoden, Mrs. Patricia Khan, and Mrs. Robin Keirnan-Sanchez, for their technical support. I also would like to extend my thanks to all faculties of the Department of Pharmaceutics, staffs, graduate students, and post-doc fellows who were my colleagues for their support and friendship.

TABLE OF CONTENTS

page

ACKNOWLEDGMENTS 4

LIST OF TABLES 8

LIST OF FIGURES 10

ABSTRACT 13

CHAPTER

1 INTRODUCTION 15

Background 15
Voriconazole 15
Mechanisms of Action 16
Drug Stability 17
Animal Pharmacokinetic Studies 17
Human Pharmacokinetic Studies 17
In Vitro and *In Vivo* Pharmacodynamic Studies 18
Clinical Efficacy 20
Microdialysis 21
Principle of Microdialysis 22
Features of Microdialysis 22
Application in PK/PD Studies 23
The PK/PD Approaches 24
Hypothesis and Objectives 25

2 MEASUREMENT OF VORICONAZOLE ACTIVITY AGAINST *CANDIDA* ISOLATES USING TIME-KILL METHODS VALIDATED BY HIGH PERFORMANCE LIQUID CHROMATOGRAPHY 30

Background 30
Specific Aims 30
Materials and Methods 30
Antifungal Agents 30
Test Isolates 30
Antifungal Susceptibility Testing 31
Antifungal Carryover 31
Time-kill Experiments 32
Postantifungal Effect (PAFE) Experiments 32
HPLC for Determination of Voriconazole in Stock Solution and RPMI Medium 32
Calibration Curves for Voriconazole in Stock Solution and RPMI Medium 33
Statistical Analysis 33
Results 34

Stability of Voriconazole in Stock Solution and RPMI Medium 34
Minimum Inhibitory Concentration (MIC) 34
Time-kills and Postantifungal Effect (PAFE) 34
Discussion 36

3 APPLYING PHARMACOKINETIC/PHARMACODYNAMIC MATHEMATICAL MODEL ACCURATELY DESCRIBES THE ACTIVITY OF VORICONAZOLE AGAINST *CANDIDA* SPP. *IN VITRO* 50

Background 50
Specific Aim 51
Materials and Methods 51
Mathematical Modelling of Time–kill Data 51
Simulations of Expected Time–kill Curves Using Human PK Data 51
Statistical Analysis 52
Results 52
An Adapted Sigmoidal E_{max} Model Provides the Best Fit for Voriconazole Time–kill Data against Candida Isolates 52
Human PK Data for Voriconazole Can Be Used to Simulate Expected Time–kill 54
Discussion 55

4 PHARMACODYNAMIC STUDY IN DYNAMIC SYSTEM FOR DESCRIBING THE ACTIVITY OF VORICONAZOLE AGAINST *CANDIDA* SPP. *IN VITRO* 62

Background 62
Specific Aim 62
Materials and Methods 63
Antifungal Agents 63
Test Isolates 63
Softwares 63
Dynamic Model Design 63
Time-kill Experiments in the Dynamic Model 65
Results 66
Discussion 69

5 IN VITRO MICRODIALYSIS OF VORICONAZOLE 81

Background 81
Specific Aims 81
Materials and Methods 82
Materials 82
Methods 82
Recovery 82
Extraction efficiency method (EE) 82
Retrodialysis method (RD) 83
Microdialysis experiments 84
HPLC for determination of voriconazole 84

Calibration curves for voriconazole 85
Results 85
Stability of Voriconazole in Lactate Ringer's Solution and Plasma 86
Protein Binding 86
Discussion 86

6 IN VIVO PHARMACOKINETIC STUDIES OF VORICONAZOLE IN RATS 91

Background 91
Specific Aims 91
Materials and Methods 92
Reagents and Equipment 92
Animals 92
Experimental Design 92
Anesthetic Procedure 93
Antiseptic Procedure 93
Blood Samples 93
Microdialysis 94
Probe calibration 94
Muscle microdialysis 95
Data Analysis 95
Noncompartmental pharmacokinetic analysis 96
Compartmental pharmacokinetic analysis and modeling 97
Results 102
Probe Recovery 102
Individual Pharmacokinetic Analysis of Total Voriconazole in Plasma after Intravenous Bolus Administration 103
Noncompartmental pharmacokinetic analysis 103
Compartmental pharmacokinetic analysis 103
One-compartment model with linear elimination analysis 104
Two-compartment model with linear elimination analysis 104
One-compartment model with nonlinear elimination 105
Two-compartment model with nonlinear elimination 105
Individual Pharmacokinetic Analysis of Unbound Voriconazole in Muscle after Intravenous Bolus Administration 106
Noncompartmental pharmacokinetic analysis 107
Compartmental pharmacokinetic analysis 107
Two-compartment model with nonlinear elimination 107
Pharmacokinetic Analysis of Average Total Voriconazole Data in Plasma and Unbound Voriconazole Data in Muscle after Intravenous Bolus Administration 108
Discussion 109

7 CONCLUSIONS 138

LIST OF REFERENCES 141

BIOGRAPHICAL SKETCH 155

LIST OF TABLES

Table		page
1-1	Pharmacokinetic parameters of voriconazole in mouse, rat, rabbit, guinea pig and dog following single and multiple administration by oral and intravenous routes	26
1-2	Pharmacokinetic (PK) properties of triazole antifungals	27
2-1	Percentage (%) of voriconazole maintenance in stock solution and RPMI medium at different temperatures	38
2-2	Minimum inhibitory concentration (MIC) of voriconazole against Candida isolates	38
2-3	*Candida albicans* ATCC90029 in constant concentration experiments	39
2-4	*Candida albicans* SC5314 in constant concentration experiments	39
2-5	*Candida glabrata* 1 in constant concentration experiments	40
2-6	*Candida glabrata* 2 in constant concentration experiments	40
2-7	*Candida parapsilosis* 1 in constant concentration experiments	41
2-8	*Candida parapsilosis* 2 in constant concentration experiments	41
2-9	Summarized voriconazole time-kill data against Candida isolates	42
2-10	*Candida albicans* ATCC90029 in PAFE experiments	42
2-11	*Candida glabrata* 2 in PAFE experiments	43
2-12	*Candida glabrata* 1 in PAFE experiments	43
2-13	*Candida parapsilosis* 1 in PAFE experiments	44
2-14	*Candida parapsilosis* 2 in PAFE experiments	44
3-1	Pharmacodynamic parameters and goodness of fit criteria against Candida isolates	57
3-2	Steady-state pharmacokinetic parameters in plasma as calculated by two-compartment model analysis	58
4-1	*Candida albicans* ATCC90029 in changing concentration experiments	71
4-2	*Candida glabrata* 1 in changing concentration experiments	72
4-3	*Candida glabrata* 2 in changing concentration experiments	73

4-4 Candida parapsilosis 1 in changing concentration experiments 74

4-5 Candida parapsilosis 2 in changing concentration experiments 75

4-6 Pharmacodynamic parameters and goodness of fit criteria against Candida isolates in the dynamic infection model 76

5-1 List of materials 88

5-2 Extraction efficiency (EE) method for measuring voriconazole recovery 89

5-3 Retrodialysis (RD) method for measuring voriconazole recovery 89

5-4 Rat plasma protein binding data of voriconazole measured by *in vitro* microdialysis 90

5-5 Human plasma protein binding data of voriconazole measured by *in vitro* microdialysis 90

6-1 Recovery data of voriconazole using retrodialysis (RD) method in rats muscle 112

6-2 Total plasma voriconazole (5 mg/kg) individual noncompartmental PK analysis 113

6-3 Total plasma voriconazole (10 mg/kg) individual noncompartmental PK analysis 114

6-4 Comparison of objective function value (OFV) and Akaike information criterion (AIC) value from rats total plasma voriconazole PK analysis using different models 115

6-5 One-compartment model with linear elimination for rat total plasma voriconazole PK analysis 116

6-6 Two-compartment model with linear elimination for rat total plasma voriconazole PK analysis 116

6-7 One-compartment with non-linear elimination model for rat total plasma voriconazole PK analysis 117

6-8 Two-compartment with non-linear elimination model for rat total plasma voriconazole PK analysis 117

6-9 Unbound muscle voriconazole (5 mg/kg) individual noncompartmental pharmacokinetics analysis 118

6-10 Unbound muscle voriconazole (10 mg/kg) individual noncompartmental pharmacokinetics analysis 119

6-11 Rat total plasma and unbound muscle voriconazole PK analysis using two-compartment with non-linear elimination model 120

LIST OF FIGURES

Figure		page
1-1	Structural relationship among azole drugs	28
1-2	Plasma voriconazole concentration-time profiles following *i.v.* dosing and following oral dosingof voriconazole	29
2-1	Susceptibility of voriconazole against Candida isolates	45
2-2	Culture flasks for voriconazole against Candida isolates *in vitro*	45
2-3	Time-kill curves for voriconazole against Candida isolates	46
2-4	Voriconazole did not demonstrate PAFEs	47
2-5	Chromatogram of voriconazole which concentration was determined from peak area	48
2-6	Voriconazole concentrations in culture media throughout the duration of time-kill experiments by HPLC	48
2-7	Voriconazole concentrations in PAFE experiments by HPLC	49
3-1	Plasma VOR concentration-time profiles simulated with a two-compartment PK model	59
3-2	Fitted time-kill curves derived using the mathematical model for constant concentrations of voriconazole	60
3-3	Simulations of candidal time–kills and plasma voriconazole concentration–time profiles.	61
4-1	Concentration elimination curve of voriconazole in the dynamic infection model	77
4-2	Time-kill curves from the dynamic *in vitro* model.	78
4-3	Fitted time-kill curves were derived by our mathematical model for changing concentrations of voriconazole.	79
4-4	Using parameters from dynamic models to simulate candidal time-kills and plasma voriconazole concentration-time profiles	80
6-1	Cascade pharmacokinetic one-compartment model with non-linear elimination of voriconazole scheme	121
6-2	Cascade pharmacokinetic two-compartment model with non-linear elimination of voriconazole scheme	121

6-3 Dosage of 5 mg/kg *i.v.* bolus: total voriconazole concentration in rat plasma. 122

6-4 Dosage of 10 mg/kg *i.v.* bolus: total voriconazole concentration in rat plasma 123

6-5 The PK plots using one-compartment with linear elimination model for PK analysis of rat total plasma voriconazole data 124

6-6 Goodness of fit plots for observed vs predicted concentrations using one-compartment with linear elimination model for PK analysis of rat total plasma voriconazole concentration data. 125

6-7 Goodness of fit plots for residuals using one-compartment with linear elimination model for PK analysis of rat total plasma voriconazole concentration data. 125

6-8 The PK plots using two-compartment with linear elimination model for PK analysis of rat total plasma voriconazole data. 126

6-9 Goodness of fit plots for observed vs predicted concentrations using two - compartment with linear elimination model for PK analysis of rat total plasma voriconazole concentration data. 127

6-10 Goodness of fit plots for residuals using two-compartment with linear elimination model for PK analysis of rat total plasma voriconazole concentration data. 127

6-11 The PK plots using one-compartment with non-linear elimination model for PK analysis of rat total plasma voriconazole data 128

6-12 Goodness of fit plots for observed vs predicted concentrations using one-compartment with non-linear elimination model for PK analysis of rat total plasma voriconazole concentration data. 129

6-13 Goodness of fit plots for residuals using one-compartment with non-linear elimination model for PK analysis of rat total plasma voriconazole concentration data. 129

6-14 The PK plots using two-compartment with non-linear elimination model for PK analysis of rat total plasma voriconazole data 130

6-15 Goodness of fit plots for observed vs predicted concentrations using two-compartment with non-linear elimination model for PK analysis of rat total plasma voriconazole concentration data. 131

6-16 Goodness of fit plots for residuals using two-compartment with non-linear elimination model for PK analysis of rat total plasma voriconazole concentration data. 131

6-17 Dosage of 5 mg/kg *i.v.* bolus: unbound voriconazole concentration in rat muscle 132

6-18 Dosage of 10 mg/kg *i.v.* bolus: unbound voriconazole concentration in rat muscle 133

6-19 The PK plots using two-compartment with non-linear elimination model for analysis of rat total plasma and unbound muscle voriconazole data. 134

6-20 Goodness of fit plots for observed vs predicted concentrations using two-compartment with non-linear elimination model for PK analysis of rat total plasma and unbound muscle voriconazole concentration data. 135

6-21 Goodness of fit plots for residuals using two-compartment with non-linear elimination model for PK analysis of rat total plasma and unbound muscle voriconazole concentration data. 135

6-22 Dosage of 5 mg/kg *i.v.* bolus in rat: average plasma and muscle PK data analysis using two-compartment with non-linear elimination model.....136

6-23 Dosage of 10 mg/kg *i.v.* bolus in rat: average plasma and muscle PK data analysis using two-compartment with non-linear elimination model.....137

Abstract of Dissertation Presented to the Graduate School
of the University of Florida in Partial Fulfillment of the
Requirements for the Degree of Doctor of Philosophy

PHARMACOKINETICS/PHARMACODYNAMICS OF VORICONAZOLE

By

Yanjun Li

August 2008

Chair: Hartmut Derendorf
Major: Pharmaceutical Sciences

Candida spp. is the most common cause of opportunistic mycoses worldwide, especially the invasive opportunistic mycotic infection. Oropharyngeal candidiasis is the most common opportunistic infection associated with AIDS. Candidemia is the fourth most common bloodstream infection in the developed world and is associated with mortality rates of up to 38% despite treatment with available antifungals. Voriconazole, a triazole agent that is effective in treating candidiasis and aspergillosis, inhibits ergosterol synthesis by blocking the action of 14α-demethylase.

It has also lowered toxicity compared with previous antifungal agents; however, it is used to cure candidiasis inside the human body after oral administration or *i.v.* injection. Empiric antifungal therapy is initiated as the first measure dealing with fungal infection, and there are no suitable mathematical models of voriconazole antifungal activity established for rational guidance to maximize efficiency and minimize toxicity.

The aim of these studies was to develop an optimal pharmacokinetic/pharmacodynamic (PK/PD) model to predict clinical outcome and improve the effectiveness of voriconazole. The PK/PD model integrates the pharmacokinetics of unbound voriconazole with in vitro antifungal activity against certain Candida strains for rational dosing of this agent.

In these studies, we measured voriconazole activity against Candida isolates using time-kill methods validated by high performance liquid chromatography *in vitro* and a pharmacokinetic/pharmacodynamic mathematical model based on time-kill curves against different Candida strains was used to accurately describe the antifungal activity of voriconazole. Using this model, pharmacodynamic studies in dynamic system for describing the activity of voriconazole against Candida spp. were conducted. Moreover, *in vitro* microdialysis was performed to determine protein binding of voriconazole in both rat and human plasma. Also, *in vivo* microdialysis in Wistar rats after intravenous administration of voriconazole was conducted to evaluate unbound muscle concentrations of voriconazole and to compare the free tissue concentration to free plasma concentration. We investigated the voriconazole PK profile by analyzing the total concentrations in plasma and unbound concentrations in muscle and developed a population PK model to fit the voriconazole PK data in rats using NONMEM.

These studies provided new insights to improve the drug clinical efficacy by using the developed voriconazole PK/PD model.

CHAPTER 1
INTRODUCTION

Background

In the past two decades, the incidence of invasive fungal infections, especially in immunocompromised patients, such as AIDS patients have risen significantly. Invasive fungal infections are growing in frequency and optimal selection and dosing of antifungal agents are important. Agents administered for invasive infections are amphotericin B, flucytosine, and azole antifungals. Azoles, a class of organic compounds having a five-membered heterocyclic ring with two double bonds, have gained attention as useful drugs with antifungal activity *in vitro* against a broad spectrum of fungal pathogens. The azole antifungal agents inhibit the synthesis of ergosterol by blocking the action of cytochrome P450 14a-demethylase (P45014DM) [1-4]. The structure of six main azole drugs including ketoconazole, fluconazole, itraconazole, voriconazole, ravuconazole, and posaconazole is shown in Figure 1-1 [5, 6]. Antimicrobial PD describes the relationship between drug exposure and treatment efficacy. Therapeutic outcome predictions based upon these PD relationships have correlated well in treatment against both susceptible and resistant pathogens. The potential value of using PK/PD parameters as guides for establishing optimal dosing regimens for new and old drugs, for new emerging pathogens and resistant organisms, for setting susceptibility breakpoints, and for reducing the cost of drug development should make the continuing search for the therapeutic rationale of antifungal dosing of animals and humans worthwhile [1, 7].

Voriconazole

Voriconazole (UK-109,496) is a triazole that is structurally related to fluconazole (Figure 1-1) [5, 8]. It is developed by Pfizer Pharmaceuticals (http://www.pfizer.com) and its clinical use was approved by the Food and Drug Administration (FDA) in May 2002. The trade name of

voriconazole is Vfend™ [9]. Voriconazole recently has gained increasing attention as a new class of azole antifungal drug with its lower toxicity and expanded antifungal activity against *Candida* spp. compared with previous antifungal therapies, and also with its advantage of high activity against *Aspergillus* species [10-12]. Voriconazole is fungistatic and exhibits no PAFE against *Candida albicans* [13-15]. Time-kill and PAFE data are limited against *C. glabrata* and do not exist against *C. parapsilosis* isolates. Moreover, standard time-kill and PAFE methodologies, although widely used, have not been validated for voriconazole or other antifungals by direct measurements of drug concentrations [16].

Mechanisms of Action

All azole antifungal agents work principally by inhibition of P45014DM. This enzyme is in the sterol biosynthesis pathway that leads from lanosterol to ergosterol [6, 17-19]. Compared to fluconazole, voriconazole inhibits P45014DM to a greater extend. This inhibition is dose-dependent [20-22]. Voriconazole also has an enhanced antifungal spectrum that includes filamentous fungi [23-26]. Voriconazole also inhibits 24-methylene dihydrolanasterol demethylation in certain yeast and filamentous fungi. Other antifungal effects of azole compounds have been proposed and include: inhibition of endogenous respiration, interaction with membrane phospholipids, and inhibition of the transformation of yeasts to mycelial forms [19]. Other mechanisms may involve inhibition of purine uptake and impairment of triglyceride and/or phospholipid biosynthesis [27]. Cross-resistance of voriconazole with other azole antifungals has been demonstrated, probably due to common modes of action [28]. Due to the potential for cross-resistance, specific organism susceptibility data should be reviewed before selecting an antifungal for the treatment of infections.

Drug Stability

The stability of voriconazole has been tested under a variety of conditions. The voriconazole chemical and physical in-use stability has been demonstrated for 24 hours at 2° to 8°C (36° to 46°F) following reconstitution of the lyophile with water [4]. Based on a shelf-life of 90% residual potency, voriconazole in 5% dextrose solutions were stable for at least 15 days at 4°C [29]. It was repoted that the stability of voriconazole in serums and plasma was found to be stable for up to 7 days at room temperature, for 30 days frozen at −20 °C, and through 3 freeze–thaw cycles [30]. Voriconazole diluted in 0.9% Sodium Chloride or Lactated Ringers solution can be stable for 14 days at 15° to 30°C [4].

Animal Pharmacokinetic Studies

Voriconazole's pharmacokinetics and metabolism have been studied in mouse, rat, rabbit, dog, guinea pig, and humans after single and multiple administration by both oral and intravenous routes [31-36]. Its pharmacokinetics parameters have been shown in Table 1-1. Oral absorption of voriconazole is high (~75%) in animals, including rats, mice, rabbits, guinea pigs, and dogs [31, 37]. Drug distribution studies using radiolabeled ^{14}C-voriconazole 10 mg/kg in male and female rats showed extensive distribution throughout tissues. In preclinical studies in rats, voriconazole was excreted in both urine and feces, with the majority of drug eliminated within 48 hours of administration [37].

Human Pharmacokinetic Studies

Voriconazole is orally and parenterally active. Bioavailability is up to 96% with peak plasma levels occurring 1-2 hours after dosing. Plasma protein binding is roughly 58% and is not affected by renal or hepatic disease. The volume of distribution is 4.6L/kg, indicating widespread distribution in the body [37, 38]. With administration of the recommended intravenous (IV) or oral loading dose, steady-state concentrations are reached within 24 hours. Without the loading dose,

accumulation must occur for 6 days to reach steady state. Oral steady state plasma concentrations have ranged from 2.1 to 4.8 mg/L (peak) and 1.4 to 1.8 mg/L (trough). Mean C_{max} and area under the curve (AUC) are reduced by 34% and 24%, respectively, following a high fat meal. The absorption of voriconazole is not affected by increases in gastric pH [37, 38]. Voriconazole displays nonlinear pharmacokinetics due to saturation of its metabolism. Increasing the IV dose from 3 mg/kg to 4 mg/kg twice daily and the oral dose from 200 mg to 300 mg twice daily results in roughly a 2.5 fold increase in the AUC [39, 40]. Mean plasma voriconazole concentration-time profiles after *i.v.* (day 7) and oral (day 14) administration are illustrated in Figure 1-2. C_{max} occurred at the end of the 1h *i.v.* infusion and between 1.4 and 1.8 h after oral administration [39].

Human data indicate voriconazole concentrations in the CSF are between 40% and 70% of the concentrations in the plasma [37, 38]. Voriconazole is a substrate for, is extensively metabolized by, and is an inhibitor of cytochrome P450 enzymes 2C19, 2C9 and 3A4. Enzyme CYP2C19 exhibits genetic polymorphism resulting in an approximately 4-fold higher voriconazole exposure in poor metabolizers vs. extensive metabolizers. Eight metabolites have been identified, of which three are major N-oxide metabolites. The N-oxide metabolites do not exhibit antifungal activity. Voriconazole metabolites are primarily excreted renally. Roughly 85% of a dose appears in the urine with < 2% as unchanged drug. The elimination half life has been reported as 6 hours, but in patients receiving prolonged therapy up to 6 days have been required to recover 90% of the drug in the urine and feces [37, 38]. An overview of pharmacokinetic properties of voriconazole and other triazoles from clinical studies is provided in Table 1-2.

In Vitro and *In Vivo* Pharmacodynamic Studies

Pharmacodynamics refers to the time course and intensity of drug effects on the organism, whether human or experimental animal. To describe antifungal efficacy, parameters such as

minimum inhibitory concentration (MIC), time above the MIC, time-kill curves, sub-MIC effects and post-antifungal effects (PAFEs) are used. *In vitro* and *in vivo* studies are conducted to examine the effects of the drug on antimicrobial inhibition or killing, the rate and extent of killing over time, and the duration of antimicrobial effects.

Voriconazole has broad *in vitro* antifungal activity against a variety of fungi including Candida spp., Aspergillus spp., Cryptococcus neoformans, Blastomyces dermatitidis, Coccidioides immitis, Histoplasma capsulatum, Fusarium spp., and Penicillium marneffei [41-45]. The voriconazole pharmacodynamics was evaluated using time-kill methods. It reported that voriconazole had nonconcentration-dependent activity in vitro with maximum effect observed at 3 times the MIC [46]. Voriconazole is a fungistatic agent against Candida spp. and Cryptococcus neoformans but a fungicidal drug against Aspergillus spp. [44]. Voriconazole has shown fungicidal activity in vitro against multiple Aspergillus spp., including A. terreus which is inherently amphotericin B- resistant [5]. Although voriconazole MICs for fluconazole-resistant isolates were significantly higher than those for fluconazole-susceptible isolates, it enhances activity against fluconazole-resistant Candida krusei, Candida glabrata, and Candida guilliermondii [5, 6, 47]. Some isolates which are resistant to fluconazole and/or itraconazole may, expectedly, exhibit cross-resistance to voriconazole [48, 49]. Voriconazole has no activity against the agents of Zygomycetes, such as Mucor spp. and Rhizomucor spp. , which generate considerably high voriconazole MICs [6, 50, 51].

Voriconazole has demonstrated anti-fungi activity in a number of animal models of systemic Candidiasis, pulmonary, disseminated and intravascular fungal infection [5, 6, 52, 53]. Moreover, it was found that serum voriconazole concentrations were very low and often undetectable in mice, which was due to a combination of high clearance and extensive

metabolism by cytochrome P450 enzymes. Thus, mice were abandoned as being suitable for further study of voriconazole and most subsequent work with this drug has been performed in the guinea pig [33]. In an early study, it has been shown that in neutropenic guinea pigs with systemic Candidiasis, voriconazole was more active than fluconazole or itraconazole in animals infected with C. krusei, C. glabrata, or azole-resistant strains of C. albicans [6]. A study has also been shown that voriconazole is highly efficacious in both the prevention and treatment of Aspergillus endocarditis in the guinea pig and is superior to itraconazole in these respects [54]. In 2000, voriconazole was evaluated in an immunosuppressed-guinea pig model of invasive Aspergillosis. The study indicated that voriconazole was more effective than amphotericin B or similar doses of itraconazole and improved survival and significantly reduced tissue colony counts [55]. Recently, some investigators have evaluated the efficacy of voriconazole in a systemic infection by Scedosporium apiospermum in immunodepressed guinea pigs and documented that voriconazole prolonged survival and reduced fungal load in kidney and brain tissues of the animals infected with the first strain but was unable to prolong survival or to reduce fungal load in brain tissue for the latter strain [56]. Voriconazole also demonstrated activity against Aspergillosis in the rat and rabbit animal models, although the pharmacokinetics of voriconazole in these animals are suboptimal [6]. Moreover, the Drosophila fly was also developed as a fast, high-throughput model to study the drug efficacy against Aspergillosis and Aspergillus [57]. The study documented that Toll-deficient Drosophila flies treated by voriconazole, had significantly better survival rates and lower tissue fungal burdens than control.

Clinical Efficacy

Voriconazole has been proven as a promising agent for the treatment of a number of invasive fungal infections including Candidiasis, acute and chronic invasive aspergillosis, coccidioidomycosis, cryptococcosis, fusariosis, scedosporiosis and pseudallescheriasis,

paecilomycosis and other endemic mycoses in clinical studies [5, 13, 58-63]. In a randomized, double-blind, double-dummy, multicenter trial of voriconazole and fluconazole in the treatment of esophageal candidiasis in immunocompromised patients, it proved that voriconazole was as effective as fluconazole in the treatment of biopsy-proven esophageal candidiasis in immunocompromised patients [64]. More recently, a study have shown that voriconazole was as effective as the regimen of amphotericin B followed by fluconazole in the treatment of candidemia in non-neutropenic patients, and with fewer toxic effects [65]. Interestingly, voriconazole has shown good response against disseminated hepatosplenic aspergillosis in a patient with relapsed leukemia, whereas itraconazole, amphotericin B and liposomal amphotericin have no efficacy [66]. In Phase II/III trials, voriconazole was well-tolerated and demonstrated extremely clinical efficacy in patients with fluconazole-sensitive and -resistant candida infection, aspergillosis, and various refractory fungal infections [67]. The efficacy of the combination of voriconazole and other anti-fungi drug such as caspofungin, have also studied in the therapy for invasive aspergillosis in organ transplant. It documented that combination of voriconazole and caspofungin might be considered preferable therapy for subsets of organ transplant recipients with invasive aspergillosis, such as those with renal failure or A. fumigatus infection [68].

Microdialysis

In many cases the clinical outcome of therapy needs to be determined by the drug concentration in the tissue compartment in which the pharmacological effect occurs rather than in the plasma. Microdialysis (MD) is an *in vivo* technique which allows direct measurement of unbound tissue concentrations and permits monitoring of the biochemical and physiological effects of drugs on the body throughout the body. MD is a catheter-based sampling technique that provides the opportunity to sample analytes from interstitial fluid from tissues to measure

the free pharmacologically active concentration of exogenous or endogenous compounds at a site closer to the target site than plasma [28]. The method has been used extensively in animal and human studies for decades [28, 69-72].

Principle of Microdialysis

Microdialysis is a sampling technique that is used to measure the concentration of the unbound fraction of endogenous and/or exogenous substances in the extracellular fluid of many tissues (e.g. adipose tissue, brain, heart, lung or solid tumors) [28, 73-79]. It is applicable to both animal and human studies. The basic principle is to mimic the function of a capillary blood vessel by perfusing a thin dialysis probe with physiological fluid after it is inserted in the tissue of interest by means of a guide cannula. Continuous transfer of soluble molecules from the extracellular fluid into the probe occurs by means of a semipermeable membrane covering the tip of the probe. Samples are subsequently collected either at intermittent time points for later analysis by standard chemical analytical techniques, or more recently, continuously for direct on-line analysis [28, 80-83].

Features of Microdialysis

There are many advantages of microdialysis [28, 80-83]. It is a straight-forward technique that is not too difficult to establish on a routine basis. Microdialysis sampling does not change the net fluid balance of the surrounding sample matrix and provides clean samples in which analytes are separated from further enzymatic action. Because there is no net fluid loss, samples can be collected continuously for hours or days from a single freely moving animal. Most importantly, each animal can serve as its own control, reducing the number of required subjects compared with some other methods such as direct tissue assay. It can be used in humans in a relatively non-invasive manner. Moreover, microdialysis is easily coupled with other chemical analysis, such as high performance liquid chromatography (HPLC) [83, 84], mass spectrometry (MS) [84, 85], capillary

electrophoresis (CE) [86, 87], or nuclear magnetic resonance (NMR) [88, 89]. These techniques are often combined, e.g., HPLC-MS [84, 90], HPLC-NMR [89, 91], HPLC-NMR-MS [92-94] and CE-LIF [86] to enhance the specificity, sensitivity, reliability and efficiency of separation and detection.

As with any technique, there are limitations in the application of microdialysis [80-83, 95-97]. Microdialysis requires sensitive analytical methods to measure low concentrations in small sample volumes. Implantation of the probe almost certainly leads to tissue reactions that can interfere with the physiological system under investigation. To minimize this interference, determination of optimal times after probe implantation must be determined specifically for the analyte of interest. For example, the optimal time to measure endogenous dopamine levels after probe insertion may not be the most optimal time to measure glutamate levels due to the continuing process of gliosis at the site of probe tissue damage. Another problem is associated with highly lipophilic drugs sticking to tubing and probe components, thereby complicating the relationship between dialysate and extracellular concentrations. Most importantly, microdialysis causes dilution of analyte levels in two ways. First, endogenous analyte levels may be decreased near the probe leading to a tissue reaction and change in physiological status. Second, the diluting effect of the dialysis procedure leads to lower concentrations of analyte in samples compared to tissue, requiring both sensitive analytical methods as well as the need to determine *in vivo* recovery of the analyte to calculate true concentrations in the extracellular fluid. This latter technique may impose temporal limitations (e.g. the no-net-flux method may require hours of sampling) and may be confounded by physiological conditions that change over time.

Application in PK/PD Studies

MD has opened many possibilities to study PK and PD processes in different tissues [74, 98, 99]. Its many features make this technique interesting to be applied in PK and PD studies. MD provides a clean sample, which is protein free. Because of the membrane porosity and cut-off,

large molecules such as proteins cannot get through the membrane, which allows determining the free drug concentration in the tissue [100, 101]. It is very important when only the free drug concentration is considered to be pharmacologically active.

The PK/PD Approaches

Pharmacokinetics (PK) describes and predicts the time course of drug concentrations and pharmacodynamics (PD) refers to the time course and intensity of drug effects [102-105]. PK/PD models integrate the PK and PD approach, in which the variable of time is incorporated into the relationship of effect to concentration [8, 102, 106]. For voriconazole, integrating the PK and PD approaches provides information about the relationships between *in vitro* susceptibility, dosage, drug concentrations in the body and antifungal or toxicological effects, which helps developers select a rational dosage regimen for confirmatory clinical testing [106-109].

PK/PD issues have been studied most extensively for fluconazole [109-112]. A study documented that the PD characteristic of fluconazole most closely associated with outcome was the ratio of the area under the concentration-time curve from 0 to 24 h to the MIC (24 h AUC:MIC) in a murine model of candidemia [109]. In a neutropenic murine model of disseminated Candida albicans infection, the PK/PD parameters for voriconazole, ravuconazole and posaconazole were also similarly characterized, which support that the 24h AUC/MIC ratio is the critical PK/PD parameter associated with treatment efficacy [32, 113, 114].

However, an optimal mathematical model of voriconazole's antifungal effect has not been established yet. It is important to establish a mathematical model to predict clinical outcome of voriconazole combining PK data from in vivo model studies and PD data from in vitro model studies.

In conclusion, the studies of PK and PD profile of voriconazole play an important role in its clinical use. Simulation through PK/PD modeling is also an important tool to capture the

variability and uncertainty that is implicitly inherent in the azole antifungal drug's further development.

Hypothesis and Objectives

The overall hypothesis is that an optimal mathematical model of voriconazole's antifungal effect could be established to predict clinical outcome of them combining pharmacokinetic data from in vivo model studies and pharmacodynamics data from in vitro model for more rational use to improve the effectiveness of the drug therapeutics in clinic. To test the hypothesis of this study, the following specific aims were purposed:

Specific Aim 1: Measure voriconazole activity against *Candida* isolates using time-kill methods validated by high performance liquid chromatography.

Specific Aim 2: Apply pharmacokinetic/pharmacodynamic mathematical model to accurately describe the activity of voriconazole against *candida* spp. *in vitro*.

Specific Aim 3: Conduct pharmacodynamic studies in dynamic system for describing the activity of voriconazole against *Candida* spp.

Specific aim 4: Determine the value of protein binding of voriconazole in both rat and human plasma using *in vitro* microdialysis.

Specific aim 5: Investigate the voriconazole PK profile from analyzing the total voriconazole concentrations in plasma and free concentrations in muscle in rats by *in vivo* microdialysis. Develop a population PK model of voriconazole in rats using NONMEM.

Table 1-1. Pharmacokinetic parameters of voriconazole in mouse, rat, rabbit, guinea pig and dog following single and multiple administration by oral and intravenous routes [31]

Parameter	Mouse	Rat		Rabbit	Guinea pig	Dog
Sex	Male	Male	Female	Female	Female[a]	Male/Female
Number of animals[b]	3	2	2	3	1[c]	4
Plasma protein binding(%)	67	66	66	60	45	51
Intravenous						
Dose (mg/kg)	10	10	10	3	10	3
Single dose AUC_t (μg·h/ml)	41.7	18.6	81.6	1.1	38.5	32.1
Multiple dose AUC_t (μg·h/ml)[d]	8.0	6.7	13.9	1.6	22	17.9
Oral						
Dose (mg/kg)	30	30	30	10	10	6
Single dose C_{max}(μg/ml)	12.4	9.5	16.7	1	4.1	6.5
Single dose T_{max} (μg·h/ml)	2	6	1	1	8	3
Single dose AUC_t (μg·h/ml)	98.8	90	215.6	3.2	29	88.8
Multiple dose AUC_t (μg·h/ml)[d]	35.3	32.3	57.4	4.4	32.3	52.2
Apparent bioavailability(%)	81	159	88	87	75	138

[a] Male animals were used for single oral dose study.
[b] Number of animals per time point, except for dog and rabbit studies, which involved serial bleeding.
[c] n=3 per time for single oral dose study in guinea pigs.
[d] Once daily for up to 10 days (minimum 5 days), except guinea pig multiple oral (three times daily).

Table 1-2. Pharmacokinetic properties of triazole antifungals [8, 115-118]

Property	Fluconazole	Itraconazole	Voriconazole	Posaconazole
Bioavailability	>90%	50%–75%	>95%	Variable (depending on dosage regime and food)
Protein binding	11%	99%	58%	>98%
Volume of distribution(L/kg)	0.7–0.8	11	4.6	7–25
T_{max} (h)	2–4	4–5	1–2	3–6
CL (L/h/kg)	0.014	0.2-0.4	0.2-0.5	0.2-0.5
Metabolism	Hepatic: 11% metabolized	Hepatic: CYP3A4	Hepatic: CYP2C19, 2C9, 3A4	Hepatic: glucuronidation to inactive metabolites
Elimination half-life	22–31 hours	35–64 hours	6–24 hours (variable)	15–35 hours
Elimination route	80% excreted unchanged in urine	Hepatic; <1% excreted unchanged in urine	Hepatic; <2% excreted unchanged in urine	<1% excreted unchanged in urine; 66% excreted unchanged in feces

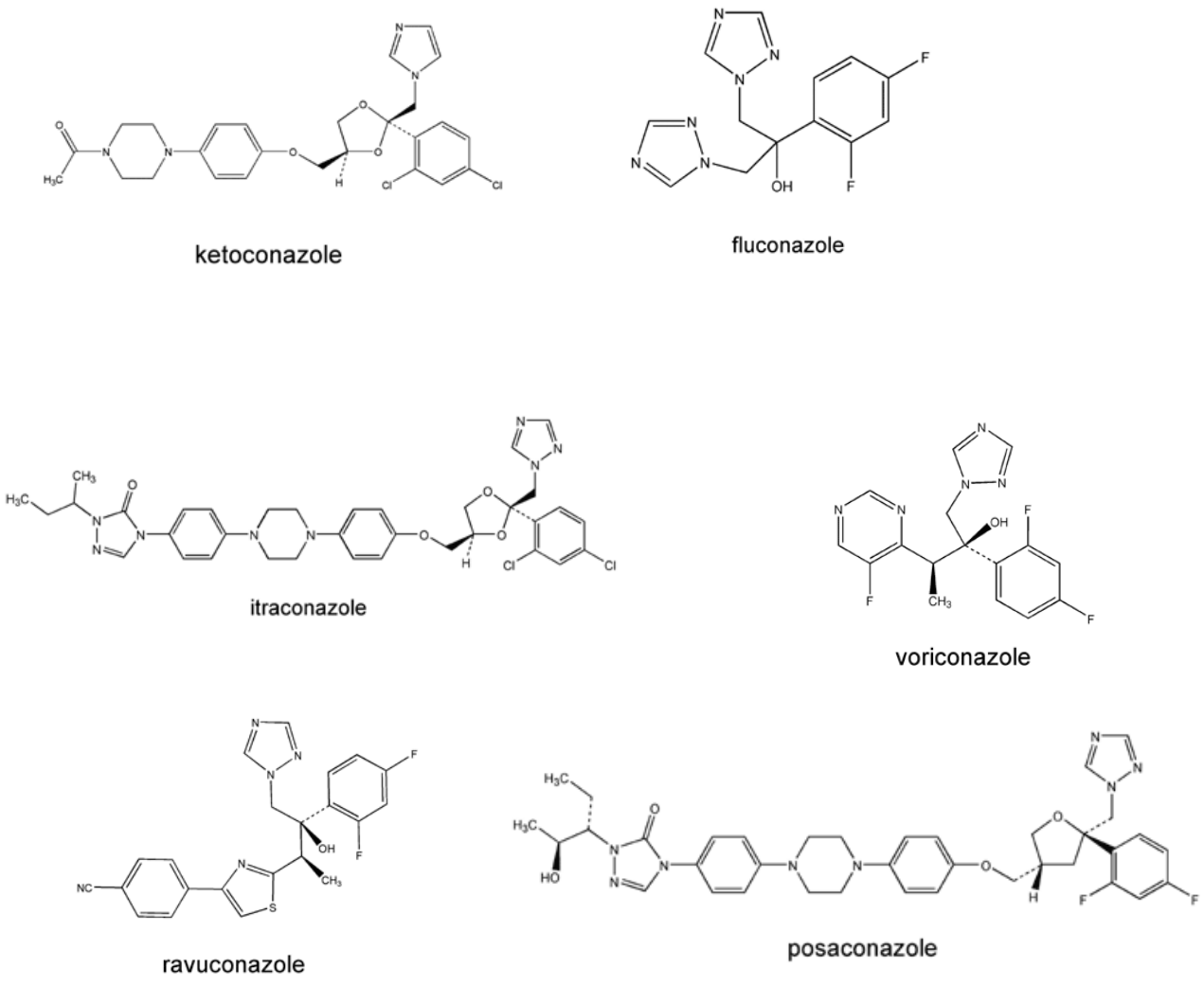

Figure 1-1. Structural relationship among azole drugs [5, 6]

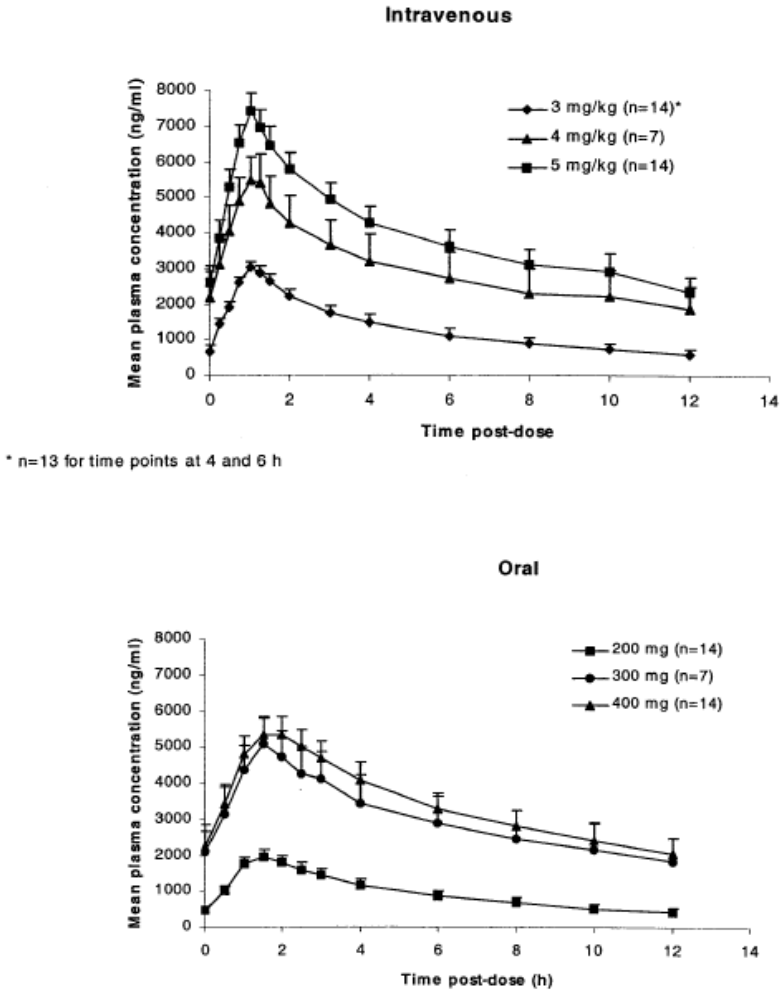

Figure 1-2. Plasma voriconazole concentration-time profiles following *i.v.* dosing (day 7) and following oral dosing (day 14) of voriconazole [39]

CHAPTER 2
MEASUREMENT OF VORICONAZOLE ACTIVITY AGAINST *CANDIDA* ISOLATES USING TIME-KILL METHODS VALIDATED BY HIGH PERFORMANCE LIQUID CHROMATOGRAPHY

Background

Voriconazole is a triazole agent that inhibits ergosterol synthesis by blocking the action of 14α-demethylase. The drug is fungistatic and exhibits no postantifungal effect (PAFE) against Candida albicans (1, 3–5, 7, 9). Time-kill and PAFE data for Candida glabrata are limited (1, 7) and do not exist for Candida parapsilosis isolates. Moreover, standard time-kill and PAFE methodologies, although widely used, have not been validated for voriconazole or other antifungals by direct measurement of drug concentrations.

Specific Aims

This study was to develop an high performance liquid chromatography (HPLC) assay to validate the results of time-kill and PAFE experiments for voriconazole against *C. albicans* reference strains (ATCC 90029 and SC5314), and *C. glabrata* and *C. parapsilosis* bloodstream isolates (two each).

Materials and Methods

Antifungal Agents

Stock solutions of voriconazole (Pfizer, New York, N.Y.) were prepared using sterile water. Stock solutions were separated into unit-of-use portions and stored at -80°C until used.

Test Isolates

Eight strains were studied: 2 references (*C. albicans*: ATCC 90029 and SC 5314) and 6 clinical (3 *C. albicans*, 2 *C. glabrata* and 1 *C. parapsilosis*).

Antifungal Susceptibility Testing

MICs were determined using E-test (Figure 2-1). The inoculum was prepared from Sabouraud glucose agar subcultures incubated at 35°C for 24 h and the resulting suspension was adjusted spectrophotometrically to a density equivalent to a 0.5 MacFarland standard at 530 nm (1.5×10^6 CFU/ml). The solidified medium was inoculated by dipping a sterile cotton swab into the respective undiluted stock inoculum suspension and streaking evenly in three directions over the entire surface of a 150 mm diameter RPMI agar plate. The plate was permitted to dry for at least 15 min before the E-test strips with antifungal were placed on the medium surface [46].

Antifungal Carryover

Prior to time-kill experiments, assessment of the effect of solubilized voriconazole on colony count determinations. A fungal suspension was prepared with each test isolate to yield an inoculum of approximately 5×10^3 CFU/ml. One hundred-microliter volumes of these suspensions were added to 900µl volumes of sterile water or sterile water plus voriconazole at concentrations ranging from 0.0625 to 16 times the MIC. This dilution resulted in a starting inoculum of approximately 5×10^2 CFU/ml. Immediately following addition of the fungal inoculum to a test tube, the tube was vortexed and a 50-µl sample was removed and plated without dilution on potato dextrose agar plates (Remel, Lenexa, Kans.) for determination of viable colony counts. Following 48 h of incubation at 35°C, the number of CFU was determined. Tests were conducted in quintuplicate. The mean colony count data for each agent at each multiple of the MIC tested were compared with the data for the control. Significant antifungal carryover was defined as a reduction in the mean number of CFU per milliliter of >25% compared with the colony count for the control [46].

Time-kill Experiments

Time-kill experiments were performed in duplicate at 0.25×, 1×, 4× and 16× MIC. Before testing, isolates were subcultured twice on potato dextrose agar plates. Colonies from a 24- to 48-h culture were suspended in 9 ml of sterile water and adjusted to a 0.5 McFarland turbidity standard. 100 µl of the adjusted fungal suspension was then added to either growth medium alone (control) or a solution of RPMI plus an appropriate amount of voriconazole stock solution. These procedures resulted in a starting inoculum of approximately 1×10^5 to 5×10^5 CFU/ml concentrations and a voriconazole concentration of 0.0625×, 0.25×, 1×, 4×, or 16 × MIC (Figure 2-2). Test solutions were placed on an orbital shaker and incubated with agitation at 35°C. At predetermined time points of 2, 4, 8, 12, and 24 h, 100µl samples were obtained from each solution, serially diluted in sterile water, and plated (100 µl) on potato dextrose agar plates for CFU determination. The lower limit of reproducibly quantifiable CFU according to these methods was 50 CFU/ml [46, 119].

Postantifungal Effect (PAFE) Experiments

PAFE experiments for control testing (no drug) and testing at 0.25, 1, 4, and 16 times the MIC in duplicate tubes. After 1 hour of incubation, the cells were centrifuged at 1,400 × *g* for 10 min, washed three times, and then resuspended in warm RPMI medium (9 ml) prior to reincubation. At predetermined time points of 2, 4, 8, 12, and 24 h, 100µl samples were obtained from each solution, serially diluted in sterile water, and plated (100 µl) on potato dextrose agar plates for CFU determination [119].

HPLC for Determination of Voriconazole in Stock Solution and RPMI Medium

An HPLC protocol for measuring voriconazole in Stock Solution and RPMI media was developed based an existing assay method with a calibration range of 0.2–10 µg/ml

voriconazole in human plasma [120], 5–10 µg/ml voriconazole in guinea pig plasma [121]. The analytical column was Kromasil C18, 5 mm, 250×4.6 mm (Hichrom, Reading, UK) with a 10×3.2 mm guard cartridge (Hichrom, Reading, UK) packed with the same material at 25°C in an Agilent 1100 Series apparatus. The mobile phase was acetonitrile-ammonium phosphate buffer (pH 6.0; 0.04 M) (1:1 v:v) and was degassed by filtration through a 0.45 mm nylon filter under vacuum. The flow rate was 0.8 ml/min and all chromatography was carried out at ambient temperature (~21°C). Voriconazole concentrations were determined from peak areas detected by UV absorption at 255 nm with a retention time of 8.2 min; the maximum sensitivity was 0.025µg/ml. Samples of Stock Solution and RPMI medium were diluted with 2 volumes of acetonitrile-ammonium phosphate buffer and centrifuged at full speed in a microcentrifuge for 10 min. The supernatants were applied to the column in 200µl sample volumes.

Calibration Curves for Voriconazole in Stock Solution and RPMI Medium

Stock solutions of voriconazole (1 µg/µl) were prepared in distilled water and diluted in RPMI medium to give 100 µg/ ml. Standards were prepared by adding the diluted voriconazole solution to appropriate volumes of Stock Solution and RPMI medium to give a concentrations of 0.025, 0.1, 0.2, 0.5, 1, 2, 4, 8 and 16 µg/ ml. Calibration curves were constructed by plotting the peak area of voriconazole against concentration using a weighted (1:X2) least squares regression for HPLC data analysis.

Statistical Analysis

When data are expressed as the mean ± SD, group mean differences were ascertained with analysis of variance (ANOVA). The results were considered significant if the probability of error was < 0.05.

Results

Stability of Voriconazole in Stock Solution and RPMI Medium

The *in vitro* stability of voriconazole in stock solution (PH = 7.0) and RPMI medium (PH= 7.0) were studied. There was no color change or precipitation in the preparations and pH remained stable during the period of the studies. The results showed that voriconazole in stock solution were found stable at -80°C, -4°C at least for 6 months and one week, respectively. In RPMI medium, voriconazole were found stable at room temperature and 37°C for at least 72 hours, and stable -80°C at least for 6 months (Table 2-1). The loss of voriconazole was less than 5% of the starting concentration at all conditions.

Minimum Inhibitory Concentration (MIC)

The MICs of all isolates were within the susceptible range, as measured by Etest and microdilution methods (Table 2-2) [122, 123].

Time-kills and Postantifungal Effect (PAFE)

For time-kills and PAFEs, colonies from 48-hour cultures on Sabouraud dextrose agar (SDA) were suspended in 9 ml sterile water [46, 119]. One microliter of a 0.5 McFarland suspension was added to 10 ml of RPMI 1640 medium with or without voriconazole (0.25×, 1×, 4×, and 16× MIC), and the solution was incubated at 35°C with agitation. The maximal voriconazole concentration in these experiments was 3.04µg/ml (16× MIC for *C. glabrata* isolate 1). For time-kills, 100 µl from each solution was serially diluted at desired time points (0, 2, 4, 8, 12, 24, 36, 48, 60, and 72 h) and plated on Sabouraud dextrose agar for colony enumeration. For PAFEs experiments, *Candida* cells were collected after 1 h of incubation, washed three times, and resuspended in warm RPMI 1640 medium (9 ml); colonies were enumerated at the desired time points.

Voriconazole exhibited dose-response effects against all *Candida* isolates during time-kill experiments (Figure 2-3; Table 2-2), as higher concentrations resulted in greater growth inhibition or killing. The range of maximal growth inhibition of isolates at 1× and 4× MICs was -0.61- to –2.78-log and –0.53- to –2.99log, respectively, compared to those of controls. At 16× MIC, the range of maximal growth inhibition was –0.58- to –4.15log (Table 2-3, 2-4, 2-5, 2-6, 2-7, 2-8 and 2-9). The results of PAFE experiments for the tested isolates are listed in Tables of 2-10, 2-11, 2-12, 2-13, and 2-14. Voriconazole did not demonstrate PAFEs as shown from Figure 2-4 which is the profile of the concentration of colony forming units versus the time.

Voriconazole at 16× MIC was fungicidal against *C. parapsilosis* isolate 2, reducing the starting inoculum by –2.21log at 24 h (fungicidal is defined as a > 2-log reduction of starting inoculum). Although kills did not achieve fungicidal levels for other isolates, voriconazole at 4× and 16× MIC reduced the starting inocula of *C. glabrata* isolate 2 and *C. parapsilosis* isolate 1 (Table 2-2). Of note, voriconazole was consistently fungistatic at 1× to 16× MICs, and the effect persisted for 72 h. Indeed, maximal inhibition of the four *C. albicans* and *C. glabrata* isolates at 4× and 16× MIC (compared to starting inocula) was not evident until 48 to 72 h. The two *C. parapsilosis* isolates, on the other hand, were maximally inhibited by 24 to 36 h.

The time-kill curves of the *C. parapsilosis* isolates also differed from those of the other isolates at early time points. The *C. parapsilosis* isolates at 4× and 16× MIC were inhibited from entering the exponential growth phase, and dose-response effects were clearly evident by 8 h. The growth rates of *C. albicans* and *C. glabrata* isolates in the presence of voriconazole did not differ from those of controls during early exponential

phase, but dose-response effects became increasingly apparent as exponential growth continued (8 to 24 h).

In our HPLC protocol for measuring voriconazole concentrations during time-kill and PAFE experiments, a 250- by 4.6-mm analytic column with 10- by 3.2-mm guard cartridge (Hichrom, Reading, United Kingdom) was packed with a 5-μm-particle-size Kromasil column at 25°C in an Agilent 1100 series apparatus [120, 121]. Mobile phase acetonitrile-ammonium phosphate buffer (pH 6.0; 0.04 M; 1:1 vol:vol) was degassed by filtration through a 0.45-μm nylon filter under vacuum; the flow rate was 0.8 ml/min. Voriconazole concentrations were determined for peak areas detected by UV absorption at 255 nm with an 8.2-min retention time (Figure 2-5). For each isolate, we tested RPMI 1640 medium containing at least one dose of voriconazole between 1× and 16× MICs. Samples were diluted with 2 volumes of acetonitrile-ammonium phosphate buffer and centrifuged at full speed in a microcentrifuge for 10 min, and the supernatants (200 μl) were applied to the column. The maximum sensitivity was 0.025μg/ml, and the method produced linear results over a range of 0.025 to 12.8μg/ml ($r^2 \geq 0.9996$). In each instance, we confirmed that voriconazole concentrations remained constant throughout the duration of time-kill experiments (Figure 2-6), and the drug was fully removed during PAFE experiments (Figure 2-7).

Discussion

Voriconazole were stable at all the conditions covered in our studies. Our findings in time-kill studies conclusively demonstrate that voriconazole exerts prolonged fungistatic activity against *C. albicans*, *C. glabrata* and *C. parapsilosis* at concentrations that are achievable in human sera with routine dosing (the medians of the average and maximum voriconazole plasma concentrations in clinical trials were 2.51 and 3.79 μg/ml,

respectively) [124]. Our findings are potentially relevant clinically, since certain *C. parapsilosis* isolates exhibit diminished susceptibility to echinocandin antifungals and *C. glabrata* isolates can develop resistance to fluconazole and other antifungal agents. Although voriconazole caused >2-log kill of one *C. parapsilosis* isolate, further studies will be needed to accurately define the extent to which the drug might be fungicidal against clinical isolates.

To our knowledge, this is the first study to verify standard time-kill and PAFE methodologies by directly measuring drug concentrations. We describe a simple and reproducible HPLC method that has a broad, clinically relevant dynamic range and does not require internal standards. The sensitivity of voriconazole measurements within liquid media was greater than that previously reported for human or guinea pig plasma (0.2 to 10 and 5 to10 μg/ml, respectively) [120, 121]. Based on our findings, we can assume that previous studies of azoles that showed fungistatic anticandidal activity and no PAFEs were conducted under the conditions of steady-state drug concentrations assumed by investigators. This demonstration is crucial as efforts to use pharmacodynamic data to develop optimal antifungal treatment strategies move forward. In particular, HPLC methods will be essential to the design of dynamic *in vitro* models to assess the pharmacodynamics of voriconazole and other agents prior to the achievement of steady-state conditions.

Table 2-1. Percentage (%) of voriconazole maintenance in stock solution and RPMI medium at different temperatures (Mean ± SD, n = 3)

	VOR in stock solution		VOR in RPMI medium		
Storage time	1.02 mg/ml	9.96 mg/ml	0.20 μg/ml	1.02 μg/ml	10.13 μg/ml
1mon (-80 °C)	99.8±0.8	99.4±0.5	99.0±0.6	100.1±0.9	100.1±0.6
6mon (-80 °C)	98.4±1.7	98.8±0.6	97.5±1.7	97.4±1.0	99.5±0.6
1d (4 °C)	99.8±0.3				
7d (4 °C)	98.6±0.7				
24h (25 °C)			99.2±0.7	99.0±0.6	100.3±0.4
72h (25 °C)			99.0±0.7	98.6±1.7	98.4±1.9
24h (37 °C)			100.0±0.4	99.0±0.6	100.3±0.6
72h (37 °C)			97.0±0.9	97.4±1.6	97.7±0.7

Table 2-2. Minimum inhibitory concentration (MIC) of voriconazole against Candida isolates (n=3)

Isolate	MIC(μg/ml)
C. albicans ATCC90029	0.008
C.albicans SC5314	0.012
C. glabrata 1	0.19
C. glabrata 2	0.032
C. parapsilosis 1	0.008
C. parapsilosis 2	0.016

Table 2-3. Voriconazole against *Candida albicans* ATCC90029 in constant concentration experiments (Data of CFU/mL, Mean ± SD, n = 3)

Time (h)	Control	SD	0.25×MIC	SD	1×MIC	SD	4×MIC	SD	16×MIC	SD
0	1.00E+05	0.00E+00	1.00E+05	0.00E+00	1.00E+05	0.00E+00	1.00E+05	0.00E+00	1.00E+05	0.00E+00
2	1.23E+05	5.13E+03	1.04E+05	6.20E+03	1.18E+05	3.76E+03	1.22E+05	1.21E+04	1.07E+05	2.21E+04
4	2.84E+05	9.81E+03	2.06E+05	1.28E+04	2.51E+05	3.50E+04	2.09E+05	3.44E+04	1.76E+05	5.22E+04
8	6.70E+05	9.24E+04	5.43E+05	1.14E+05	5.38E+05	4.33E+04	4.87E+05	5.72E+04	3.85E+05	4.89E+04
12	1.49E+06	2.71E+05	9.38E+05	1.52E+05	8.84E+05	4.75E+04	6.11E+05	9.06E+04	4.78E+05	2.23E+04
24	9.54E+06	2.57E+05	3.32E+06	1.19E+06	6.33E+05	1.81E+04	5.58E+05	7.55E+04	5.00E+05	6.81E+04
48	1.07E+07	5.78E+05	2.54E+06	2.00E+05	3.25E+05	1.17E+05	2.52E+05	8.03E+04	2.27E+05	1.14E+05

Table 2-4. Voriconazole against *Candida albicans* SC5314 in constant concentration experiments (Data of CFU/mL, Mean ± SD, n = 2)

Time (h)	Control	SD	0.25×MIC	SD	1×MIC	SD	4×MIC	SD	16×MIC	SD
0	1.00E+05	0.00E+00	1.00E+05	0.00E+00	1.00E+05	0.00E+00	1.00E+05	0.00E+00	1.00E+05	0.00E+00
2	9.67E+04	1.71E+03	9.46E+04	1.51E+04	1.14E+05	8.02E+03	9.28E+04	1.15E+04	8.20E+04	9.21E+03
4	1.77E+05	2.11E+04	1.28E+05	6.96E+03	1.28E+05	2.66E+04	1.18E+05	1.97E+04	1.00E+05	2.11E+04
8	8.78E+05	2.44E+05	5.31E+05	1.92E+05	3.99E+05	1.35E+05	2.75E+05	8.31E+04	2.88E+05	1.10E+05
12	1.08E+06	1.96E+05	7.14E+05	4.46E+04	4.24E+05	1.70E+05	2.97E+05	3.88E+04	3.54E+05	1.53E+05
24	1.30E+06	1.06E+05	7.93E+05	5.74E+04	2.80E+05	6.57E+04	3.40E+05	1.40E+05	2.95E+05	1.13E+05
48	1.25E+06	1.55E+05	7.00E+05	9.44E+04	2.46E+05	9.56E+04	2.79E+05	8.14E+02	2.71E+05	6.26E+04

Table 2-5. Voriconazole against *Candida glabrata* 1 in constant concentration experiments (Data of CFU/mL, Mean ± SD, n = 2)

Time (h)	Control	SD	0.25×MIC	SD	1×MIC	SD	4×MIC	SD	16×MIC	SD
0	1.00E+05	0.00E+00	1.00E+05	0.00E+00	1.00E+05	0.00E+00	1.00E+05	0.00E+00	1.00E+05	0.00E+00
2	1.06E+05	1.77E+04	1.03E+05	1.24E+04	1.08E+05	1.58E+04	1.05E+05	2.04E+04	1.00E+05	1.80E+04
4	1.15E+05	1.47E+04	1.11E+05	2.79E+04	1.46E+05	6.29E+04	1.19E+05	3.41E+04	1.31E+05	3.37E+04
8	1.76E+05	7.00E+04	1.54E+05	6.41E+04	1.63E+05	7.19E+04	1.61E+05	5.35E+04	1.70E+05	5.59E+04
12	5.25E+05	6.45E+03	5.35E+05	4.15E+04	4.22E+05	1.07E+05	2.85E+05	2.55E+04	3.61E+05	2.85E+04
24	2.46E+06	5.70E+04	1.39E+06	2.76E+05	7.32E+05	1.80E+05	6.96E+05	1.52E+05	6.20E+05	1.10E+04
48	3.86E+06	2.49E+05	2.19E+06	3.90E+04	1.05E+06	4.87E+05	7.45E+05	8.02E+04	4.36E+05	4.11E+04

Table 2-6. Voriconazole against *Candida glabrata* 2 in constant concentration experiments (Data of CFU/mL, Mean ± SD, n = 2)

Time (h)	Control	SD	0.25×MIC	SD	1×MIC	SD	4×MIC	SD	16×MIC	SD
0	1.00E+05	0.00E+00	1.00E+05	0.00E+00	1.00E+05	0.00E+00	1.00E+05	0.00E+00	1.00E+05	0.00E+00
2	9.60E+04	3.97E+02	1.01E+05	1.63E+04	1.01E+05	3.62E+03	8.67E+04	1.41E+04	9.96E+04	1.83E+04
4	1.20E+05	2.64E+03	1.25E+05	2.84E+04	1.24E+05	5.68E+03	1.11E+05	1.26E+04	1.11E+05	2.68E+04
8	4.86E+05	2.51E+05	4.28E+05	1.66E+05	3.52E+05	7.74E+04	2.78E+05	8.54E+04	2.81E+05	9.87E+04
12	1.23E+06	4.34E+05	8.90E+05	6.26E+04	6.03E+05	1.25E+05	3.37E+05	4.88E+04	2.94E+05	4.36E+04
24	5.34E+06	9.61E+05	1.08E+06	2.01E+05	5.80E+05	2.78E+04	4.26E+05	1.39E+04	3.52E+05	6.21E+04
48	7.11E+06	1.41E+06	2.96E+05	1.42E+05	6.91E+04	3.16E+04	3.74E+04	1.26E+04	3.47E+04	1.44E+04

Table 2-7. Voriconazole against *Candida parapsilosis* 1 in constant concentration experiments (Data of CFU/mL, Mean ± SD, n = 2)

Time (h)	Control	SD	0.25×MIC	SD	1×MIC	SD	4×MIC	SD	16×MIC	SD
0	1.00E+05	0.00E+00	1.00E+05	0.00E+00	1.00E+05	0.00E+00	1.00E+05	0.00E+00	1.00E+05	0.00E+00
2	1.06E+05	8.26E+03	9.41E+04	2.25E+04	9.62E+04	8.26E+03	1.00E+05	6.56E+03	1.03E+05	2.44E+03
4	1.67E+05	6.03E+03	1.41E+05	1.33E+04	1.39E+05	2.05E+02	1.36E+05	3.57E+03	1.30E+05	8.87E+03
8	9.97E+05	9.36E+03	6.39E+05	1.98E+04	2.71E+05	5.42E+04	2.30E+05	3.12E+03	1.94E+05	3.28E+03
12	1.84E+06	4.52E+05	1.64E+06	3.35E+05	3.74E+05	2.73E+04	1.48E+05	7.51E+04	1.25E+05	4.19E+04
24	7.26E+06	2.44E+06	5.32E+06	1.51E+06	6.67E+05	1.41E+05	1.25E+05	8.30E+03	1.21E+05	1.34E+04
48	3.45E+07	2.51E+06	2.72E+07	1.06E+07	3.47E+06	5.73E+05	1.28E+05	3.71E+04	9.06E+04	3.60E+04

Table 2-8. Voriconazole against *Candida parapsilosis* 2 in constant concentration experiments (Data of CFU/mL, Mean ± SD, n = 2)

Time (h)	Control	SD	0.25×MIC	SD	1×MIC	SD	4×MIC	SD	16×MIC	SD
0	1.00E+05	0.00E+00	1.00E+05	0.00E+00	1.00E+05	0.00E+00	1.00E+05	0.00E+00	1.00E+05	0.00E+00
2	1.10E+05	7.07E+03	1.04E+05	1.41E+03	9.49E+04	3.18E+03	9.55E+04	2.33E+04	8.55E+04	7.00E+03
4	1.36E+05	1.70E+04	1.25E+05	2.12E+03	1.09E+05	1.27E+04	1.08E+05	9.90E+03	8.00E+04	2.68E+04
8	3.51E+05	1.77E+04	4.25E+05	7.85E+04	7.44E+04	1.58E+04	6.47E+04	1.88E+04	2.32E+04	7.79E+03
12	1.16E+06	2.05E+05	9.15E+05	9.69E+04	8.09E+04	2.00E+04	3.07E+04	9.76E+03	1.26E+04	1.41E+03
24	5.60E+06	3.04E+05	6.08E+06	2.57E+06	7.12E+04	3.04E+03	1.15E+04	2.98E+03	2.78E+03	3.07E+03
48	1.02E+07	2.21E+06	1.42E+07	4.53E+06	5.35E+05	5.69E+05	5.15E+04	2.87E+04	1.73E+03	7.14E+02

Table 2-9. Summarized voriconazole time-kill data against Candida isolates

Isolate	MIC(μg/ml)[b]	Maximum log kill at[a] :								
		24h			24-48h			>48h		
		1x MIC	4x MIC	16x MIC	1x MIC	4x MIC	16x MIC	1x MIC	4x MIC	16x MIC
C. albicans ATCC90029	0.008	-1.23	-1.34	-1.34	**-1.77**	-1.84	**-1.96**	-1.63	**-1.90**	-1.89
C.albicans SC5314	0.012	**-0.61**	-0.51	-0.54	-0.56	**-0.53**	**-0.58**			
C. glabrata 1	0.19	-0.43	-0.49	-0.59	-0.74	-0.78	-1.00	**-0.99**	**-1.08**	**-1.17**
C. glabrata 2	0.032	-1.02	-1.10	-1.15	-2.23	-2.39	-2.49	**-2.78**	**-2.99**	**-3.02**
C. parapsilosis 1	0.008	**-0.99**	-1.64	-1.68	-0.91	**-2.67**	**-2.74**	-0.67	-2.37	-2.69
C. parapsilosis 2	0.016	**-1.86**	**-2.70**	-3.93	-1.03	-2.13	-3.94	-0.88	-1.12	**-4.15**

[a] Time-kill data are presented as the maximum difference between the growth of the control isolate (grown in the absence of voriconazole) and that of the isolate in the presence of various voriconazole concentrations at ≤ 24 h, 24 to 48 h, and > 48 h. The maximum growth inhibition of each isolate at the given concentrations is shown in bold.

[b] MICs, as determined by Etest and the Clinical and Laboratory Standards Institute (formerly NCCLS) broth microdilution method [123], were within twofold agreement.

Table 2-10. Voriconazole against *Candida albicans* ATCC90029 in PAFE experiments (Data of CFU/mL, Mean ± SD, n =2)

Time (h)	Control	SD	0.25×MIC	SD	1×MIC	SD	4×MIC	SD	16×MIC	SD
0	3.00E+05	1.98E+04	3.04E+05	1.56E+04	2.95E+05	7.78E+03	3.15E+05	7.07E+03	2.87E+05	1.48E+04
2	3.20E+05	2.83E+03	3.15E+05	2.05E+04	2.89E+05	2.12E+03	3.28E+05	5.66E+03	3.35E+05	6.36E+04
4	5.65E+05	7.07E+03	6.15E+05	1.48E+05	5.15E+05	3.54E+04	6.20E+05	1.27E+05	5.75E+05	1.34E+05
8	1.75E+06	1.41E+05	1.99E+06	7.64E+05	1.66E+06	2.47E+05	1.91E+06	3.11E+05	2.17E+06	1.20E+06
12	5.10E+06	2.83E+05	5.40E+06	4.24E+05	4.65E+06	7.07E+04	4.35E+06	2.12E+05	5.30E+06	7.07E+05
24	1.55E+07	1.27E+06	1.80E+07	3.89E+06	1.46E+07	1.06E+06	1.60E+07	4.17E+06	1.61E+07	3.68E+06
48	2.56E+07	2.69E+06	2.84E+07	7.07E+06	2.77E+07	4.88E+06	2.24E+07	1.34E+06	2.93E+07	5.02E+06

Table 2-11. Voriconazole against *Candida glabrata* 2 in PAFE experiments (Data of CFU/mL, Mean ± SD, n =2)

Time (h)	Control	SD	0.25×MIC	SD	1×MIC	SD	4×MIC	SD	16×MIC	SD
0	2.61E+05	1.77E+04	2.31E+05	2.12E+03	2.38E+05	4.24E+03	2.62E+05	4.95E+03	2.44E+05	1.27E+04
2	2.48E+05	2.47E+04	2.18E+05	4.81E+04	2.66E+05	1.48E+04	2.43E+05	5.23E+04	2.30E+05	1.77E+04
4	5.55E+05	2.12E+04	4.80E+05	4.24E+04	5.20E+05	4.24E+04	6.00E+05	2.83E+04	5.30E+05	2.83E+04
8	1.37E+06	7.07E+04	1.48E+06	1.34E+05	1.20E+06	7.07E+03	1.58E+06	9.90E+04	1.79E+06	1.20E+05
12	3.19E+06	6.36E+04	3.08E+06	8.49E+04	3.35E+06	2.12E+05	3.00E+06	1.41E+05	3.60E+06	1.06E+05
24	1.48E+07	7.07E+05	1.59E+07	2.76E+06	1.80E+07	4.81E+06	1.54E+07	6.36E+05	1.67E+07	4.24E+05
48	1.91E+07	5.66E+05	1.54E+07	1.41E+05	1.75E+07	1.34E+06	1.72E+07	3.54E+05	1.97E+07	1.56E+06

Table 2-12. Voriconazole against *Candida glabrata* 1 in PAFE experiments (Data of CFU/mL)

Time (h)	Control	0.25×MIC	1×MIC	4×MIC	16×MIC
0	2.58E+05	2.35E+05	2.58E+05	2.67E+05	2.77E+05
2	2.37E+05	2.15E+05	2.37E+05	2.39E+05	2.64E+05
4	3.40E+05	3.07E+05	3.53E+05	2.60E+05	3.10E+05
8	8.60E+05	6.70E+05	1.06E+06	7.00E+05	1.03E+06
12	1.41E+06	1.62E+06	1.53E+06	1.05E+06	1.15E+06
24	7.80E+06	7.00E+06	7.00E+06	7.80E+06	6.80E+06
48	1.15E+07	1.29E+07	1.35E+07	1.16E+07	1.34E+07

Table 2-13. Voriconazole against *Candida parapsilosis* 1 in PAFE experiments (Data of CFU/mL)

Time (h)	Control	0.25×MIC	1×MIC	4×MIC	16×MIC
0	2.89E+05	3.40E+05	3.10E+05	2.70E+05	2.84E+05
2	2.51E+05	2.85E+05	2.95E+05	2.46E+05	2.67E+05
4	4.80E+05	6.80E+05	6.40E+05	6.00E+05	6.27E+05
8	9.90E+05	1.69E+06	1.12E+06	1.55E+06	1.70E+06
12	2.40E+06	3.42E+06	2.50E+06	3.04E+06	3.16E+06
24	1.46E+07	2.18E+07	1.47E+07	1.64E+07	2.00E+07
48	3.22E+07	3.04E+07	3.02E+07	3.03E+07	3.69E+07

Table 2-14. Voriconazole against *Candida parapsilosis* 2 in PAFE experiments (Data of CFU/mL)

Time (h)	Control	0.25×MIC	1×MIC	4×MIC	16×MIC
0	1.81E+05	1.79E+05	1.42E+05	1.55E+05	1.79E+05
2	1.38E+05	1.36E+05	1.40E+05	1.46E+05	1.34E+05
4	1.34E+05	1.61E+05	1.54E+05	2.20E+05	1.40E+05
8	4.10E+05	6.00E+05	3.66E+05	6.50E+05	4.70E+05
12	1.34E+06	1.40E+06	1.33E+06	1.92E+06	1.48E+06
24	1.37E+07	1.60E+07	1.45E+07	1.95E+07	1.21E+07
48	2.26E+07	2.29E+07	2.36E+07	2.43E+07	2.00E+07

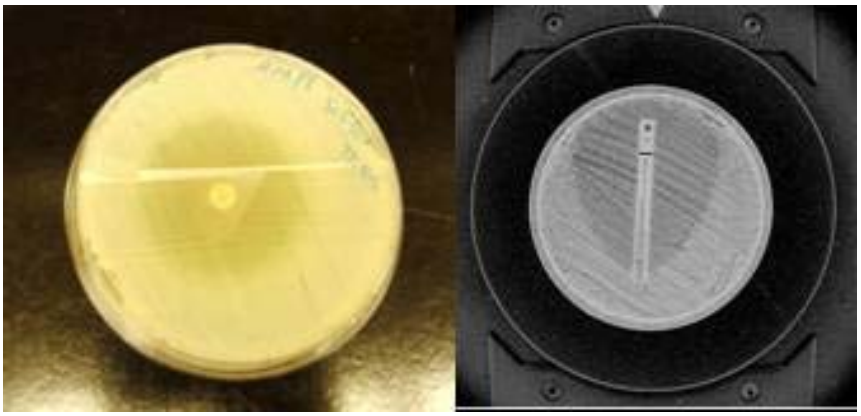

A B

Figure 2-1. Susceptibility of voriconazole against Candida isolates were determined by disc diffusion, E-test and the Clinical and Laboratory Standards Institute broth microdilution method. A) Disc diffusion. B) E-test.

Figure 2-2. Culture flasks for voriconazole against Candida isolates *in vitro*

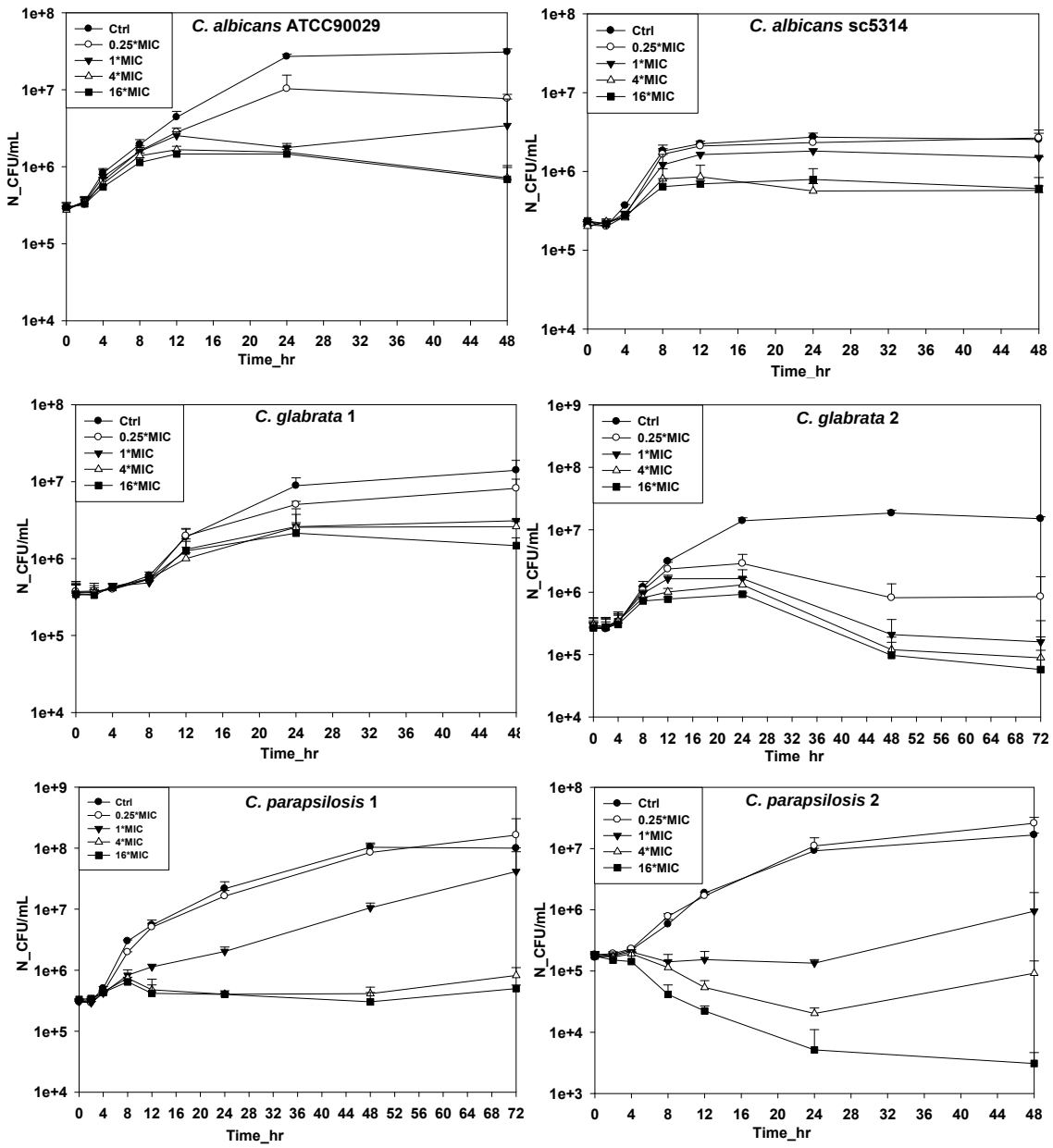

Figure 2-3. Time-kill curves for voriconazole against Candida isolates (Mean ± SD, n=3 for C. albicans ATCC90029, n=2 for other tested strains, without significant differences in results by ANOVA)

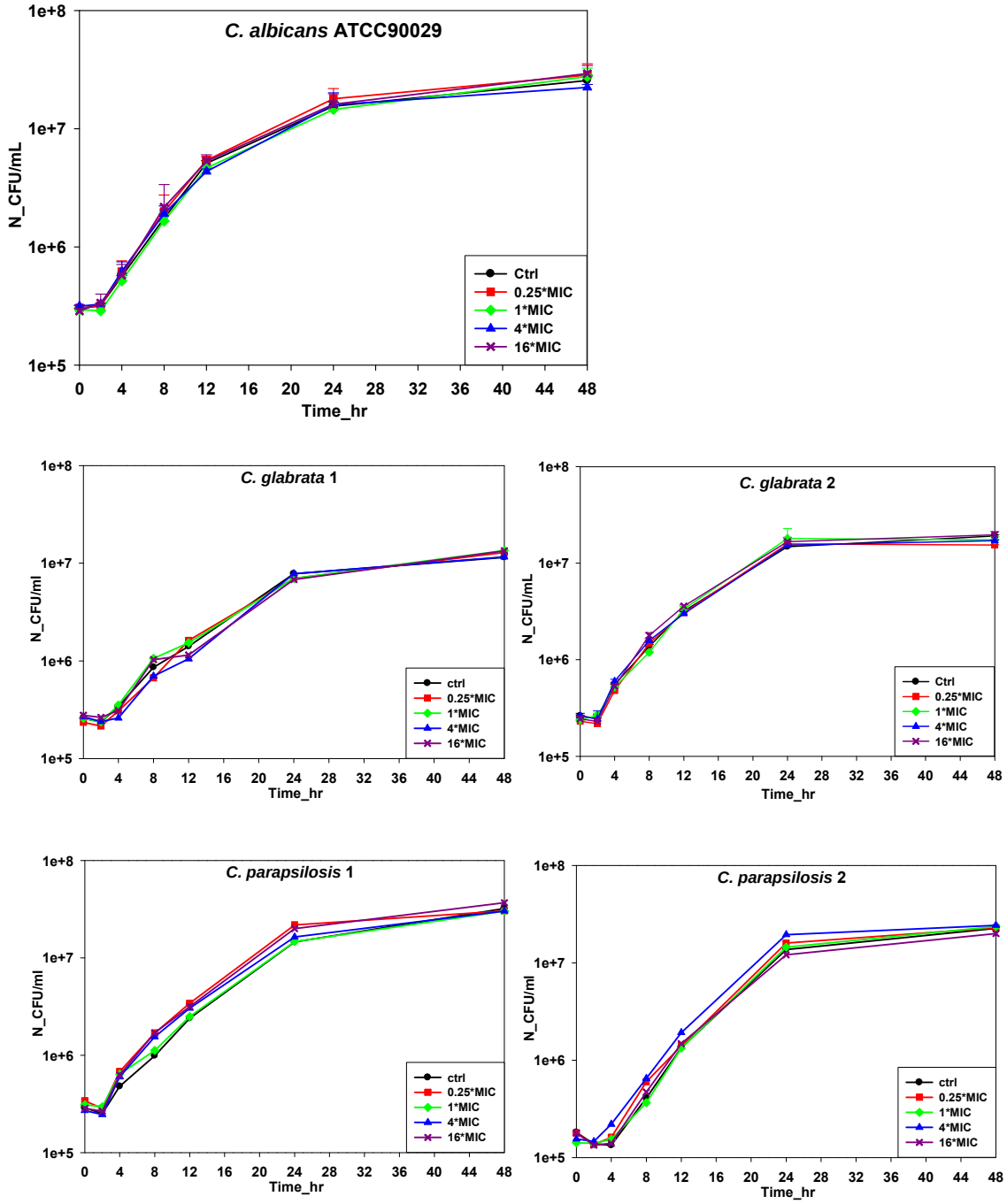

Figure 2-4. Voriconazole did not demonstrate PAFEs. (Mean ± SD, n=2 for C. albicans ATCC90029, C. glabrata 2, without significant differences in results by ANOVA; n=1 for other three tested strains.)

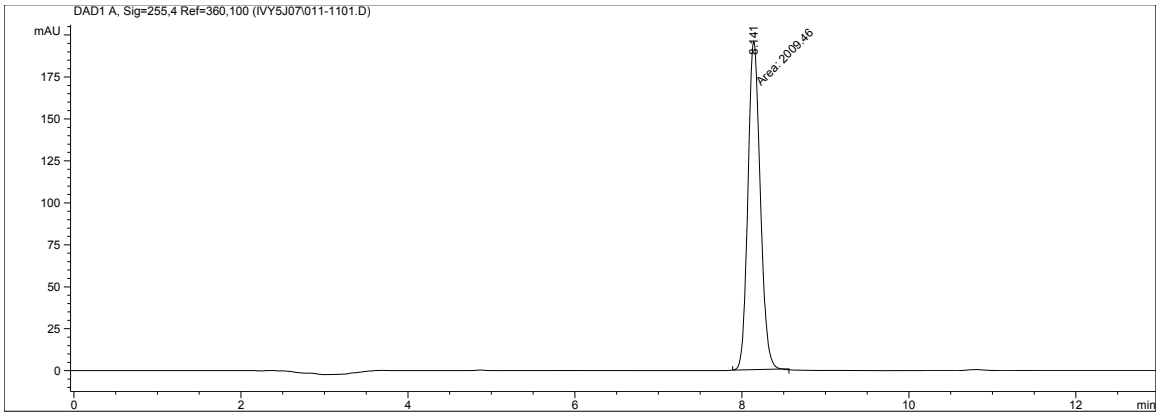

Figure 2-5. Chromatogram of voriconazole which concentration was determined from peak area detected by UV absorption at 255 nm with around an 8.2 minute retention time

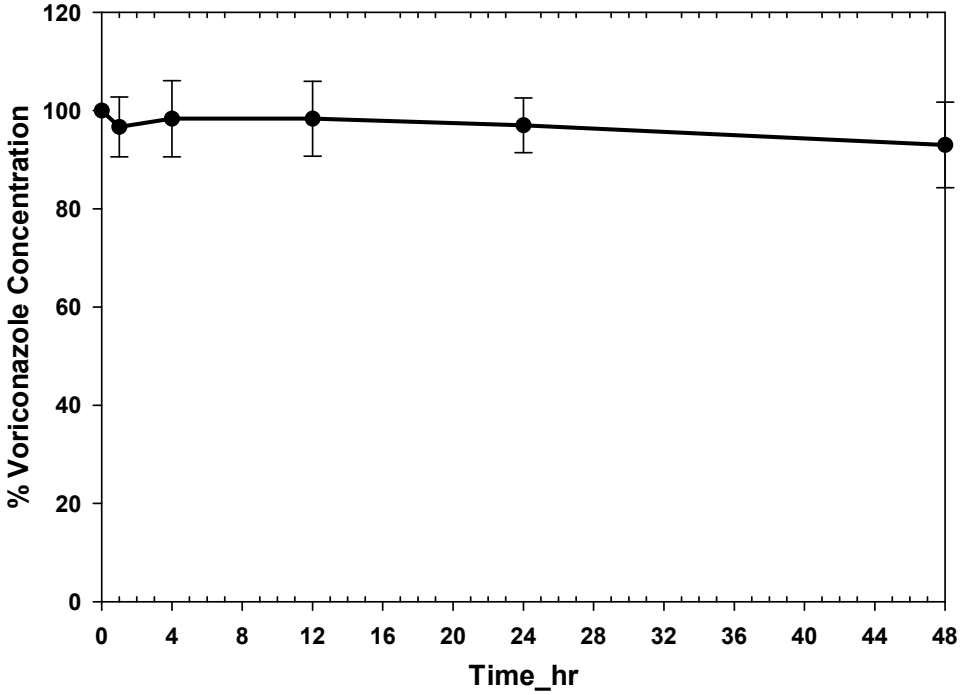

Figure 2-6. Voriconazole concentrations in culture media throughout the duration of time-kill experiments by HPLC: Representative data for a 48-h time-kill experiment with *C. glabrata* isolate 1 are presented. (Mean ± SD, n=3, without significant differences in results by ANOVA)

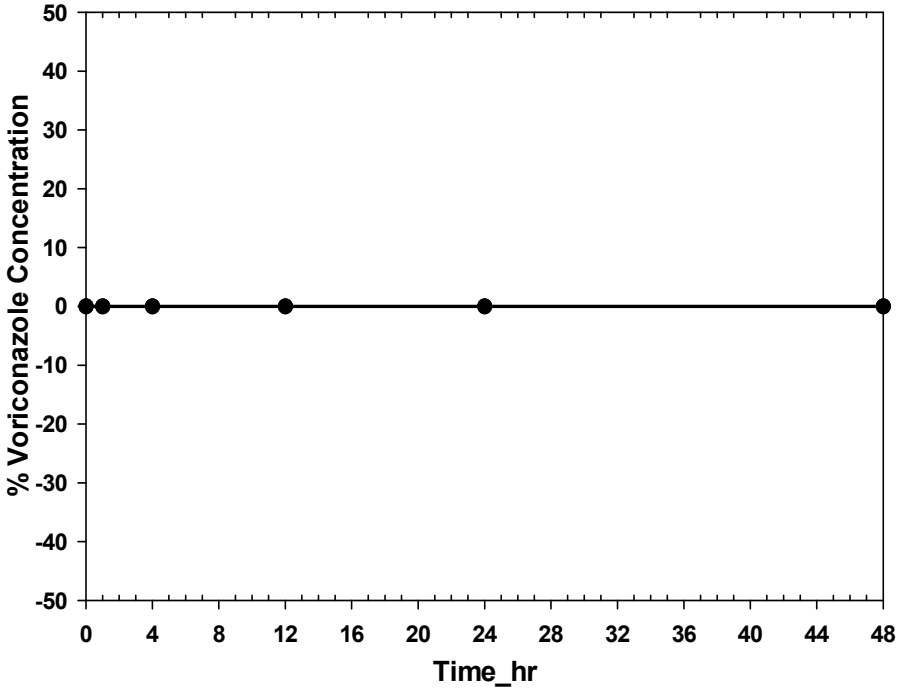

Figure 2-7. Voriconazole concentrations in PAFE experiments by HPLC: Representative data for a 48-h time-kill experiment with *C. glabrata* isolate 1 are presented. (Mean ± SD, n=3, without significant differences in results by ANOVA)

CHAPTER 3
APPLYING PHARMACOKINETIC/PHARMACODYNAMIC MATHEMATICAL MODEL ACCURATELY DESCRIBES THE ACTIVITY OF VORICONAZOLE AGAINST *CANDIDA* SPP. *IN VITRO*

Background

Time–kill curves are attractive tools for studying the pharmacodynamics of antimicrobial agents as they provide detailed information about antimicrobial efficacy as a function of both time and concentration [125]. Although time–kill curves can be studied using animal models of infection, *in vitro* models offer significant advantages in cost, convenience and time, as well as permitting direct investigation of the antimicrobial–microbe interaction in a controlled and reproducible manner [126]. The results of specific time–kill experiments can be accurately described using pharmacokinetic/ pharmacodynamic (PK/PD) mathematical models. By using PK data derived from clinical trials or animal experiments, mathematical models can be used to simulate the expected kill curves for different doses and dosing regimens of an antimicrobial agent [127]. As such, PK/PD modelling is a potentially powerful technique for defining optimal antimicrobial treatment strategies.

Voriconazole is a triazole antifungal agent effective in the treatment of patients with candidiasis [8, 65]. We recently performed time–kill experiments against two strains each of *Candida albicans*, *Candida parapsilosis* and *Candida glabrata* using voriconazole concentrations of 0.25×, 1×, 4× and 16× the minimum inhibitory concentration (MIC) and measuring colony counts at 0, 2, 4, 8, 12, 24, 36, 48, 60 and 72 h [22]. We demonstrated that voriconazole exhibited dose–response effects against all isolates, as higher concentrations resulted in enhanced killing of *Candida* spp. The ranges of maximal growth inhibition of isolates at concentrations of 1× and 4× MIC were −0.61

to −2.78 log and −0.53 to −2.99 log, respectively, compared with controls. At 16× MIC, the range of maximal growth inhibition was −0.58 to −4.15 log.

Specific Aim

The objectives of the present study were to develop a PK/PD mathematical model to fit our time–kill data and to use the model to simulate the expected kill curves for typical intravenous and oral dosing regimens.

Materials and Methods

Mathematical Modelling of Time–kill Data

The methods and results of antifungal susceptibility testing and time–kill curve experiments for voriconazole against *Candida* isolates were described previously [22]. During time–kill experiments, aliquots were taken at each time point and examined under the microscope to exclude hyphal formation or clumping. The voriconazole MICs against the isolates ranged from 0.008 to 0.19μg/mL. Fitting of time–kill data was performed with a series of models using the Scientist® 3.0 non-linear least squares regression software program (MicroMath, Salt Lake City, UT), as detailed in the Results and Discussion section. To determine the model that best fits the data for each isolate, graphs were visually inspected for goodness of fit and several criteria were considered, including model selection criterion (MSC), coefficient of determination (R^2) and the correlation between measured and calculated data points.

Simulations of Expected Time–kill Curves Using Human PK Data

PK parameters were extracted from published data sets of humans receiving voriconazole using XyExtract v2.5(Wilton and Cleide Pereira da Silva, Campina Grande, Para´ıba, Brazil) and the data were analyzed by WinNonlin 5.2 (Pharsight Corporation, Mountain View, CA) to describe the best absorption model. The Scientist® 3.0 software

program was then used to simulate plasma concentration–time profiles for multiple dosing of voriconazole (τ = 12 h). Simulations of expected kill curves for each isolate were made using steady-state PK parameters in the mathematical model that was shown earlier to best fit the time–kill data.

Statistical Analysis

When data are expressed as the mean ± SD, group mean differences were ascertained with analysis of variance (ANOVA). The results were considered significant if the probability of error was < 0.05.

Results

An Adapted Sigmoidal E_{max} Model Provides the Best Fit for Voriconazole Time–kill Data against Candida Isolates

Fitting of the time–kill data was started with a simple, commonly used E_{max} model [127].

$$\frac{dN}{dt} = \left(k_s - \frac{k_{max} \cdot C}{EC_{50} + C} \right) \cdot N \qquad (3\text{-}1)$$

In this model, dN/dt is the change in number of *Candida* as a function of time, k_s (h^{-1}) is the candidal growth rate constant in the absence of voriconazole, k_{max} (h^{-1}) is the maximum killing rate constant (i.e. maximum effect),EC_{50} (mg/L) is the concentration of voriconazole necessary to produce 50% of maximum effect, C (mg/L) is the concentration of voriconazole at any time (t) and N (colony-forming units (CFU)/mL) is the number of viable *Candida*. Since voriconazole concentrations did not change during the time–kill experiments, C was constant for the entire fitted time period.

The E_{max} model does not account for the fact that isolates have not yet reached the logarithmic growth phase at time zero or for the delay in the onset of killing by

voriconazole. To compensate for these delays, an exponential correction factor ($1-\exp^{-zt}$) was incorporated into the preceding model. Since the delays in the onset of candidal growth and voriconazole killing were not necessarily equivalent, they were assigned different adaptation rate constants (i.e. delay in growth = ($1-\exp^{-\alpha t}$) and delay in killing = ($1-\exp^{-\beta t}$)):

$$\frac{dN}{dt} = \left[k_s \cdot \left(1 - e^{-\alpha t}\right) - \left(\frac{k_{\max} \cdot C}{EC_{50} + C} \right) \cdot \left(1 - e^{-\beta t}\right) \right] \cdot N \qquad (3\text{-}2)$$

Model (2) was adapted by considering the maximum number of *Candida* (N_{max}), which potentially corrected for the limitations of space and nutrients that are inherent in *in vitro* systems:

$$\frac{dN}{dt} = \left[k_s \cdot \left(1 - \frac{N}{N_{\max}}\right) \cdot \left(1 - e^{-\alpha t}\right) - \left(\frac{k_{\max} \cdot C}{EC_{50} + C} \right) \cdot \left(1 - e^{-\beta t}\right) \right] \cdot N \qquad (3\text{-}3)$$

In the final model, a Hill factor (h) was incorporated, which modified the steepness of the slopes and smoothed the curves:

$$\frac{dN}{dt} = \left[k_s \cdot \left(1 - \frac{N}{N_{\max}}\right) \cdot \left(1 - e^{-\alpha t}\right) - \left(\frac{k_{\max} \cdot C^h}{EC_{50}{}^h + C^h} \right) \cdot \left(1 - e^{-\beta t}\right) \right] \cdot N \qquad (3\text{-}4)$$

The fitted time–kill curves of the six *Candida* isolates were generated using the different models in the absence of voriconazole (control) or in the presence of constant concentrations (mg/L) of voriconazole. In Model (4), Hill factor values ranging from 0 to 4 were tested. In general, the curve fittings for all PD data were acceptable. The best fits for each isolate were obtained using Model (4); the PD parameters and goodness of fit criteria were excellent for all voriconazole–*Candida* isolate pairings, with MSC≥2.46 and R^2 ≥0.95. The fitted curves for Model (4) are shown in Figure 3-2. The PD parameters of

voriconazole against the six *Candida* isolates and the goodness of fit criteria are presented in Table 3-1.

In time–kill experiments, PD effects can be described by at least three parameters: *k*s, the growth rate constant of the organism in the absence of drug; *k*max, the maximum killing rate constant of the drug against the organism; and EC50 (the concentration of drug necessary for 50% of its maximum effect) [125, 127]. The EC_{50} values calculated in the present study demonstrate that voriconazole was highly effective at easily achievable serum levels against each of the six *Candida* isolates (EC_{50} range 0.002–0.05 mg/L) (Table 3-1). Moreover, the rates of maximal killing by voriconazole were highly correlated with the growth rates of the isolates (Pearson's correlation coefficient = 0.9861). In other words, the data suggest that voriconazole achieved its highest kill rates against the most rapidly proliferating organisms.

Human PK Data for Voriconazole Can Be Used to Simulate Expected Time–kill Curves

Mathematical models can be used to simulate the expected kill curves for different doses and dosing regimens of antimicrobials by substituting the concentration term with PK parameters collected in vivo and accounting for protein binding [127]. To simulate time–kill curves that might be expected for voriconazole under typical dosing regimens, we first extracted PK parameters from published data sets of humans receiving the drug intravenously (3 mg/kg twice a day (bid)) and orally (200 mg bid) in steady-state [39]. Plasma concentration profiles for intravenous and oral dosing were found to be best characterized by two-compartment models of zero- and first-order absorption, respectively. Some of the PK parameters are listed in Table 3-2.

Applying the PK parameters for the two dosing regimens, we simulated plasma concentration–time profiles for multiple dosing of voriconazole (τ = 12 h), assuming plasma protein binding of 58% (Figure 3-2) [8]. We then used the steady-state

PK parameters to generate simulations for voriconazole activity against each of the *Candida* isolates in the present study (Figure 3-2). As shown, voriconazole showed fungistatic activity against all six strains. For five of the six strains, simulated kills were virtually identical for the intravenous and oral regimens. The exception was *C. parapsilosis* 2, for which the effects of intravenous dosing were greater. By collecting PK data for a range of voriconazole doses and dosing regimens during clinical trials or animal models, we should be able to use the mathematical model to predict treatment strategies that might be most effective against a given *Candida* isolate.

Discussion

A pharmacokinetic/pharmacodynamic (PK/PD) mathematical model was also developed in our studies to fit voriconazole time–kill data against *Candida* isolates *in vitro* and used the model to simulate the expected kill curves for typical intravenous and oral dosing regimens. Although PD studies comparing the efficacy of various voriconazole regimens against *Candida* isolates are feasible in animal models [32], they are laborious, expensive and complicated. *In vitro* models permit direct study of the interaction between fungi and fungal agents in a controlled and reproducible manner and allow direct comparisons of different agents and dosing strategies in a more convenient and faster way [126].

We have shown that it is feasible to describe precisely the time–kill activity of voriconazole against *Candida* isolates by using an adapted sigmoidal E_{max} model that corrects for delays in candidal growth and the onset of voriconazole activity, saturation of

the number of *Candida* that can grow in the *in vitro* system and the steepness of the concentration–response curve. We established the PK/PD models and simulated the expected voriconazole activity for typical intravenous and oral dosing regimens by using PK data collected *in vivo* and accounting for protein binding. A limitation of the present study design was that voriconazole concentrations were constant. In the future, we will characterize voriconazole–*Candida* interactions using a dynamic in vitro system in which drug concentrations change over time in a manner consistent with the PK profile in humans. Based on the success of the present study, it should also be feasible to model accurately the time–kill data for changing voriconazole concentrations. In conclusion, we demonstrated that the activity of voriconazole against *Candida* isolates can be accurately described using a mathematical model. We anticipate that this approach will be an efficient method for devising optimal voriconazole treatment strategies against candidiasis.

Table 3-1. Pharmacodynamic parameters and goodness of fit criteria against Candida isolates

Parameter(unit)	*C. abicans* ATCC90029	*C. abicans* SC5314	*C. glabrata* 1	*C. glabrata* 2	*C. parapsilosis* 1	*C. parapsilosis* 2
C (mg/L)	**0.002/0.008/0.032/0.128**	**0.003/0.012/0.048/0.192**	**0.0475/0.19/0.76/3.04**	**0.008/0.032/0.128/0.512**	**0.002/0.008/0.032/0.128**	**0.004/0.016/0.064/0.256**
K_s (h^{-1})	**0.28**	**0.87**	**0.24**	**0.26**	**0.22**	**0.66**
K_{max} (h^{-1})	**0.34**	**0.72**	**0.29**	**0.35**	**0.24**	**0.63**
EC_{50} (mg/L)	**0.0015**	**0.0030**	**0.05**	**0.0042**	**0.0066**	**0.012**
alpha	**1.24**	**0.19**	**0.14**	**0.58**	**0.26**	**0.072**
beta	**0.069**	**0.11**	**0.032**	**0.059**	**0.23**	**0.19**
N_{max} (CFU/mL)	**1.09E+07**	**1.21E+06**	**3.85E+06**	**6.57E+06**	**3.48E+07**	**6.95E+06**
h	**2.13**	**2.77**	**1.16**	**2.32**	**1.49**	**3.84**
MSC/R^2	**4.68/0.99**	**3.58/0.99**	**4.76/0.995**	**4.33/0.99**	**5.63/0.997**	**4.91/0.95**

k_s: fungal growth rate constant in the absence of voriconazole
k_{max}: maximum killing rate constant (maximum effect)
EC_{50}: concentration of voriconazole necessary to produce 50% of maximum effect
alpha: constant used to fit the initial lag phase for the growth
beta: constant used to fit the initial lag phase for the inhibition or killing
h: Hill factor
MSC: model selection criteria

Table 3-2. Steady-state pharmacokinetic parameters in plasma as calculated by two-compartment model analysis

Parameter (unit)	Dose regimen	
	200mg oral	3mg/kg/h *i.v.*
C_{max} (mg/L)	1.59	2.66
T_{max} (h)	1.72	1.00
α (h^{-1})	0.443	1.260
β (h^{-1})	0.139	0.120
F	0.9	1.0
CL/F (L/h)	17.9	14.2
Vd_{ss}/F (L)	98.9	109.7
Vd_{area}/F (L)	128.5	117.9

i.v.: intravenous
C_{max}: maximum concentration
T_{max}: time to C_{max}
α: macro rate constant associated with the distribution phase
β: macro rate constant associated with the elimination phase
F: bioavailability
CL/*F*: systemic clearance
Vd_{ss}/F: apparent volume of distribution at steady-state
Vd_{area}/F: apparent volume of distribution

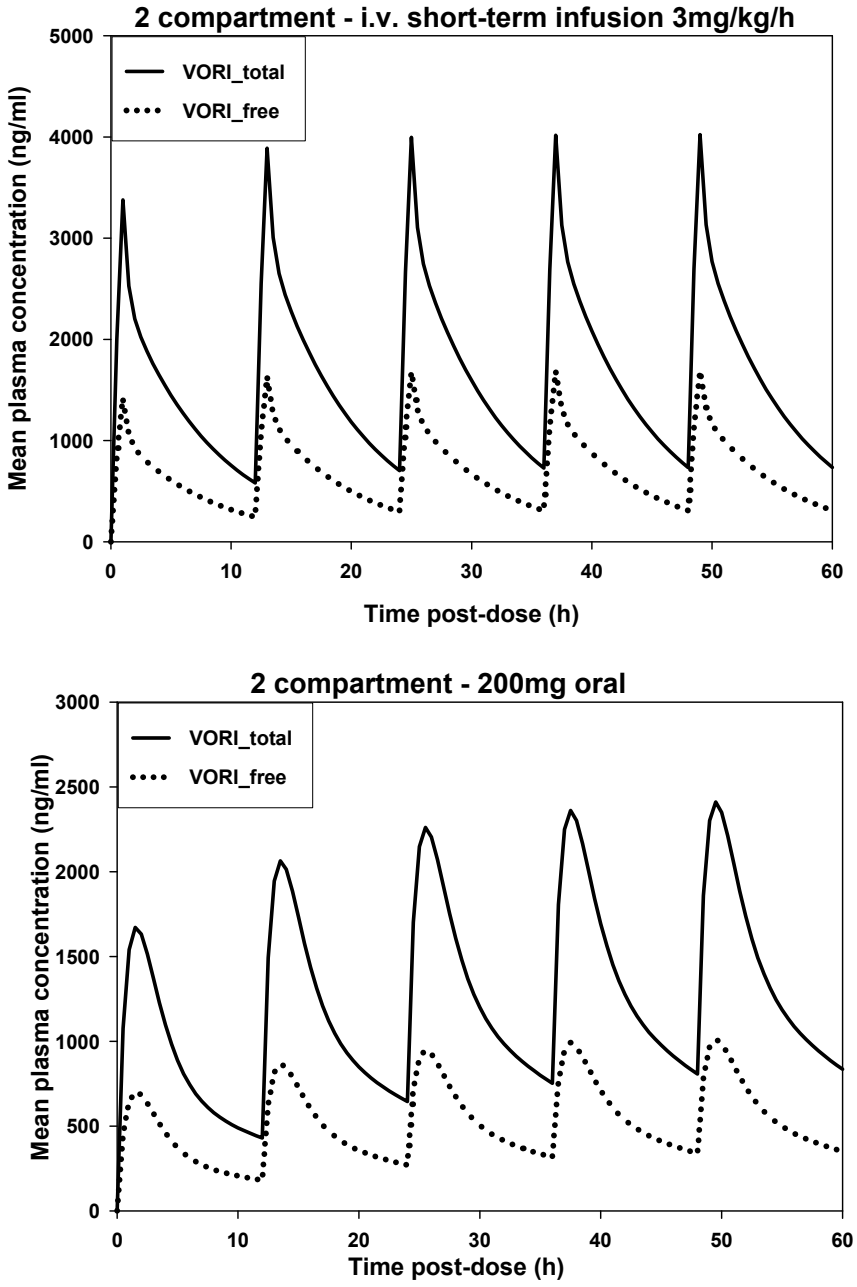

Figure 3-1. Plasma VOR concentration-time profiles simulated with a two-compartment PK model. (PK data were extracted from published paper[39]). Short-term intravenous (3mg/kg/h, bid, T=1h); Oral administration (200mg, bid, F=0.9); fb = 58%

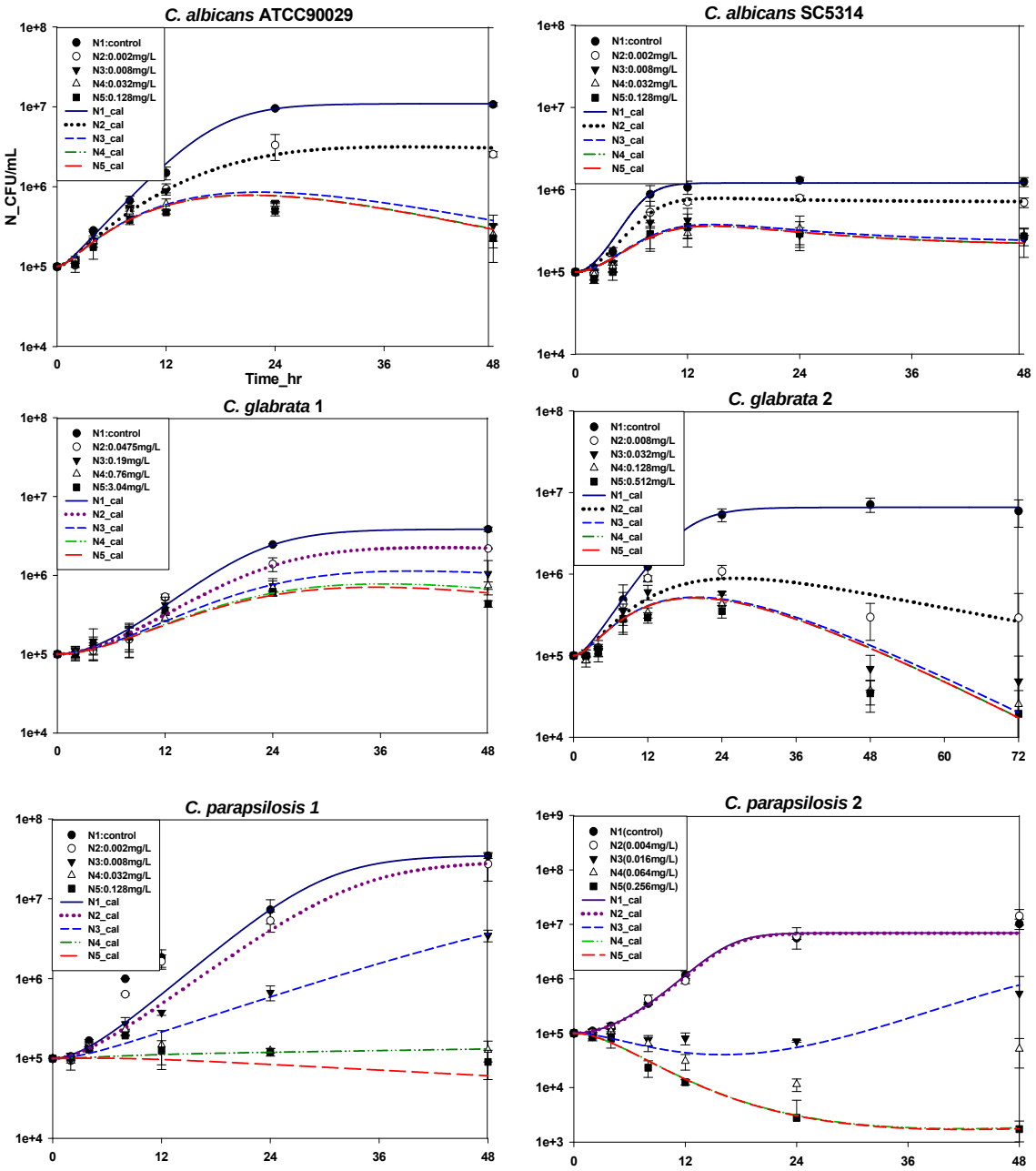

Figure 3-2. Fitted time-kill curves derived using the mathematical model for constant concentrations of voriconazole (Mean ± SD; n = 3 for *Candida albicans* ATCC90029 and n = 2 for the other strains, without significant differences in results by analysis of variance (ANOVA)). Voriconazole concentrations were 0×, 0.25×, 1×, 4× and 16× the minimum inhibitory concentrations (listed as N1-N5, respectively, in the individual figure legends).

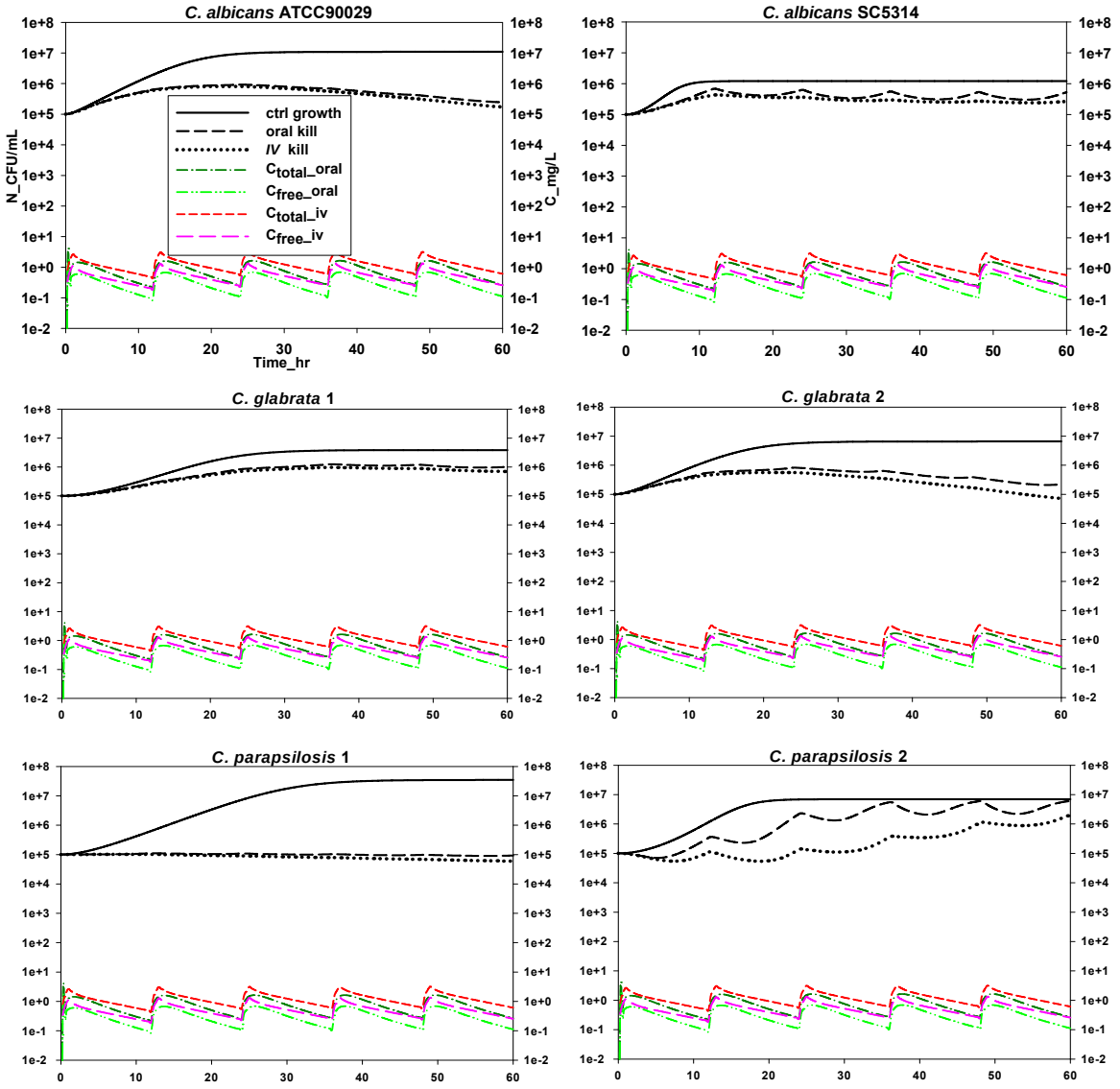

Figure 3-3. Simulations of candidal time–kills and plasma voriconazole concentration–time profiles. The simulations of time–kills are shown for short-term intravenous (*i.v.)* infusion (····) and oral dosing of voriconazole (---). Control growth is in the absence of drug (—). The simulated plasma concentration–time profiles for multiple doses of voriconazole (τ = 12 h) are shown for short-term i.v. infusion (τ = 1 h, infusion rate = 3 mg/kg/h, twice a day (bid)) and oral administration (200 mg, bid, F = 0.9). Free voriconazole concentrations were calculated assuming plasma protein binding level of 58%.

CHAPTER 4
PHARMACODYNAMIC STUDY IN DYNAMIC SYSTEM FOR DESCRIBING THE ACTIVITY OF VORICONAZOLE AGAINST *CANDIDA* SPP. *IN VITRO*

Background

Voriconazole is a lipophilic triazole antifungal agent that exhibits potent activity *in vitro* and *in vivo* against a variety of fungi including *Candida* spp., *Aspergillus* spp., *Cryptococcus neoformans*, *Blastomyces dermatitidis*, *Coccidioides immitis*, *Histoplasma capsulatum*, *Fusarium* spp. and *Penicillium marneffei* [41-43]. Using standard *in vitro* time-kill methodologies, we and others have shown that voriconazole exerts prolonged fungistatic activity and no post-antifungal effect against diverse *Candida* spp., including *C. albicans*, *C. glabrata* and *C. parapsilosis* [8, 22]. In a follow-up study, we developed a mathematical model that accurately described the activity of voriconazole against *Candida* spp. during time-kill experiments [102]. After identifying and validating the *in vitro* pharmacodynamic (PD) parameters derived from our experiments, we used pharmacokinetic (PK) data extracted from human data sets to simulate the expected kill curves *in vivo* for typical intravenous and oral dosing regimens of voriconazole. Indeed, by using PK data from human clinical trials or animal studies to simulate kill curves for different doses and dosing regimens of voriconazole or other antimicrobial agents, PK/PD modeling is potentially a powerful technique for defining optimal treatment strategies [127].

The major limitation of our earlier studies was that voriconazole concentrations remained constant over time at fixed multiples of the minimum inhibitory concentration (MIC) [22, 46, 102, 128, 129].

Specific Aim

The first objective of the present study was to develop a dynamic time-kill methodology in which voriconazole concentrations diminished in a manner consistent with the serum PK profile in humans. After we characterized the interaction between voriconazole and five *Candida*

isolates using the dynamic *in vitro* system, our objectives were to fit our mathematical model to the changing concentration kill-curves and to use human PK data to simulate expected kill curves *in vivo*.

Materials and Methods

Antifungal Agents

Stock solutions of voriconazole (Pfizer, New York, N.Y.) were prepared using sterile water. Stock solutions were separated into unit-of-use portions and stored at -80°C until used.

Test Isolates

Five strains were studied: 1 reference (*Candida albicans* ATCC 90029) and 4 clinical (2 *Candida glabrata* and 2 *Candida parapsilosis*).

Softwares

PK parameters were extracted from published data sets of humans receiving voriconazole using XyExtract v2.5(Wilton and Cleide Pereira da Silva, Campina Grande, Para´ıba, Brazil) and the data were analyzed by WinNonlin 5.2 (Pharsight Corporation, Mountain View, CA) to describe the best absorption model. The Scientist® 3.0 software program was then used to simulate plasma concentration–time profiles for multiple dosing of voriconazole (τ = 12 h).

Dynamic Model Design

In the infection model, the voriconazole was introduced as an intravenous bolus and was eliminated at constant rate according to the first order kinetics:

$$C = C_0 \cdot e^{-k_e t} \tag{4-1}$$

$$C = \frac{A}{V_0} \tag{4-2}$$

Where C_0 is the initial voriconazole concentration in the flask, t is the time that has elapsed since the loading of voriconazole, C is the voriconazole concentration at time t, and ke is the voriconazole elimination rate constant.

For any two points of time t,

$$C_1 = C_0 \cdot e^{-k_e t_1} \tag{4-3}$$

$$C_2 = C_0 \cdot e^{-k_e t_2} \tag{4-4}$$

$$C_1 = \frac{A_1}{V_0} \tag{4-5}$$

$$C_2 = \frac{A_2}{V_0} = \frac{A1 - C_1 \cdot \Delta V}{V_0} \tag{4-6}$$

From equations 4-3, 4-4, 4-5 and 4-6, equation 4-7 could be derived:

$$C_0 \cdot e^{-k_e t_1} - C_0 \cdot e^{-k_e t_2} = \frac{C_0 \cdot e^{-k_e t_1} \cdot \Delta V}{V_0} \tag{4-7}$$

Reconstitute equation 4-7,

$$\Delta V = V_0 \cdot (1 - e^{-k_e (t_1 - t_2)}) \tag{4-8}$$

As $\Delta t = t_1 - t_2$,

$$\Delta V = V_0 \cdot (1 - e^{-k_e \cdot \Delta t}) \tag{4-9}$$

Where V_0 is the initial volume of medium in the flask, and Δt is the time period of replacing voriconazole-free medium.

The K_e could be calculated using a certain half-life ($t_{1/2}$):

$$K_e = \frac{\ln 2}{t_{1/2}} \tag{4-10}$$

As shown in Figure 4-1, every 2 hours (Δt), 4.13 ml (ΔV) of voriconazole containing medium were replaced by the same volume of voriconazole-free medium in order to simulate an *in vivo* half-life of 6 hours.

Time-kill Experiments in the Dynamic Model

The MICs of voriconazole against a *C. albicans* reference strain (ATCC 90029) and *C. glabrata* and *C. parapsilosis* clinical isolates (two each), as determined by E-test and the Clinical and Laboratory Standards Institute (formerly NCCLS) broth microdilution method, were consistent with previous reports [22, 46, 123]; values were within two-fold agreement by the two methods (Table 2-1). In our previous time-kill experiments, voriconazole at constant concentrations of 1×, 4× and 16×MIC inhibited growth of the isolates in a dose-dependent manner [22]. The dynamic time-kill experiments were performed in duplicate against each isolate (inocula of 1×10^5 to 5×10^5 CFU/mL). Colonies from 24-hour cultures on Sabouraud dextrose agar (SDA) plates were suspended in 9 mL of sterile water and adjusted to UV absorbance of 0.84-0.86 at 535nm; 200μL of the suspension were added to 20 mL (V_0) of RPMI 1640 (Sigma Chemical Co.) buffered to a pH of 7.0 with MOPS (morpholinepropanesulfonic acid; RPMI 1640 medium) without voriconazole, and incubated at 35°C with continuous agitation. After 2 hours pre-incubation, voriconazole was added at starting concentrations of 0.25×, 1×, 4×, or 16×MIC. The drug was introduced as a bolus and eliminated at constant rate according to first order kinetics which was described previously. Prior to the removal of voriconazole-containing medium at each time point, 100 μL aliquots were obtained from each solution, serially diluted, and plated on SDA plates to enumerate CFUs. Voriconazole concentrations during time-kill experiments were verified by serial HPLC measurements [22].

Results

Voriconazole exhibited dose-response effects against all Candida isolates during the dynamic time-kill experiments, as higher starting concentrations resulted in greater growth inhibition or killing (Figures 4-2). The time-kill data in the dynamic time-kill experiments for individual isolates were listed in the tables of Table 4-1, 4-2, 4-3, 4-4, 4-5. Of note, starting concentrations of 4× and 16×MIC resulted in growth inhibition or killing of all five isolates; results with 16×MIC starting concentrations were clearly superior to 4×MIC starting concentrations for four isolates (*C. albicans* ATCC90029, *C. glabrata* 2, *C. parapsilosis* 1, and *C. parapsilosis* 2). On balance, the results were consistent with those observed for constant concentrations of 4× and 16×MIC against the same isolates in our earlier time-kill study [22]. In the present study, results with 1× MIC starting concentrations were significantly inferior to 4× and 16×MIC against all five isolates (Figure 4-2). In fact, 1× MIC starting concentrations caused slight growth inhibition of only two strains (*C. albicans* ATCC90029 and *C. glabrata* 1); for the remaining three isolates, the 1× MIC growth curves did not differ significantly from controls grown in the absence of voriconazole. These results differed from constant concentrations of 1× MIC in the previous study, for which growth inhibition and kills of all isolates were significantly compared to controls. In fact, growth inhibition and kills at constant concentrations of 1× MIC approached those seen at constant concentrations of 4× and 16×MIC against three isolates (*C. albicans* ATCC90029, *C. glabrata* 1 and *C. glabrata* 2).

We used our previously developed sigmoidal E_{max}-model to fit time-kill data for each voriconazole-Candida pairing in the dynamic experiments [102, 127]. The model accounts for delays in the onset of both Candida growth and voriconazole-induced kill, the saturation of Candida growth, and incorporates a Hill factor that modifies the steepness of the slopes and smoothes the curves:

$$\frac{dN}{dt} = \left[k_s \cdot \left(1 - \frac{N}{N_{\max}} \right) \cdot \left(1 - e^{-\alpha t} \right) - \left(\frac{k_{\max} \cdot C^h}{EC_{50}{}^h + C^h} \right) \cdot \left(1 - e^{-\beta t} \right) \right] \cdot N \qquad (4\text{-}11)$$

In this model, dN/dt is the change in number of *Candida* as a function of time, k_s (h^{-1}) is the candidal growth rate constant in the absence of voriconazole; k_{max} (h^{-1}) is the maximum killing rate constant; EC_{50} (mg/L) is the concentration of voriconazole necessary to produce 50% of maximum effect; C (mg/L) is the concentration of voriconazole at any time (t); N (CFU/mL) is the number of viable *Candida*; α is the constant used to fit the initial lag phase for the growth; β is the constant used to fit the initial lag phase for the inhibition or killing; and h is the Hill factor.

Simultaneous fitting of the model to the changing concentration kill-curves was performed using Scientist3.0 non-linear least squares regression software program (MicroMath, Salt Lake City, UT) as previously described [102]. Graphs were visually inspected for quality of fit and several criteria were considered, including model selection criterion (MSC), coefficient of determination (R^2) and the correlation between measured and calculated data points. For each isolate, goodness of fit criteria was excellent, with MSC ≥ 2.71 and $R^2 \geq 0.97$ (Table 4-6, Figure 4-3). Similarly, PD parameters were excellent (Table 4-6). The EC_{50} values (drug concentrations necessary for 50% of maximum effect) indicate that voriconazole was highly effective against each of the five isolates at easily achievable serum levels (range: 0.005 to 0.08 mg/L); these values were comparable to those obtained in the earlier constant concentration experiments (range: 0.0015 to 0.05 mg/L). As in the previous study, voriconazole achieved its highest rates of kill against the most rapidly proliferating isolates.

To simulate the expected kill curves for different doses and dosing regimens of voriconazole, we substituted the concentration term in our model with PK parameters collected

in vivo [39, 102]. PK data were extracted from published data sets of humans receiving voriconazole intravenously (3 mg/kg twice a day (bid)) or orally (200 mg bid) using XyExtract v2.5 (Wilton and Cleide Pereira da Silva, Campina Grande, Paraíba, Brazil). Plasma concentration profiles for intravenous and oral dosing were best characterized by two-compartment models of zero- and first-order absorption, respectively (analysis by WinNonlin 5.2, Pharsight Corporation, Mountain View, CA). PK parameters for the two dosing regimens are presented in Table 2. These values were used to simulate the respective voriconazole plasma concentration-time profiles (τ = 12 h; Scientist® 3.0 software program) (Figure 4-4). The PK parameters for two dosing regimens were then applied to the E_{max}-model to simulate the expected *in vivo* kill curves, assuming plasma protein binding of 58% [8].

Simultaneous fitting of the identified model to the changing concentration kill-curves was performed in Scientist® 3.0 non-linear least squares regression software program (MicroMath, Salt Lake City, UT) as previously described [102]. To determine the model that best fits the data for each isolate, graphs were visually inspected for quality of fit and several criteria were considered, such as model selection criterion (MSC), coefficient of determination (R^2) and the correlation between measured and calculated data points.

In the current study, we employed a dynamic in vitro model to determine time-kill curves of voriconazole against C. *albicans* reference strain, C. *glabrata* and C. *parapsilosis* bloodstream isolates (2 each) at ×0.25, ×1, ×4 and 16×MIC. The MICs were determined by Etest and the Clinical and Laboratory Standards Institute (formerly NCCLS) broth microdilution method [22, 46, 123], and were within twofold agreement (Table 2-1).

We characterized voriconazole-Candida interactions using the dynamic *in vitro* system in which drug concentrations change over time in a manner consistent with the PK profile in

humans [39, 102] (Table 3-2). PK parameters were extracted from published data sets of human receiving voriconazole using XyExtract v2.5 (Wilton and Cleide Pereira da Silva, Campina Grande, Paraíba, Brazil) and the data were analyzed by WinNonlin 5.2 (Pharsight Corporation, Mountain View, CA) to describe the best absorption model. The Scientist® 3.0 software program was then used to simulate plasma concentration-time profiles for multiple dosing of voriconazole (τ = 12 h). Simulations of expected kill curves for each isolate were made using the PK parameters for two dosing regimens in the Emax-model as described above, assuming plasma protein binding of 58% [8].

As shown in Figure 4-4, the simulated kill curves predicted that voriconazole would exert prolonged fungistatic activity against all five isolates, resulting in diminishing Candidal concentrations over time. Indeed, for three isolates (*C. albicans* ATCC90029, *C. parapsilosis* 1 and *C. parapsilosis* 2), reductions from starting inocula over 60 hours were predicted to exceed 2-logs. Of note, kill curves for four isolates were almost identical for the IV and oral dosing regimens. The exception was *C. parapsilosis* 2, for which the effects of IV dosing were predicated to be greater than oral dosing.

Discussion

Our study is noteworthy for several reasons. To our knowledge, this is the first report of time-kill experiments against Candida isolates using an *in vitro* method that mimics changing voriconazole concentrations *in vivo* rather than testing constant concentrations. The most striking finding from our study was that starting voriconazole concentrations of 1× MIC were largely ineffective at inhibiting the growth of isolates, whereas starting concentrations of both 4× and 16×MIC significantly inhibited all isolates. The data from the dynamic model, therefore, suggest that clinicians should aim for peak serum concentrations of voriconazole ≥ 4×MIC in treating their patients with candidemia. Since the median of maximum voriconazole plasma

concentrations in clinical trials was 3.79 μg/ml [124], a target peak concentration ≥ 4×MIC fits well with the recently proposed breakpoint MICs ≤ 1 μg/mL for voriconazole susceptibility [122].

Second, we demonstrated that it is possible to accurately fit the data from our dynamic model using an adapted E_{max} mathematical model. Moreover, we used the mathematical model to simulate expected kill curves for typical dosing regimens of voriconazole by substituting the concentration term with PK data collected *in vivo* and accounting for protein binding. In this regard, our approach of combining *in vitro* time-kill data with existing *in vivo* PK data might serve as a model for future studies to define the optimal use of antifungal agents. Although PD studies comparing the efficacy of various regimens of voriconazole and other antifungals are feasible in animal models [32], they are complicated, laborious and expensive. *In vitro* time-kills permit direct study of the interaction between antifungals and fungi in a controlled and reproducible manner, and they allow direct comparisons of different agents and dosing strategies in a more convenient, faster and cheaper way that does not expend animal lives [126]. Finally, our data predict that typical IV and oral dosing regimens of voriconazole are comparable in their ability to kill most Candida isolates *in vitro*. As such, the data lend support to the practice of switching to oral voriconazole to complete a course of therapy of invasive candidiasis among patients who have exhibited clinical and microbiologic responses to initial parenteral antifungal therapy.

In conclusion, we have shown that the PK/PD relationship of voriconazole against Candida spp. can be accurately modeled in a dynamic *in vitro* system that mimics *in vivo* conditions. PK/PD modeling approaches such as ours merit further investigation as tools to define optimal treatment regimens of voriconazole and other antifungal agents against candidiasis.

Table 4-1. Voriconazole against *Candida albicans* ATCC90029 in changing concentration experiments (Data of CFU/mL, Mean ± SD, n = 3)

Time (h)	Control	SD	0.25×MIC	SD	1×MIC	SD	4×MIC	SD	16×MIC	SD
0	1.00E+05	0.00E+00	1.00E+05	0.00E+00	1.00E+05	0.00E+00	1.00E+05	0.00E+00	1.00E+05	0.00E+00
2	2.13E+05	5.98E+04	1.66E+05	4.04E+04	1.63E+05	3.32E+04	1.85E+05	3.86E+04	1.72E+05	5.24E+04
4	3.25E+05	7.81E+04	2.72E+05	5.40E+04	2.84E+05	2.16E+04	2.50E+05	3.81E+04	2.42E+05	8.13E+04
6	4.62E+05	8.61E+04	4.25E+05	8.52E+04	3.89E+05	4.60E+04	2.92E+05	4.01E+04	2.96E+05	6.86E+04
8	6.83E+05	1.51E+05	6.25E+05	7.77E+04	4.46E+05	6.18E+04	3.30E+05	7.16E+04	1.62E+05	2.58E+03
10	1.06E+06	1.67E+05	9.69E+05	1.08E+05	8.45E+05	9.47E+04	2.00E+05	1.71E+04	7.80E+04	3.92E+03
12	1.88E+06	2.36E+05	1.94E+06	5.03E+05	9.42E+05	7.51E+04	1.27E+05	3.16E+03	3.03E+04	4.35E+03
14	2.53E+06	5.20E+05	2.67E+06	6.74E+05	1.04E+06	1.85E+04	9.23E+04	6.31E+03	2.13E+04	6.21E+03
16	4.71E+06	1.62E+06	3.66E+06	1.54E+06	1.38E+06	2.71E+05	7.99E+04	1.39E+04	1.86E+04	4.58E+03
18	7.05E+06	3.85E+06	6.03E+06	2.85E+06	1.91E+06	3.47E+05	7.24E+04	1.83E+04	1.18E+04	2.54E+03
20	9.43E+06	1.68E+06	8.21E+06	1.83E+06	2.46E+06	2.00E+05	6.83E+04	1.41E+04	1.07E+04	1.99E+03
22	1.11E+07	2.89E+06	9.34E+06	2.91E+06	3.36E+06	3.72E+05	4.04E+04	9.00E+03	9.42E+03	1.10E+03
24	1.45E+07	1.48E+06	1.15E+07	7.47E+05	3.82E+06	4.91E+05	4.42E+04	5.10E+03	1.10E+04	2.96E+03

Table 4-2. Voriconazole against *Candida glabrata* 1 in changing concentration experiments (Data of CFU/mL, Mean ± SD, n = 2)

Time (h)	Control	SD	0.25×MIC	SD	1×MIC	SD	4×MIC	SD	16×MIC	SD
0	1.00E+05	0.00E+00	1.00E+05	0.00E+00	1.00E+05	0.00E+00	1.00E+05	0.00E+00	1.00E+05	0.00E+00
2	1.42E+05	1.67E+04	1.17E+05	2.07E+04	1.29E+05	2.37E+03	1.04E+05	1.04E+04	1.04E+05	7.22E+03
4	2.04E+05	1.58E+04	1.66E+05	1.06E+04	1.95E+05	2.68E+04	1.64E+05	5.69E+04	1.68E+05	4.36E+04
6	2.59E+05	5.81E+04	2.29E+05	8.03E+03	2.49E+05	8.48E+04	1.87E+05	5.75E+04	1.88E+05	4.00E+04
8	3.27E+05	4.91E+04	2.72E+05	5.58E+04	2.60E+05	8.17E+04	2.13E+05	6.09E+04	1.87E+05	1.67E+04
10	3.90E+05	1.17E+05	2.96E+05	4.97E+04	2.92E+05	1.07E+05	2.54E+05	7.58E+04	2.01E+05	3.16E+04
12	6.18E+05	2.36E+05	5.50E+05	1.47E+05	4.60E+05	1.73E+05	3.59E+05	7.56E+04	3.34E+05	7.96E+04
14	9.20E+05	9.91E+04	1.01E+06	4.91E+04	7.20E+05	4.30E+04	3.58E+05	1.45E+04	3.65E+05	8.58E+04
16	1.32E+06	2.05E+04	1.13E+06	8.66E+04	8.32E+05	3.31E+04	5.05E+05	1.15E+05	4.40E+05	9.53E+02
18	1.90E+06	2.96E+04	1.48E+06	1.88E+05	1.06E+06	2.52E+04	5.69E+05	6.91E+04	4.46E+05	1.37E+03
20	2.66E+06	2.28E+05	1.60E+06	2.40E+04	1.19E+06	9.47E+04	5.57E+05	5.27E+04	4.64E+05	4.67E+02
22	4.03E+06	8.75E+05	2.37E+06	3.97E+05	1.70E+06	2.11E+04	5.38E+05	3.66E+04	4.01E+05	1.39E+04
24	4.13E+06	7.98E+05	2.97E+06	6.44E+05	1.76E+06	5.27E+04	5.60E+05	1.68E+04	3.89E+05	1.40E+04

Table 4-3. Voriconazole against *Candida glabrata* 2 in changing concentration experiments (Data of CFU/mL, Mean ± SD, n = 2)

Time (h)	Control	SD	0.25×MIC	SD	1×MIC	SD	4×MIC	SD	16×MIC	SD
0	1.00E+05	0.00E+00	1.00E+05	0.00E+00	1.00E+05	0.00E+00	1.00E+05	0.00E+00	1.00E+05	0.00E+00
2	1.57E+05	5.31E+04	1.31E+05	1.09E+04	1.41E+05	2.86E+03	1.10E+05	1.18E+04	1.21E+05	9.25E+02
4	2.21E+05	1.58E+04	1.79E+05	1.08E+04	2.27E+05	2.20E+04	1.82E+05	7.21E+03	1.69E+05	4.62E+04
6	3.07E+05	7.51E+04	2.61E+05	3.51E+04	3.79E+05	8.15E+04	2.42E+05	8.49E+04	2.07E+05	5.75E+04
8	4.35E+05	1.20E+05	3.84E+05	2.51E+04	4.21E+05	9.94E+04	3.20E+05	9.63E+04	2.40E+05	1.87E+04
10	5.43E+05	8.13E+04	5.41E+05	1.96E+03	5.96E+05	1.72E+05	4.04E+05	9.96E+04	3.06E+05	4.68E+04
12	9.80E+05	4.67E+05	7.28E+05	7.96E+04	6.89E+05	1.70E+05	4.28E+05	7.68E+04	3.33E+05	4.29E+04
14	1.24E+06	2.20E+05	1.07E+06	5.29E+01	8.48E+05	2.28E+05	4.48E+05	8.55E+04	3.53E+05	3.85E+04
16	2.22E+06	8.49E+05	1.81E+06	3.12E+05	1.50E+06	4.50E+05	7.17E+05	2.06E+05	4.55E+05	1.12E+04
18	3.54E+06	1.21E+06	2.80E+06	1.03E+06	2.52E+06	9.34E+05	7.77E+05	1.56E+05	5.06E+05	1.37E+05
20	4.40E+06	1.27E+06	3.42E+06	8.45E+05	3.11E+06	8.76E+05	8.36E+05	1.72E+05	4.93E+05	9.74E+04
22	5.80E+06	2.40E+06	4.87E+06	1.16E+06	3.30E+06	8.54E+05	7.65E+05	1.87E+05	4.45E+05	7.21E+04
24	5.95E+06	1.77E+06	5.54E+06	1.46E+06	3.42E+06	8.15E+05	7.89E+05	2.01E+05	4.32E+05	3.21E+04

Table 4-4. Voriconazole against Candida parapsilosis 1 in changing concentration experiments (Data of CFU/mL, Mean ± SD, n = 2)

Time (h)	Control	SD	0.25×MIC	SD	1×MIC	SD	4×MIC	SD	16×MIC	SD
0	1.00E+05	0.00E+00	1.00E+05	0.00E+00	1.00E+05	0.00E+00	1.00E+05	0.00E+00	1.00E+05	0.00E+00
2	1.86E+05	7.74E+04	1.89E+05	1.03E+04	2.06E+05	4.45E+04	1.80E+05	4.99E+04	1.72E+05	4.79E+04
4	4.80E+05	2.20E+05	3.66E+05	2.91E+04	3.87E+05	3.68E+04	4.18E+05	2.75E+04	2.73E+05	9.65E+04
6	8.96E+05	3.56E+05	6.49E+05	4.19E+04	6.16E+05	4.00E+03	4.96E+05	9.34E+04	3.87E+05	1.77E+05
8	1.70E+06	4.70E+05	1.46E+06	1.08E+05	9.61E+05	3.02E+05	1.88E+05	3.16E+04	1.64E+05	7.10E+04
10	2.43E+06	4.01E+05	2.30E+06	4.47E+05	1.60E+06	3.22E+05	1.44E+05	6.45E+03	7.09E+04	1.95E+04
12	3.60E+06	1.38E+06	3.63E+06	2.02E+06	3.02E+06	1.29E+06	1.11E+05	2.48E+04	3.27E+04	8.60E+03
14	5.88E+06	1.88E+06	5.35E+06	2.58E+05	4.71E+06	2.37E+06	1.37E+05	1.23E+04	4.42E+04	1.74E+04
16	8.48E+06	2.81E+06	8.55E+06	1.99E+05	6.44E+06	2.76E+06	1.71E+05	2.10E+04	5.59E+04	2.58E+04
18	1.06E+07	2.20E+06	1.21E+07	2.89E+06	8.27E+06	2.81E+06	1.64E+05	4.07E+04	4.54E+04	2.31E+04
20	1.54E+07	2.45E+06	1.43E+07	1.46E+06	1.13E+07	2.20E+06	2.16E+05	9.19E+03	5.28E+04	2.01E+04
22	1.89E+07	4.79E+06	1.27E+07	1.17E+05	1.11E+07	3.23E+06	3.20E+05	8.26E+04	5.73E+04	2.71E+04
24	2.27E+07	3.06E+05	1.67E+07	7.17E+06	1.37E+07	3.39E+06	5.32E+05	2.16E+05	5.95E+04	2.56E+04

Table 4-5. Voriconazole against Candida parapsilosis 2 in changing concentration experiments (Data of CFU/mL, Mean ± SD, n = 2)

Time (h)	Control	SD	0.25×MIC	SD	1×MIC	SD	4×MIC	SD	16×MIC	SD
0	1.00E+05	0.00E+00	1.00E+05	0.00E+00	1.00E+05	0.00E+00	1.00E+05	0.00E+00	1.00E+05	0.00E+00
2	1.85E+05	3.82E+04	1.63E+05	4.84E+04	1.35E+05	4.03E+03	1.84E+05	8.69E+04	1.33E+05	7.26E+04
4	2.58E+05	3.30E+04	2.75E+05	4.05E+04	2.37E+05	5.48E+04	1.19E+05	3.61E+04	5.66E+04	4.88E+03
6	3.80E+05	1.86E+05	3.07E+05	1.21E+05	3.60E+05	1.76E+05	1.06E+05	4.04E+04	5.40E+04	1.47E+04
8	5.20E+05	2.29E+05	6.18E+05	1.21E+05	6.14E+05	2.69E+05	1.07E+05	3.22E+04	2.86E+04	3.83E+03
10	1.62E+06	4.52E+05	1.59E+06	2.18E+04	1.23E+06	3.62E+05	8.58E+04	5.19E+03	2.22E+04	1.35E+04
12	2.32E+06	3.79E+04	2.51E+06	4.20E+05	1.87E+06	2.45E+05	8.59E+04	4.97E+04	1.22E+04	6.37E+03
14	2.23E+06	3.06E+05	2.74E+06	3.13E+04	2.97E+06	4.30E+03	9.11E+04	4.51E+04	1.17E+04	1.35E+03
16	3.09E+06	5.82E+05	2.96E+06	5.50E+05	2.86E+06	2.18E+05	1.67E+05	9.81E+03	1.44E+04	2.70E+02
18	4.16E+06	1.28E+06	5.42E+06	2.64E+06	4.25E+06	1.47E+06	2.97E+05	5.19E+04	1.16E+04	4.84E+03
20	4.57E+06	1.12E+06	5.23E+06	1.25E+05	4.19E+06	1.05E+06	3.50E+05	5.63E+04	9.13E+03	3.80E+03
22	5.23E+06	4.25E+05	5.47E+06	8.45E+05	4.86E+06	6.69E+05	4.97E+05	2.07E+05	1.63E+04	7.84E+03
24	5.73E+06	1.41E+06	6.83E+06	1.86E+06	3.79E+06	4.23E+05	7.40E+05	3.68E+05	1.29E+04	6.77E+03

Table 4-6. Pharmacodynamic parameters and goodness of fit criteria against Candida isolates in the dynamic infection model

Parameter(unit)	***C. abicans* ATCC90029**	***C. glabrata* 1**	***C. glabrata* 2**	***C. parapsilosis* 1**	***C. parapsilosis* 2**
C (mg/L)[a]	**0.002/0.008/0.032/0.128**	**0.0475/0.19/0.76/3.04**	**0.008/0.032/0.128/0.512**	**0.002/0.008/0.032/0.128**	**0.004/0.016/0.064/0.256**
$\mathbf{K_s}$ (h^{-1})	**0.29**	**0.17**	**0.19**	**0.32**	**0.30**
$\mathbf{K_{max}}$ (h^{-1})	**0.45**	**0.27**	**0.38**	**0.49**	**0.50**
$\mathbf{EC_{50}}$ (mg/L)	**0.005**	**0.074**	**0.0810**	**0.007**	**0.017**
α	**1.21**	**5.55**	**6.98**	**9.81**	**9.34**
β	**0.556**	**0.061**	**0.085**	**0.25**	**0.70**
$\mathbf{N_{max}}$ (CFU/mL)	**1.65E+07**	**1.87E+07**	**2.48E+07**	**1.96E+07**	**5.88E+06**
h	**1.42**	**0.86**	**0.89**	**1.79**	**2.86**
MSC/R^2	**3.58/0.98**	**3.68/0.99**	**2.71/0.97**	**3.19/0.98**	**3.08/0.98**

C_{max}: maximum voriconazole concentration
k_s: fungal growth rate constant in the absence of voriconazole
k_{max}: maximum killing rate constant (maximum effect)
EC_{50}: concentration of voriconazole necessary to produce 50% of maximum effect
α: constant used to fit the initial lag phase for the growth
β: constant used to fit the initial lag phase for the inhibition or killing
h: Hill factor
MSC: model selection criteria

[a] Values of voriconazole concentrations of 0.25×, 1×, 4× and 16× MIC, respectively.

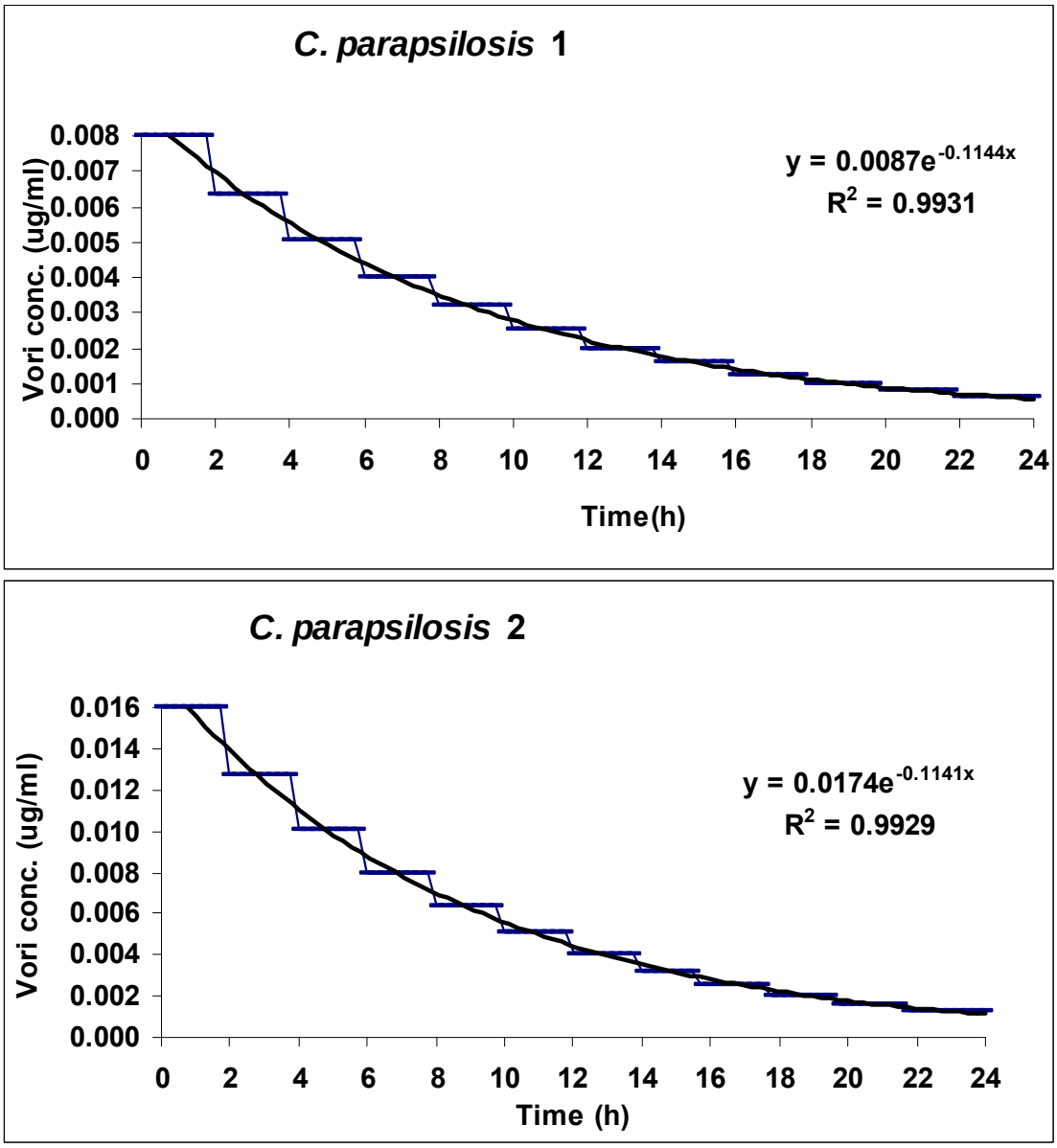

Figure 4-1. Concentration elimination curve of voriconazole in the dynamic infection model

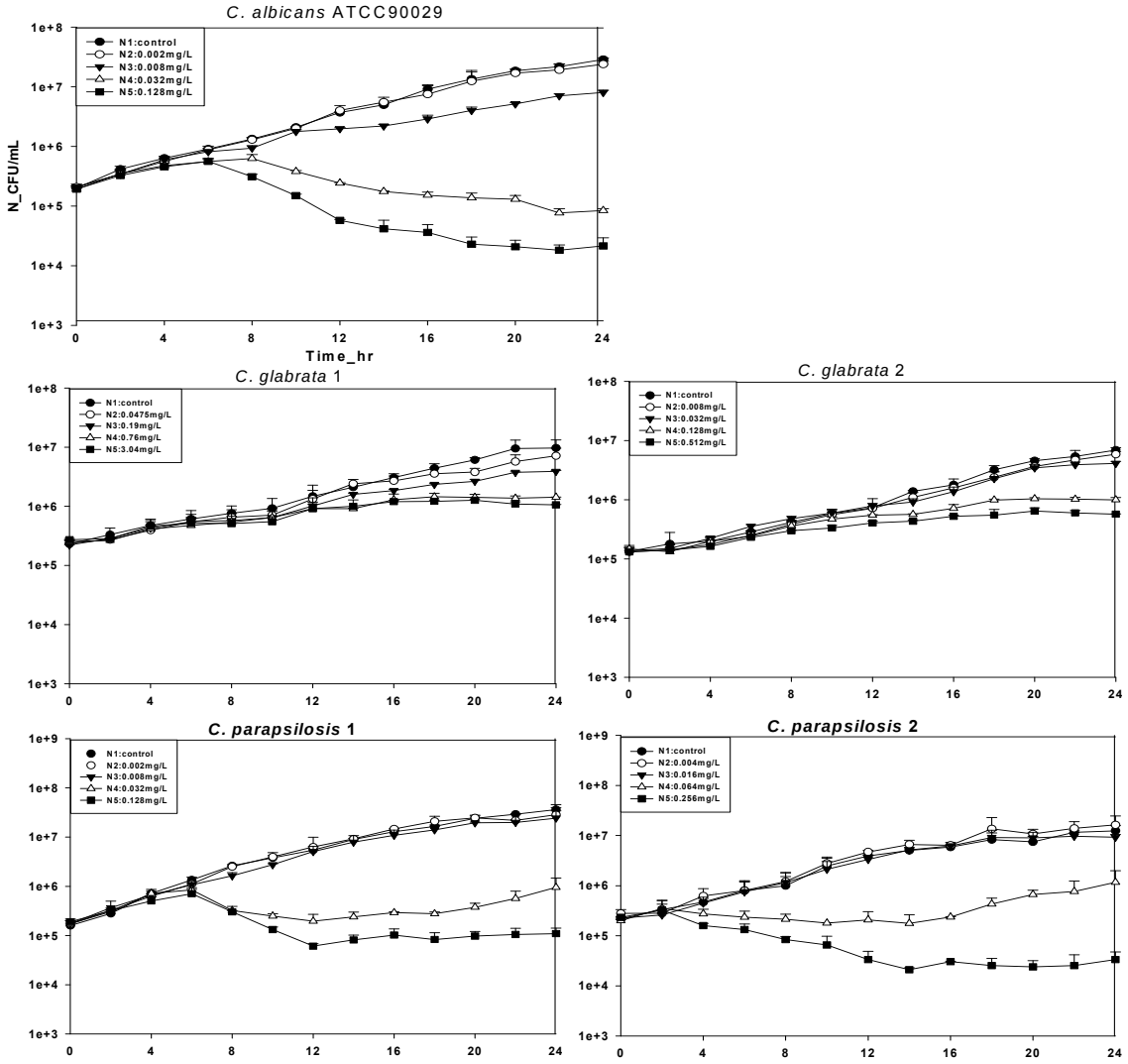

Figure 4-2. Time-kill curves from the dynamic *in vitro* model (Mean ± SD; n=3, without significant differences in results by ANOVA). Voriconazole concentrations were 0×, 0.25×, 1×, 4× and 16×MICs (listed as N1-N5 in the individual figure legends).

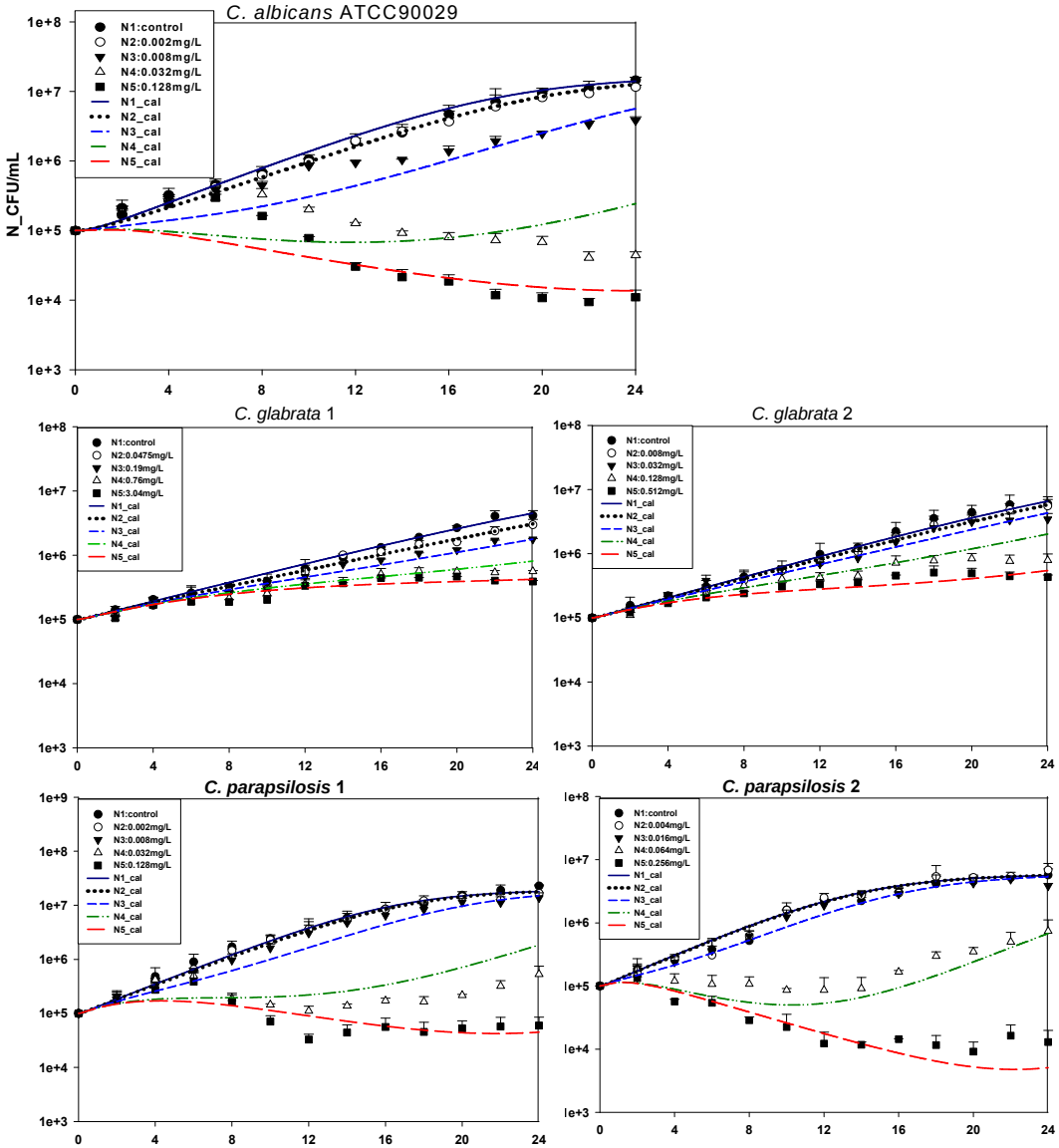

Figure 4-3. Fitted time-kill curves were derived by our mathematical model for changing concentrations of voriconazole (Mean ± SD; n=3, without significant differences in results by ANOVA). Voriconazole concentrations were 0×, 0.25×, 1×, 4× and 16×MICs (listed as N1-N5 in the individual figure legends).

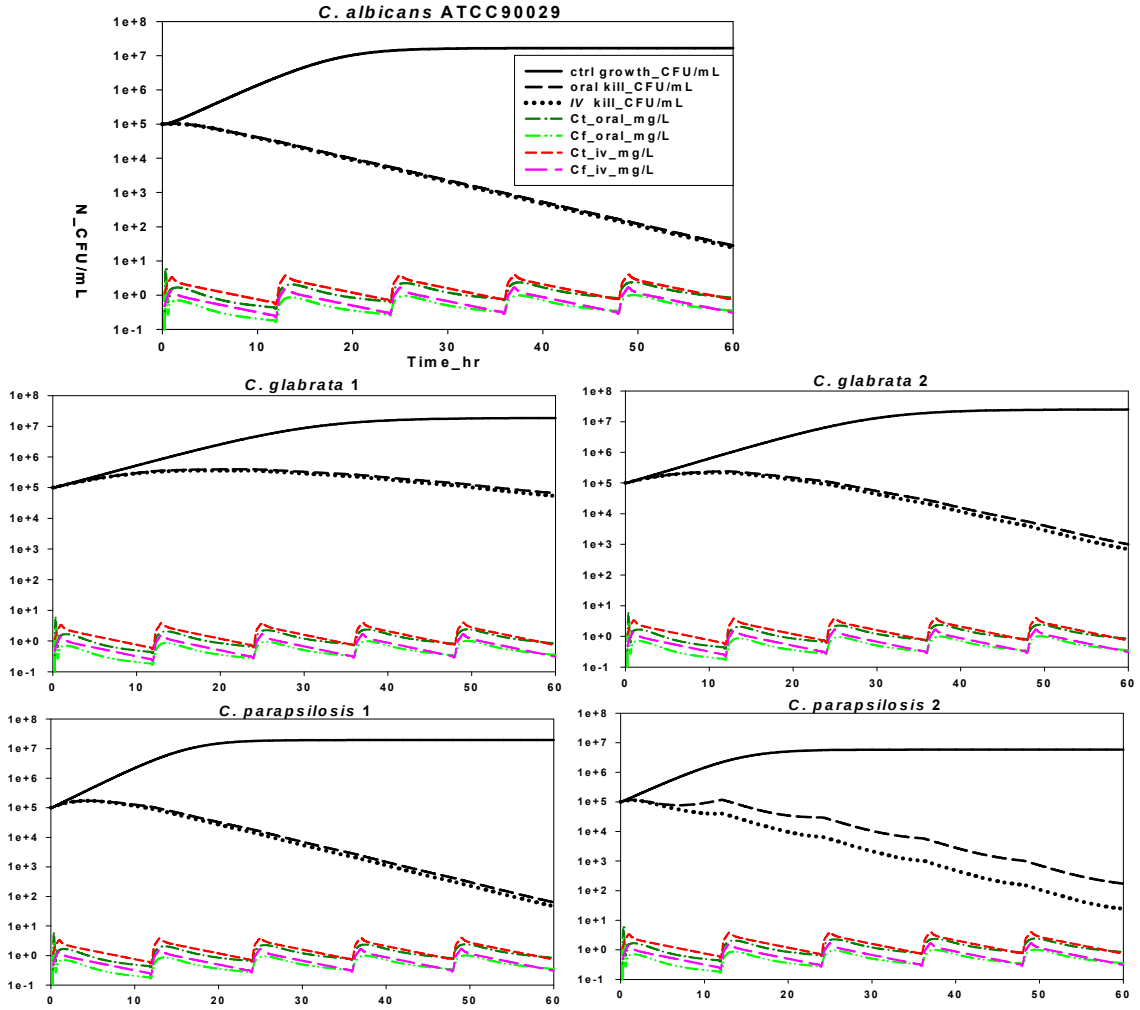

Figure 4-4. Using parameters from dynamic models to simulate candidal time-kills and plasma voriconazole concentration-time profiles: The simulations of time-kills are shown for short-term IV infusion (····) and oral dosing of voriconazole (---). Control growth is in the absence of drug (—). The simulated plasma concentration-time profiles for multiple doses of voriconazole (τ=12h) are shown for short-term intravenous (IV) infusion (T=1h, infusion rate=3mg/kg/h, bid); and oral administration (200mg, bid, F=0.9). Free voriconazole concentrations were calculated assuming plasma protein binding level of 58%.

CHAPTER 5
IN VITRO MICRODIALYSIS OF VORICONAZOLE

Background

Microdialysis is a dynamic technique which has been employed for the *in vivo* measurement of a variety of drugs and endogenous compounds in different tissues [73, 99]. The applicability of this technique can be limited by drug lipophilicity which can impair the diffusion through microdialysis semi-permeable membrane [130, 131]. Voriconazole is a moderately lipophilic (Log D7.4 = 1.8) antifungal triazolic agent [31]. The determination of the recovery (the fraction of the free drug at the site of sampling which dialyses into the probe) is essential for voriconazole to estimate the free drug levels in the tissue. There are several factors which affect drug's relative recovery including the drug's physico-chemical properties, flow rate, probe's characteristics such as type, membrane length and diameter, experimental conditions such as temperature and matrix tortuosity of the interested tissues, when the recovery is determined *in vivo* [99]. For determining the *in vitro* recovery of voriconazole in microdialysis, a straight-forward approach was undertaken and the calibration methods directly were used to determine the free, unbound drug concentration. For practical reasons, the two most common methods are the extraction efficiency method (EE) and retrodialysis (RD) method.

Specific Aims

The objective of *in vitro* microdialysis (MD) study was to assess the feasibility of doing microdialysis of voriconazole, to determine the *in vitro* recovery of this compound and to determine the value of protein binding of voriconazole in both rat and human plasma *in vitro*.

Materials and Methods

Materials

All materials are listed in Table 5-1 unless otherwise stated.

The CMA/20 probe, with a membrane length of 10 mm and a molecular cutoff of 20 kDa was used for the experiments. The probe was connected to a 1000 µl Gastight syringe by a Perifix screw connector (B. Braun). A microinfusion pump (Harvard Apparatus Syringe Pump Model ´22´) was used to keep the flow through the probe constant.

All the solvents used in the HPLC analysis were of HPLC grade.

Methods

Recovery

The *in vitro* recovery of voriconazole was determined by two different methods: extraction efficiency (EE) and retrodialysis (RD). All methods were carried out at 37ºC. Each procedure is described in the following sections.

Extraction efficiency method (EE)

In the EE method, blank Lactated Ringer's (LR) solution was pumped through the microdialysis (MD) probe at a flow rate of 1.5µL/min. The MD probe was then placed into the sample tube, which was a glass tube filled with approximately 6 ml of drug solution, starting with the lowest concentration and fixed in place with adhesive tape. Six different voriconazole concentrations of 0.5, 1, 2, 5, 10 and 40 µg/ml were used in this experiment with all prepared in lactated Ringer's solution. To guarantee equal concentrations throughout the whole tube, the solution was stirred at approximately 100rpm. Voriconazole was diffused from the sample tube into the MD probe and were measured in the dialysate. Samples were collected every 20 minutes after the end of the 2

hours equilibration time. A total of 5 samples were collected for each experiment. The concentrations were determined by a validated HPLC/UV method and plotted versus time. All experiments were performed in triplicates. The percent recovery (R%) for the EE method is then calculated as followed:

$$R\% = \frac{C_{dialysate}}{C_{sol}} \times 100 \quad (5\text{-}1)$$

Where R% is the recovery in percentage, C_{sol} is the average voriconazole concentration in the tube before and after the experiment, and $C_{dialysate}$ is the voriconazole concentration in the dialysate.

Retrodialysis method (RD)

In RD method, the syringes contained the voriconazole solution that was pumped through the MD probe at a flow rate of 1.5μL/min. The MD probe was placed into a sample tube that was filled with blank LR solution and fixed in place with adhesive tape. To guarantee equal concentrations throughout the whole tube, the solution was stirred at approximately 100rpm. The voriconazole was diffused out of the probe into the sample tube. The loss of voriconazole over the membrane was then determined while determining $C_{dialysate}$. Samples are collected every 20 minutes after the end of the 2 hours equilibration time. A total of 5 samples were collected for each experiment. The voriconazole concentrations were determined by a validated HPLC/UV method and plotted versus time. All experiments were performed in triplicates. The percent recovery (R%) for the RD method was then calculated as followed:

$$R\% = \frac{(C_{perfusate} - C_{dialysate})}{C_{perfusate}} \times 100 \quad (5\text{-}2)$$

$C_{perfusate}$ is the average voriconazole concentration in the perfusate before and after the experiment, and $C_{dialysate}$ is the voriconazole concentration in the dialysate.

Microdialysis experiments

The *in vitro* recovery of the voriconazole was determined by the extraction efficiency method (EE). In this method, blank Ringer's solution was pumped through the microdialysis probe (CMA/20), which was placed into a testing tube filled with approximately 6 ml of voriconazole solution. Six different voriconazole concentrations of 0.5, 1, 2, 5, 10 and 40 μg/ml were tested in this experiment with all prepared in lactated Ringer's solution. After placing the probe in the drug solution, it was allowed to equilibrate for 10 minutes at flow rate of 5μl/min followed by 2 hours at 1.5μl/min. Subsequently dialysate samples were collected every 20 minutes after the equilibration period. A total of 5 samples were collected for each experiment, and the experiment was triplicate for each concentration. The voriconazole concentration in the dialysates and in the tube before and after the experiments was determined by the HPLC/UV method described above. The probe recovery determined by the extraction efficiency was calculated by the equation 5-1. The protein binding was determined by the extraction efficiency was calculated by the equation 5-3.

$$protein\ binding\ \% = (1 - \frac{C_{dialysate}}{R\% \times C_{sol}}) \times 100 \qquad (5\text{-}3)$$

HPLC for determination of voriconazole

An HPLC protocol for measuring voriconazole in Lactated Ringer's solution and human or rat plasma was developed based an existing assay method with a calibration range of 0.025–16 μg/ml voriconazole as being described previously in Materials and Methods of Chapter 2. Voriconazole samples in Lactated Ringer's solution were

measured using HPLC/UV method directly. Plasma samples were extracted before the measurement using HPLC/UV method as being described previously [120] with modification. Briefly, plasma samples were centrifuged at 1,700 × *g* for 5 min. An aliquot (150 µl) was pipetted into a 1.5 ml Eppendorf tube and acetonitrile (240 µl) was then added. The mixture was mixed briefly by vortex, centrifuged at 1,200 × *g* for 5 min after standing for 10 min at room temperature and supernatant was transferred to a new Eppendorf tube. This step was repeated one more time. Then 50 µl of the supernatant plus 50 µl of 0.04 M Ammonium Phosphate buffer (pH 6.0) was applied for HPLC system.

Calibration curves for voriconazole

Stock solutions of voriconazole (1 µg/ µl) were prepared in distilled water and diluted in Lactated Ringer's solution or plasma to give 100 µg/ ml. Standards were prepared by adding the diluted voriconazole solution to appropriate volumes of Lactated Ringer's solution or plasma to give a concentrations of 0.025, 0.1, 0.2, 0.5, 1, 2, 4, 8 and 16 µg/ ml. The plasma standards were also extracted before injecting to HPLC system. Calibration curves were constructed by plotting the peak area of voriconazole against concentration using a weighted ($1/X^2$) least squares regression for HPLC data analysis.

Results

The HPLC data printout from the integrator was transferred into EXCEL 2003 (Microsoft Corporation) spreadsheets. With the equation obtained from the Weighted ($1:X^2$) Linear Regression, the voriconazole concentrations rom Lactated Ringer's solution, rat and human plasma samples were calculated [132].

Stability of Voriconazole in Lactate Ringer's Solution and Plasma

The *in vitro* stability of voriconazole in Lactate Ringer's solution and human and rat plasma were studied. The results showed that voriconazole in Lactate Ringer's solution, human and rat plasma were found stable at -80°C for at least 6 months, at -4°C at least for 72 hours, room temperature and 37°C for at least 24 hours which is consistent with previous report [4, 30].

Protein Binding

The results of recovery for both extraction efficiency (EE) and retrodialysis (RD) methods were summarized in Table 5-2 and 5-3. As shown from the tables, the *in vitro* recovery of this compound from both extraction efficiency (EE) and retrodialysis methods (RD) were quite similar with 51.1% ± 2.6% (mean ± SD) (ranging from 46.2% to 56.3%) for EE method and 51.9% ± 2.9% (mean ± SD) (ranging from 45.3% to 57.8%) for RD method. The results of protein binding of voriconazole in presence of different drug concentrations in rat and human plasma were summarized in Table 5-4 and 5-5. The protein binding of voriconazole in rat plasma is 66.2% ± 2.2% (mean ± SD) (ranging from 61.5% to 70.3%) and that in human plasma is 57.0% ± 2.8% (mean ± SD) (ranging from 50.9% to 62.1%).

Discussion

This experiment confirmed that the performance of voriconazole microdialysis was feasible. It has been reported in the literature that recoveries were dependent on the method used for the determination as well as on the flow rate, but independent of drug concentration [133]. In our current study, the recoveries of voriconazole were independent of both the methods (EE and RD) and drug concentrations.

Only the free or unbound fraction of drug is available for antimicrobial activity according to the "free drug hypothesis" of anti-infective agents. Voriconazole exhibits moderate plasma protein binding with values of 66% in rat plasma and 58% in human plasma, which was measured by ^{14}C Voriconazole [31]. The binding is independent of dose or plasma drug concentrations [8]. Our current study is the first time to report the voriconazole protein binding with *in vitro* microdialysis method as our knowledge. The average plasma protein binding of voriconazole in rat and human is 66.2% and 57.0%, respectively, which is consistent with the previous publications [8, 31]. Moreover, we also confirmed that the protein binding in rat and human plasma was independent of the drug concentrations. The free drug concentrations provided a better correlation to outcome than total drug concentrations. Free drug concentrations must be considered when examining the relationship between pharmacokinetic parameters and *in vivo* activity. Microdialysis provided a simple, clean method for determining the free drug concentration *in vitro* and in *vivo*.

Table 5-1. List of materials

Materials	Resource
Voriconazole	Pfizer, New York, NY
Acetonitrile	Fisher, HPLC grade, Pittsburgh, PA
Ammonium Phosphate	Sigma, HPLC grade, St. Louis, MO
Lactated Ringer's solution (USP)	Abbott, Chicago, IL
Rat plasma	Wistar, Harlan Sprague-Dawley, Indianapolis, IN
Human plasma	Civitan Regional blood system, Gainesville, FL
CMA/20 probe	Stockholm, Sweden
Balance AB104	Mettler, Toledo, Hightstown, NJ
Vortex	Kraft Apparatus model PV-5, Fisher, Pittsburgh, PA
Pipette tips	Fisher, Pittsburgh, PA
Tubes microcentrifuge	Fisher, Pittsburgh, PA
Centrifuge	Fisher model 235V, Pittsburgh, PA

Table 5-2. Extraction efficiency (EE) method for measuring voriconazole recovery

Recovery	Concentration (μg/ml)						Average
(%)	0.51	1.04	2.06	5.13	10.31	41.47	
1	50.6	50.7	46.8	56.3	52.6	50.6	
2	46.6	51.8	53.4	52.8	54.4	46.1	
3	46.2	52.0	52.2	51.5	56.2	49.6	
Mean (%)	47.8	51.5	50.8	53.5	54.4	48.8	51.1
SD (%)	2.4	0.7	3.5	2.4	1.8	2.3	2.6

Table 5-3. Retrodialysis (RD) method for measuring voriconazole recovery

Recovery	Concentration (μg/ml)						Average
(%)	0.52	0.99	1.96	5.12	10.39	40.37	
1	49.9	51.6	49.4	56.2	57.8	47.6	
2	47.1	51.8	53.5	52.3	55.7	51.5	
3	45.3	53.2	53.7	54.3	52.7	51.2	
Mean (%)	47.4	52.2	52.2	54.3	55.4	50.1	51.9
SD (%)	2.3	0.9	2.5	1.9	2.6	2.2	2.9

Table 5-4. Rat plasma protein binding data of voriconazole measured by *in vitro* microdialysis

Protein binding	Concentration (μg/ml)						Average
(%)	0.53	1.13	2.22	5.42	11.09	41.19	
1	61.5	64.9	66.0	65.8	66.9	70.3	
2	62.4	66.7	68.5	68.5	69.2	63.2	
3	61.7	69.1	63.3	68.4	68.7	65.7	
Mean (%)	61.9	66.9	65.9	67.5	68.2	66.4	66.2
SD (%)	0.4	2.1	2.6	1.5	1.2	3.6	2.2

Table 5-5. Human plasma protein binding data of voriconazole measured by *in vitro* microdialysis

Protein binding	Concentration (μg/ml)						Average
(%)	0.54	1.09	2.16	5.55	11.15	41.13	
1	50.9	51.8	56.5	57.6	61.2	62.1	
2	55.9	55.9	56.6	60.2	60.8	60.3	
3	56.8	54.4	51.5	59.8	55.9	57.9	
Mean (%)	54.6	54.0	54.9	59.2	59.3	60.1	57.0
SD (%)	3.2	2.1	2.9	1.4	2.9	2.1	2.8

CHAPTER 6
IN VIVO PHARMACOKINETIC STUDIES OF VORICONAZOLE IN RATS

Background

Voriconazole is an antifungal agent which has been shown to be effective in the treatment of patients with candidiasis [134-136]. The effectiveness of voriconazole and other antifungal agents is determined by the sensitivity of the fungi and the concentrations achieved at the site of infection [34, 131, 137]. However, the site of infection is generally not the blood. Therefore, in many infections concentrations in organ tissues, extracellular fluids, and inflammatory cells rather than plasma concentrations determine the clinical outcome and may allow a better prediction of the therapeutic effect than plasma concentrations [73, 74, 95, 99, 138-141]. Microdialysis has been used to study drug free levels in many tissues and organs, such as muscle, adipose tissue, bile, blood, eye, skin, brain, lung, and so on [73, 74]. It is an established technique for studying physiological, pharmacological, and pathological changes of many drugs such as antibiotics [142, 143], anti-cancer drugs [95, 144-146], and psychoactive compounds [137, 147-149] in both preclinical and clinical studies.

Specific Aims

The objective of this project is to study the distribution profile of voriconazole in the body by measuring its concentration in plasma, muscle. To evaluate unbound muscle concentrations of voriconazole in Wistar rats by microdialysis after intravenous administration of voriconazole and to compare the free tissue concentration to free plasma concentration. To develop a population PK model of voriconazole in rats using NONMEM®.

Materials and Methods

Reagents and Equipment

All of them have been described in Table 5-1 in Chapter 5 unless otherwise stated.

Isoflurane, USP was distributed by Webster Veterinary. Supply, Charlotte, NC

Animals

Wistar male rats (Harlan Sprague-Dawley, Indianapolis, IN) were used in the project.

Previous studies with other azole drugs have indicated that rat is a suitable test model to investigate tissue distribution using microdialysis [133, 137, 147, 148]. The rats were shipped to ACS a couple of days before the study starts in order to reduce stress and adapt them to the researcher. In the experiment, the rats were weighed before the surgery and dose administration. The body weight of male Wistar rats used in this experiment was ranged from 350g to 400g and age of 2-4 months. The animals were numbered in the sequence of the experiments without identifying devices such as tattoos or collar numbers since this project involved non-survival surgical experiment.

Experimental Design

Two groups of anesthetized male Wistar rats of six each were administered intravenously with either 5mg/kg or 10 mg/kg dose of voriconazole. Total plasma concentrations as well as unbound concentrations in thigh muscle were measured over 8-hour period by microdialysis. Animals were sacrificed at the end of the study. The data were analyzed by both non-compartmental and compartmental pharmacokinetic approaches.

The study was performed with the approval of the Institutional Animal Care and Use Committee (IACUC) of the University of Florida (Protocol # F109). The animals

were housed in the Animal Care Services (ACS) at the Health Science Center, University of Florida according to the standard husbandry procedures.

Anesthetic Procedure

Isoflurane has been used in the surgical procedure for anesthesia in rats in many reports [150-153]. In our studies, the rats were anesthetized by using Isotec-4 isoflurane vaporizer (SurgiVet/ Smiths Medical, Waukesha, WI**)** from ACS. After placing the rat in the induction chamber, the flowmeter was adjusted to 0.8-1.5L/min and the isoflurane vaporizer was adjusted to 2% which was marked as "2". Anesthesia was confirmed by the absence of reflexes after pinching the rat's footpads. After anesthesia, the rat was immobilized in a supine position on a dissecting board by holding the paws with rubber bands, which was attached to pins on each corner of the board. For maintenance of anesthesia, a mask connected to the Bain Circuit was used for the rat, and the flowmeter was adjusted to 400-800mL/min. The footpads were pinched in a regular basis (every 15 min) during the experiment. The rat was kept normothermic on an electric heating pad.

Antiseptic Procedure

This project involved non-survival surgical experiment. The surgery sites were disinfected by swiping the area with 70% isopropyl alcohol and skin areas of surgery sites were shaved before surgery.

Blood Samples

Blood sample were collected by a polyethylene catheter (inner diameter of 0.3 mm and outer diameter of 0.7 mm) introduced in the carotid. After initial insertion and following each sampling, the catheter was irrigated with 300µl 100 IU pre-warmed heparinized saline. Blood samples (100µl) were collected in heparinized tubes before the dose was administered (time zero) and at 10, 30, 60, 90, 120, 180, 240, 300, 360, 480min

after drug administration. The blood samples were centrifuged at approximately 2000 rpm for 10 minutes at room temperature and the supernatant of plasma was transferred to a new Eppendorf tube. This step was repeated one more time. Then plasma samples were kept at -80 °C until analyzed.

Microdialysis

Probe calibration

The left hind leg muscle was used for insertion of a microdialysis probe after skin area was shaved and cut open. Before introducing the probe itself, a guide plastic cannula was introduced in the muscle with the help of a 23-guage needle. Afterwards, the plastic cannula was kept in place and the needle was removed and replaced by the microdialysis probe. After inserting the probe, the plastic cannula was removed by tearing it out while holding the probe in place.

Probe calibration was performed before drug administration. The probe was initially perfused with lactated Ringer's solution (NaCl 137 mM, KCl 1.0 mM, $CaCl_2$ 0.9 mM, $NaHCO_3$ 1.2 mM) at a flow rate of 2 μl /min for 30 minutes using a Harvard Apparatus 22 injection pump, model 55-4150. After equilibration, the probe was calibrated by retrodialysis. In this method, the syringe with lactated Ringer's solution was replaced by a syringe with a voriconazole solution of 1 or 2μg/ml. The drug solution was initially pumped at a flow of 5 μl/min for 5 min and after the flow was changed back to 2 μl/min. The probe was allowed to equilibrate for 0.5 hour before samples were collected. The samples for the calibration procedure were collected very 20 minutes and a total of 3 samples were collected in each experiment. The samples were frozen at -80 ^{o}C before analyses by a validated HPLC/UV method.

Muscle microdialysis

After the probe calibration, the drug perfusion was stopped and removed instead of blank lactated Ringer's solution. The probe was perfused with lactated Ringer's solution for 30 minutes to wash out. After wash out, microdialysis samples were collected for muscle over 20-minute intervals at times 20, 40, 60, 80, and up to 480 minutes after drug administration.

The *in vivo* recovery was calculated by the same above equation of

$$R\% = \frac{C_{perfusate} - C_{dialysate}}{C_{perfusate}} \times 100 \quad (6\text{-}1)$$

The drug concentration in the tissue was calculated using the equation of

$$C_{t,free} = \frac{C_{dialysate}}{R\%} \quad (6\text{-}2)$$

$C_{t,free}$ is the muscle free concentration, $C_{dialysate}$ is the concentration in the dialysate, and R% is the percent of recovery obtained in each animal experiment.

Data Analysis

Microdialysis samples were measured using HPLC/UV method directly. Plasma samples were extracted before the measurement using HPLC/UV method as being described previously (Methods in Chapter 5) with modification. Briefly, plasma samples were thawed on ice and then centrifuged at 1,700 × *g* for 5 min. An aliquot (25 µl) was pipetted into a 0.7 ml Eppendorf tube and acetonitrile (40 µl) was then added. The mixture was mixed briefly by vortex, centrifuged at 1,200 × *g* for 5 min after standing for 10 min at room temperature and supernatant was transferred to a new Eppendorf tube. This step was repeated one more time. Then 25 µl of the supernatant plus 25 µl of 0.04 M Ammonium Phosphate buffer (pH 6.0) was applied for HPLC system.

The HPLC data was input into EXCEL 2003 (Microsoft Corporation) spreadsheets. With the equation obtained from the Weighted ($1:X^2$) Linear Regression, the rat and human plasma sample concentrations were calculated [132]. With the equation obtained from the Weighted ($1:X^2$) Linear Regression function, the rat plasma sample concentrations were calculated. Unbound concentrations in rat thigh muscle were measured by microdialysis. Individual probe recovery was determined by retrodialysis and allowed conversion of the measured dialysate concentrations to the actual unbound tissue concentrations. The data were analyzed both by noncompartmental and compartmental pharmacokinetic approaches.

Noncompartmental pharmacokinetic analysis

The following parameters were determined for each rat for both plasma and microdialysis noncompartmental pharmacokinetic analysis. The mean and standard deviation (SD) of each parameter were also determined.

The data were analyzed by WinNonlin 5.2 (Pharsight Corporation, Mountain View, CA) to describe the best absorption model. The initial concentration C_0 was determined by logarithmic back-extrapolation to t = 0 using the first two data points. The terminal elimination rate constant (k_e) was determined by linear regression of the log plasma concentrations. The terminal half-life ($t_{1/2}$) was calculated as $\ln(2)/k_e$. The area under the concentration-time curve (AUC_t) values were calculated between time 0 and the final time point at which measurable drug concentrations were observed, using the linear trapezoidal rule. AUC∞ was calculated by extrapolation from time zero to infinity with k_e. The area under the first moment curve (AUMC) was calculated from a plot of C_t versus t using the trapezoidal rule up to the last data point (C_x) at time t_x and adding the extrapolated terminal area, calculated as $C_x \cdot t_x/k_e + C_x/k_e^2$. AUMC∞ was Area under the

first moment curve when the time concentration curve is extrapolated to infinity. The mean residence time (MRT) was calculated as AUMC/AUC. Clearance (CL) was calculated by the relationship of Dose/AUC∞, and the volume of distribution was calculated by the relationship CL/*k*e. The volume of distribution at steady state (Vd_{ss}) was calculated as (Dose·AUMC)/AUC^2.

Compartmental pharmacokinetic analysis and modeling

Both the individual and average plasma and free tissue concentrations at each time point were fitted by using the modeling software of NONMEM® (UCSF, San Francisco, CA).

Rat total plasma voriconazole pharmacokinetic data were first analyzed using one- and two-compartment model with linear or nonlinear elimination (Michaelis-Menten elimination). Then rat total plasma and unbound muscle voriconazole data were analyzed simultaneously using a two-compartment model with nonlinear elimination. The schemes of one- and two-compartment model with nonlinear elimination were shown in Figure 6-1 and Figure 6-2. The models were fitted to the data using the first order (FO) method and the subroutine ADVAN1 TRANS2 (one-compartment with linear elimination), ADVAN3 TRANS4 (two-compartment with linear elimination), ADVAN10 TRANS1 (one-compartment with nonlinear elimination), and ADVAN6 TRANS1 (two-compartment with nonlinear elimination). NONMEM performs linearized maximum likelihood estimation by use of an objective function (OF). Typical values (population means) with their corresponding standard errors (SE) and the intersubject and intrasubject variabilities were expressed as coefficients of variation (CV percentage). To determine whether there was a statistically significant difference between the goodness of fit between the two models, the Akaike model selection criteria was used, which required

a decrease of two points in the objective function (minus twice the logarithm of the likelihood of the model) to accept a model with one additional parameter, as well as a comparison of diagnostic plots (observed concentrations compared with predictions and observations/predictions compared with time).

The one-compartment model with linear elimination will be parameterized in terms of CL (clearance), and V (volume of central compartment). The two-compartment model with linear elimination will be parameterized in terms of CL (clearance), V_1 (volume of central compartment), V_2 (volume of peripheral compartment), and Q (intercompartmental clearance).

The one-compartment model with nonlinear elimination will be parameterized in terms of V_{max} (maximum elimination rate), K_m (the Michaelis-Menten constant, voriconazole concentration at which the elimination is at half maximum) and V (volume of central compartment). The two-compartment model with nonlinear elimination will be parameterized in terms of V_{max} (maximum elimination rate), K_m (the Michaelis-Menten constant, voriconazole concentration at which the elimination is at half maximum), V_1 (volume of central compartment), V_2 (volume of peripheral compartment), and Q (intercompartmental clearance).

The differential equations for a two-compartment model with nonlinear elimination (Michaelis-Menten elimination) are given in following equations:

$$C1 = \frac{A(1)}{V1} \tag{6-3}$$

$$\frac{dA(1)}{dt} = k_{21} \cdot A(2) - \left(\frac{V_{\max} \cdot C_1}{K_m + C_1} \right) - k_{12} \cdot A(1) \tag{6-4}$$

$$\frac{dA(2)}{dt} = k_{12} \cdot A(1) - k_{21} \cdot A(2) \quad (6\text{-}5)$$

$$K_{12} = \frac{Q}{V_1} \quad (6\text{-}6)$$

$$K_{21} = \frac{Q}{V_2} \quad (6\text{-}7)$$

Where A(1) represents the amount of voriconazole in the central compartment, A(2) represents the amount of voriconazole in the peripheral compartment, V_{max} represents the maximal elimination rate, K_m is the Michaelis-Menten constant (voriconazole concentration at which the elimination is at half maximum), C_1 is the predicted serum concentration of voriconazole, and k_{12} and k_{21} are the intercompartmental rate constants. V_1 is the volume of central compartment, V_2 is the volume of peripheral compartment, and Q is the intercompartmental clearance.

Because free rather than protein-bound voriconazole was measured in dialysate, a scaling factor for the tissue compartments was introduced, accounting for the free fraction of voriconazole, f*u*.

$$C2 = \frac{A(2)}{V2} \times fu \quad (6\text{-}8)$$

Interindividual variability for the pharmacokinetic parameters was modeled using the following exponential error model:

$$V_{max} = \theta_1 \cdot EXP(\eta_1) \quad (6\text{-}9)$$

$$K_m = \theta_2 \cdot EXP(\eta_2) \quad (6\text{-}10)$$

$$V_1 = \theta_3 \cdot EXP(\eta_3) \quad (6\text{-}11)$$

$$Q = \theta_4 \cdot EXP(\eta_4) \quad (6\text{-}12)$$

$$V_2 = \theta_5 \cdot EXP(\eta_5) \quad (6\text{-}13)$$

Where θ is the population mean estimate (or typical value) of the corresponding pharmacokinetic parameter, and η_i's are the associated interindividual variability. The η values are independent, identically distributed random errors with mean of zero and a variance equal to ωi^2. Interindividual variability will be described by an exponential error model.

When analysising the total plasma only, we used a proportional error model for the intraindividual residual variability of plasma concentration for estimation, which was described by the following equation:

$$Cp_{ij} = \widetilde{C}p_{ij} \cdot (1 + \varepsilon_{ij,prop}) \quad (6\text{-}14)$$

where Cp_{ij} is the observed value of the j^{th} plasma concentration of individual i; $\hat{C}_{pij}$ is the predicted j^{th} plasma concentration of individual i; and $\varepsilon_{ij,\ prop}$ denote the proportional residual random errors distributed with zero means and variance $\sigma^2_{\ prop}$.

When analysising the total plasma and unbound muscle voriconazole data simultaneously, the intraindividual residual variability of total plasma concentration were estimated using a proportional model, as described previously and the unbound muscle data were using a combination of proportional and additive error model, as described by the following equation:

$$Cp_{ij} = \widetilde{C}p_{ij} \cdot (1 + \varepsilon_{ij,prop}) + \varepsilon_{ij,add} \quad (6\text{-}15)$$

where Cp_{ij} is the observed value of the j^{th} plasma concentration of individual i; $\hat{C}_{pij}$ is the predicted j^{th} plasma concentration of individual i; and $\varepsilon_{ij,\ prop}$ and $\varepsilon_{ij,\ add}$ denote the proportional and additive residual random errors distributed with zero means and variance $\sigma^2_{\ prop}$ and $\sigma^2_{\ add}$.

Plasma total voriconazole concentrations and unbound muscle voriconazole concentrations were assigned separate residual errors, ε_1, ε_2 and ε_3, respectively. The following criteria were considered to determine the best model:

In the case of nested models (one model is a subset of other, i.e., null model (without covariates) is a subset of full model (with covariates), the minimum objective function value (OFV) of the best model should be significantly smaller than the alternative model(s) based on the maximum likelihood ratio (MLR) test. The MLR test was applied when the test models fulfilled the full/reduced model definition. A full model can be made equivalent to a reduced model by setting a parameter to a fixed value. The change in OFV between the two nested models is approximately χ^2 distributed with degree of freedom equal to the number of parameters that are set to a fixed value in the reduced model. A decrease of 3.84 units in the OFV will be considered statistically significant ($p < 0.05$) for addition of one parameter during the development of the model.

In the case of non-nested models, the different structure models were evaluated based on minimization of the Akaike information criterion (AIC) value. The AIC was defined in terms of:

$$AIC = OFV + 2*p \quad (6\text{-}16)$$

where p = total number of parameters in the model (structural + error). Lower the value of AIC better the model.

A plot of voriconazole concentration (observed (DV), individual predicted (IPRED) and population predicted (PRED)) versus time for all the individual were drawn, which would give an overall trend of fitted concentrations. It could be seen that for certain individuals the population predictions are underpredicted or overpredicted.

The observed and predicted plasma concentrations would be more randomly distributed across the line of unity for the preferred model. NONMEM obtains IPRED values by the Bayesian POSTHOC option. Using the population mean estimate of parameters (prior) and each individual data (likelihood), NONMEM obtains the individual parameter estimates (posterior). From the individual parameter estimates, individual predicted concentrations (IPRED) are obtained.

A graph of DV *vs.* IPRED and DV vs. PRED (goodness of fit plots) could be looked for any bias in the predictions. Ideally the points should be uniformly distributed along the line of identity. Normally DV *vs.* IPRED is much better than DV *vs.* PRED as PRED contains unexplained variability.

Plots of the residuals (RES) *vs.* PRED and weighted residuals (WRES) *vs.* PRED (goodness of fit plots) could be looked for any unaccounted heterogeneity in the data.

The NONMEM codes were written and the initial estimation of all parameters obtained by WinNonlin was used to run NONMEM. The figures were generated with S-PLUS (Statistical Sciences, Version 6.2).

Results

Probe Recovery

The individual probe recovery in each experiment was used to convert the microdialysate concentrations to unbound tissue concentrations and all the values were summarized in Table 6-1. As shown from the tables, the *in vivo* recovery of voriconazole from retrodialysis methods (RD) were quite similar with 43.3 ± 4.2% (mean ± SD) (range from 37.6% to 48.1%) for 1 μg/ml group and 47.6 ± 4.0% (mean ± SD) (range from 43.4% to 53.6%) for 2 μg/ml group.

Individual Pharmacokinetic Analysis of Total Voriconazole in Plasma after Intravenous Bolus Administration

The experimental data of total plasma voriconazole from 5 and 10 mg/kg intravenous dose were listed in Table 6-2 and 6-3 and were analyzed by both noncompartmental pharmacokinetic analysis and compartmental pharmacokinetic analysis.

Noncompartmental pharmacokinetic analysis

After noncompartmental pharmacokinetic analysis by WinNonlin 5.2, the results of voriconazole for the total plasma data after intravenous bolus administration of 5 and 10 mg/kg were listed in Table 6-2 and 6-3. The initial concentrations (C0) were 3.78 ± 0.29 mg/L (mean ± SD) and 7.76 ± 0.18 mg/L (mean ± SD) respectively, which declined with a terminal half-life of 3.95 ± 0.34 hours (mean ± SD) and 4.92 ± 0.29 hours (mean ± SD). The areas under the curve AUC∞ were 20.53 ± 2.57 hr·mg/L (mean ± SD) and 56.07 ± 3.82 hr·mg/L (mean ± SD), respectively. The areas under the first moment curve (AUMC∞) were 121.90 ± 24.64 hr2·mg/L (mean ± SD) and 417.35 ± 43.75 hr2·mg/L (mean ± SD), respectively. The residence times (MRT∞) were 5.89 ± 0.52 hours (mean ± SD) and 7.43 ± 0.40 hours (mean ± SD), respectively. The volumes of distribution of the central compartment (Vc) were 1.33 ± 0.1 mL/g (mean ± SD) and 1.29 ± 0.03 mL/g (mean ± SD), respectively and Vdss were 1.44 ± 0.09 mL/g (mean ± SD) and 1.33 ± 0.12 mL/g (mean ± SD), respectively. The total body clearances (CL) were 0.25 ± 0.03 mL/hr/g (mean ± SD) and 0.18 ± 0.02 mL/hr/g (mean ± SD), respectively.

Compartmental pharmacokinetic analysis

The experimental data of total plasma voriconazole from 5 and 10 mg/kg intravenous dose were plotted in Figure 6-3 and 6-4 and were analyzed by both one- and

two-compartment model with linear or nonlinear elimination (Michaelis-Menten elimination) by NONMEM. Initially, all four models have applied to fit unbound plasma and muscle voriconazole PK data from 5 and 10 mg/kg intravenous dose, and the OFV and AIC value have been listed in Table 6-4. As shown in this table, the AIC value (-344.03) from two-compartment model with nonlinear elimination was the lowest, which indicated that this model might be the best to fit the total plasma voriconazole PK data in rats.

One-compartment model with linear elimination analysis

A one-compartment model with linear elimination was used to fit the data of total plasma voriconazole from 5 and 10 mg/kg intravenous dose and was able to produce a good curve fit of these data. As shown in Table 6-4, the OFV is -240.73, and the AIC is -230.73, which is the highest compared to other models. The critical parameters obtained in this analysis were listed in Table 6-5. The diagnostic plots for this one-compartment model were also shown in Figure 6-5, 6-6 and 6-7. As shown in Figure 6-5, the observed and predicted plasma concentrations were randomly distributed across the line of unity. As shown in Figure 6-6, the points of DV, IPRED and PRED were uniformly distributed along the line of identity, and in Figure 6-7, the residuals and weighted residuals plot versus predicted voriconazole concentration for this model showed a relatively uniform distribution of residuals over the concentration range.

Two-compartment model with linear elimination analysis

A two-compartment model with linear elimination was also used to fit the data of total plasma voriconazole from 5 and 10 mg/kg intravenous dose and was able to produce a good curve fit of these data. As can be seen from Table 6-4, the OFV is -295.77, and the AIC is -277.77. The critical parameters obtained in this analysis were listed in Table

6-6. The diagnostic plots for this two-compartment model were also shown in Figure 6-8, 6-9 and 6-10. The observed and predicted plasma concentrations were randomly distributed across the line of unity except some early time point data. The points of DV, IPRED and PRED were uniformly distributed along the line of identity, and the residuals and weighted residuals plot versus predicted voriconazole concentration for this model showed a relatively uniform distribution of residuals over the concentration range.

One-compartment model with nonlinear elimination

A one-compartment model with nonlinear elimination was used to fit the data of total plasma voriconazole from 5 and 10 mg/kg intravenous dose and was able to produce a good curve fit of these data. As shown in Table 6-4, the OFV is -249.17, and the AIC is -235.17. The critical parameters obtained in this analysis were listed in Table 6-7. The diagnostic plots for this one-compartment model were also shown in Figure 6-11, 6-12 and 6-13. As shown in Figure 6-11, the plot of voriconazole concentration (observed (DV), individual predicted (IPRED) and population predicted (PRED)) versus time for the entire individual gave an overall trend of fitted concentrations. The observed and predicted plasma concentrations were randomly distributed across the line of unity. As shown in Figure 6-12, the points of DV, IPRED and PRED were uniformly distributed along the line of identity, and in Figure 6-13, the residuals and weighted residuals plot versus predicted voriconazole concentration for this model showed a relatively uniform distribution of residuals over the concentration range.

Two-compartment model with nonlinear elimination

To find the best model to fit the data of total plasma voriconazole from 5 and 10 mg/kg intravenous dose, a two-compartment model with nonlinear elimination was also applied. This model was able to produce a good curve fit of these data. As shown in

Table 6-4, the OFV is -366.03, and the AIC is -344.03, which is the lowest compared to other models. The critical parameters obtained in this analysis were listed in Table 6-8. The diagnostic plots for this two-compartment model were also shown in Figure 6-14, 6-15 and 6-16. As shown in Figure 6-14, the plot of voriconazole concentration (observed (DV), individual predicted (IPRED) and population predicted (PRED)) versus time for the entire individual gave an overall trend of fitted concentrations. The observed and predicted plasma concentrations were randomly distributed across the line of unity. As shown in Figure 6-15, the points of DV, IPRED and PRED were uniformly distributed along the line of identity. As can be seen in Figure 6-16, the residuals and weighted residuals plot versus predicted voriconazole concentration for this model showed a relatively uniform distribution of residuals over the concentration range. All the diagnostic plots and AIC value have indicated that the two-compartment model with nonlinear elimination seem to adequately explain the variability of the data and fit the data better than other models.

Individual Pharmacokinetic Analysis of Unbound Voriconazole in Muscle after Intravenous Bolus Administration

The experimental data of unbound muscle voriconazole concentration from 5 and 10 mg/kg intravenous dose were obtained from rats muscle *in vivo* microdialysis based on *in vivo* recovery of voriconazole from retrodialysis methods (RD) as described previously in this chapter. All the data were listed in Table 6-9, 6-10 and were analyzed by both noncompartmental pharmacokinetic analysis and compartmental pharmacokinetic analysis.

Noncompartmental pharmacokinetic analysis

After noncompartmental pharmacokinetic analysis, the results of voriconazole for the unbound muscle data after intravenous bolus administration of 5 and 10 mg/kg were listed in Table 6-9 and 6-10. The values of terminal half-life were 2.83 ± 0.20 hours (mean ± SD) and 6.92 ± 2.29 hours (mean ± SD). The areas under the curve AUC_∞ were 7.52 ± 1.02 hr·mg/L (mean ± SD) and 24.52 ± 7.84 hr·mg/L (mean ± SD), respectively. The areas under the first moment curve ($AUMC_\infty$) were 36.72 ± 6.98 hr^2·mg/L (mean ± SD) and 267.98 ± 184.84 hr^2·mg/L (mean ± SD), respectively. The residence times (MRT_∞) were 4.85 ± 0.31 hours (mean ± SD) and 10.16 ± 3.02 hours (mean ± SD), respectively. The total body clearances (CL) were 0.68 ± 0.10 mL/hr/g (mean ± SD) and 0.43 ± 0.11 mL/hr/g (mean ± SD), respectively.

Compartmental pharmacokinetic analysis

Since the two-compartment model with nonlinear elimination is the best model to fit the total plasma voriconazole PK data in rats, the experimental data of total plasma and unbound muscle voriconazole PK data from 5 and 10 mg/kg intravenous dose were analyzed simultaneously by two-compartment model with nonlinear elimination (Michaelis-Menten elimination) by NONMEM. The experimental original unbound muscle voriconazole PK data were plotted in Figure 6-17 and 6-18.

Two-compartment model with nonlinear elimination

To find the best model to fit the data of unbound plasma and muscle voriconazole from 5 and 10 mg/kg intravenous dose, a two-compartment model with nonlinear elimination was applied. This model was also able to produce a good curve fit of these data. The critical parameters obtained in this analysis were listed in Table 6-11. The diagnostic plots for this model were also shown in Figure 6-19, 6-20 and 6-21. As shown

in Figure 6-19, the plot of total plasma and unbound muscle voriconazole concentration (observed (DV), individual predicted (IPRED) and population predicted (PRED)) versus time for the entire individual gave an overall trend of fitted concentrations. The observed and predicted plasma concentrations were randomly distributed across the line of unity. As shown in Figure 6-20, the points of DV, IPRED and PRED were uniformly distributed along the line of identity. As can be seen in Figure 6-21, the residuals and weighted residuals plot versus predicted voriconazole concentration for this model showed a relatively uniform distribution of residuals over the concentration range. It indicated that the two-compartment model with nonlinear elimination seem to adequately explain the variability of the unbound plasma and muscle voriconazole PK data.

Pharmacokinetic Analysis of Average Total Voriconazole Data in Plasma and Unbound Voriconazole Data in Muscle after Intravenous Bolus Administration

The average data of total plasma and unbound muscle voriconazole from 5 and 10 mg/kg intravenous dose were listed in Table 6-2, 6-3, 6-9 and 6-10, and were fitted simultaneously by two-compartment model with nonlinear elimination (Michaelis-Menten elimination) by NONMEM using the respective parameters of V1= 0.5 L, Q = 0.28 L/hr, Vmax = 0.34 mg/hr, Km = 1.52 mg/L. This model produced a good curve fit of the average plasma and unbound muscle voriconazole concentrations (Figure 6-10 and 6-11).

The data of unbound plasma voriconazole concentration from 5 and 10 mg/kg intravenous dose were obtained from total plasma concentration based on a protein binding of 66.2% in rat plasma, which was measured by *in vitro* microdialysis as described in Chapter 5. The average data of unbound plasma voriconazole were also calculated and plotted in the same figures (Figure 6-10 and 6-11).

Discussion

In this study, the pharmacokinetics of voriconazole in male Wistar rats in doses of 5 and 10 mg/kg given intravenously was investigated. Plasma concentrations as well as unbound tissue concentrations in thigh muscle were measured. As it is known, antifungal effect relates to the antifungal agent concentrations in plasma and tissue at the target site. The aim was to establish the relationship between plasma concentration and tissue concentration, which may allow us to predict the pharmacodynamic effect of antifungal agent and help optimize the dosage regimen.

Elimination of voriconazole from plasma does not follow simple linear pharmacokinetics in rats which is consistent with the previous report [31]. The voriconazole plasma profiles following intravenous administration (Figure 6-3, 6-4) are convex to some extent indicating the characteristic of compounds that show capacity-limited elimination. Compared the 5 mg/kg dosing regimen to 10 mg/kg, pharmacokinetic parameters are dependent upon dose. There was superproportional increase in area under the curve was seen with increasing dose in rat studies. There is 2.7-fold increase in AUC for a 2-fold increase in intravenous dose. It has been reported that voriconazole was eliminated predominantly by metabolism such as the human hepatic cytochrome P450 enzymes of CYP2C19, CYP2C9 and CYP3A4 [31]. The terminal elimination half-lives calculated for voriconazole in was 3.95h for 5mg/kg dosage and 4.92h for 10mg/kg dosage, which is similar to what has been reported in the literatures for rats [31, 154]. In Araujo, et al's report, the estimated half-life was found to be 2.4±0.6 h considering that the pharmacokinetic study was carried out for 8 h. In Roffey, et al's report, the voriconazole's plasma PK data were extracted and concentrations were fitted

to a noncompartment analysis (NCA) model using WinNonlin. The estimated half-life was found to be 4 h considering that the pharmacokinetic study was carried out for 6h.

The elimination of voriconazole was characterized by nonlinear pharmacokinetics in rats. It is likely that saturation of metabolic clearance is the cause of the nonlinearity. Compared the fit of linear with nonlinear models, 1-compartment with 2-compartment models, the 2-compartment with nonlinear elimination had the best fitting with a lowest AIC value of -344.03.

Microdialysis has been reported to be a very useful technique to measure a variety of drugs in different tissues or endogenous compounds *in vivo* [73, 133, 155]. It is very important to determine the probe recovery when applying microdialysis for a new compound if a good prediction of the true tissue levels is wanted. The recoveries of voriconazole in rat muscle were determined by retrodialysis method in our studies.

Voriconazole exhibits moderate plasma protein binding and is independent of plasma drug concentrations *in vitro.* The unbound concentrations of voriconazole in the muscle were measured directly and compared with the calculated free plasma concentrations using the average plasma protein binding of voriconazole in rat of 66.2%. The results showed that muscle had similar concentrations of unbound plasma concentrations.

We fitted plasma and tissue concentrations simultaneously. A two-compartment model with nonlinear elimination described the data well and resulted in a value of f*u* (0.38) for muscle. The f*u* can be interpreted as the free fraction of voriconazole in tissue such as in muscle which might be affected by the subject's covariates, weight, height, and the plasma albumin concentration [156, 157].

In summary, a two-compartment model with non-linear elimination was able to produce a good curve of both the individual and the average plasma and muscle voriconazole concentrations. The unbound voriconazole concentrations in muscle were almost identical with the calculated unbound plasma concentrations for different dosages indicating the muscle microdialysis sample may be used for estimating the free plasma levels for voriconazole. The free fraction of voriconazole in tissue (f*u*) can also be predicted by PK analysis.

Table 6-1. Recovery data of voriconazole using retrodialysis (RD) method in rats muscle

Animal	Recovery (%)	
	1 μg/ml	2 μg/ml
1	39.9	53.6
2	41.5	46.9
3	37.6	51.0
4	46.3	43.4
5	48.1	43.8
6	46.1	47.1
Mean (%)	43.3	47.6
SD (%)	4.2	4.0

Table 6-2. Total plasma voriconazole (5 mg/kg) individual noncompartmental pharmacokinetics analysis

Time (hr)	Concentration (mg/L)								
	51	52	53	54	55	56	Mean	SD	Median
0.17	3.46	3.94	3.58	3.52	3.14	3.50	3.52	0.26	3.51
0.50	2.98	3.35	3.20	3.12	2.75	3.01	3.07	0.21	3.06
1.00	2.63	3.05	2.82	2.72	2.48	2.54	2.71	0.21	2.67
1.50	2.39	2.68	2.64	2.59	2.25	2.33	2.48	0.18	2.49
2.00	2.27	2.54	2.40	2.35	2.09	2.11	2.29	0.17	2.31
3.00	2.14	2.36	2.22	2.05	1.89	1.79	2.08	0.21	2.10
4.00	1.86	2.07	2.01	1.83	1.74	1.59	1.85	0.18	1.85
5.00	1.68	1.73	1.78	1.48	1.46	1.30	1.57	0.19	1.58
6.00	1.42	1.52	1.52	1.23	1.19	1.01	1.31	0.21	1.32
8.00	1.03	1.07	1.06	0.84	0.86	0.72	0.93	0.14	0.95
K_e [hr^{-1}]	0.16	0.16	0.17	0.19	0.18	0.20	0.18	0.02	0.18
$t_{1/2}$ [hr]	4.26	4.37	3.99	3.67	3.92	3.48	3.95	0.34	3.95
C_0 [mg/L]	3.73	4.27	3.79	3.74	3.36	3.78	3.78	0.29	3.76
AUC_∞[(mg/L)·hr]	21.80	23.76	22.52	19.40	18.74	16.99	20.53	2.57	20.60
$AUMC_\infty$ [(mg/L)·hr^2]	140.10	150.96	137.42	105.33	110.59	87.02	121.90	24.64	124.01
MRT_∞ [hr]	6.43	6.35	6.10	5.43	5.90	5.12	5.89	0.52	6.00
V_c [mL/g]	1.34	1.17	1.32	1.34	1.49	1.32	1.33	0.10	1.33
Vd_{ss} [mL/g]	1.47	1.34	1.35	1.40	1.58	1.51	1.44	0.09	1.44
CL [mL/hr/g]	0.23	0.21	0.22	0.26	0.27	0.29	0.25	0.03	0.24

Table 6-3. Total plasma voriconazole (10 mg/kg) individual noncompartmental pharmacokinetics analysis

Time (hr)	Concentration (mg/L)								
	101	102	103	104	105	106	Mean	SD	Median
0.17	7.16	7.53	7.11	7.61	7.26	7.45	7.35	0.21	7.35
0.50	6.31	6.80	6.46	7.05	6.33	6.67	6.60	0.29	6.57
1.00	5.75	6.19	5.93	6.60	5.53	6.22	6.04	0.38	6.06
1.50	5.34	6.02	5.35	5.62	5.26	5.99	5.60	0.34	5.48
2.00	5.02	5.37	5.05	5.50	5.10	5.25	5.21	0.19	5.18
3.00	4.51	5.13	4.76	5.26	4.78	5.00	4.91	0.28	4.89
4.00	4.30	5.07	4.46	4.87	4.10	4.54	4.56	0.36	4.50
5.00	3.78	4.56	4.08	4.33	3.94	4.20	4.15	0.28	4.14
6.00	3.21	4.03	3.61	3.74	3.24	3.94	3.63	0.35	3.68
8.00	2.39	2.96	2.78	2.81	2.56	2.82	2.72	0.21	2.80
K_e [hr^{-1}]	0.15	0.15	0.13	0.14	0.14	0.14	0.14	0.01	0.14
$t_{1/2}$ [hr]	4.56	4.76	5.40	4.81	4.95	5.03	4.92	0.29	4.88
C_0 [mg/L]	7.63	7.93	7.46	7.91	7.78	7.87	7.76	0.18	7.83
AUC_∞[(mg/L)·hr]	49.88	59.62	57.69	58.13	52.84	58.29	56.07	3.82	57.91
$AUMC_\infty$ [(mg/L)·hr^2]	342.79	438.36	465.78	422.35	392.91	441.91	417.35	43.75	430.35
MRT_∞ [hr]	6.87	7.35	8.07	7.27	7.44	7.58	7.43	0.40	7.39
V_c [mL/g]	1.31	1.26	1.34	1.26	1.29	1.27	1.29	0.03	1.28
Vd_{ss} [mL/g]	1.38	1.22	1.50	1.18	1.37	1.32	1.33	0.12	1.34
CL [mL/hr/g]	0.20	0.17	0.19	0.16	0.18	0.17	0.18	0.01	0.18

Table 6-4. Comparison of objective function value (OFV) and Akaike information criterion (AIC) value from rats total plasma voriconazole PK analysis using different models

Models	Total number of parameters (p)	Objective function value (OFV)	Akaike information criterion (AIC) value
1-compartment with linear elimination	5	-240.73	-230.73
1-compartment with nonlinear elimination	7	-249.17	-235.17
2-compartment with linear elimination	9	-295.77	-277.77
2-compartment with nonlinear elimination	11	-366.03	-344.03

Table 6-5. One-compartment model with linear elimination for rat total plasma voriconazole PK analysis

Parameter estimates	Population estimate (SE%)	Between subject variability (BSV) (SE%)
CL (L/hr)	0.082 (8.7)	22.4% (37.3)
V (L)	0.58 (1.7)	5.1% (31.5)
	Residual variability	
Proportional error	5.5% (6.8)	

Note: % SE: percent standard error of the population parameter estimate.

Table 6-6. Two-compartment model with linear elimination for rat total plasma voriconazole PK analysis

Parameter estimates	Population estimate (SE%)	Between subject variability (BSV) (SE%)
CL (L/hr)	0.070 (6.7)	23.5% (28.3)
V_1 (L)	0.49 (1.7)	6.3% (28.0)
Q (L/hr)	0.35 (11.8)	10.0% (-)
V_2 (L)	0.11 (7.9)	10.0% (-)
	Residual variability	
Proportional error	3.9% (12.1)	

Note: Dashes indicate that the respective parameters tested during model building were fixed. % SE: percent standard error of the population parameter estimate.

Table 6-7. One-compartment with non-linear elimination model for rat total plasma voriconazole PK analysis

Parameter estimates	Population estimate (SE%)	Between subject variability (BSV) (SE%)
V_{max} (mg/hr)	0.86 (24.8)	9.3% (74.7)
K_m (mg/L)	4.55 (31.0)	1.0% (-)
V (L)	0.59 (1.5)	5.7% (27.5)
	Residual variability	
Proportional error	5.5% (5.9)	

Note: Dashes indicate that the respective parameters tested during model building were fixed. % SE: percent standard error of the population parameter estimate.

Table 6-8. Two-compartment with non-linear elimination model for rat total plasma voriconazole PK analysis

Parameter estimates	Population estimate (SE%)	Between subject variability (BSV) (SE%)
V_1 (L)	0.50 (1.6)	6.5% (29.8)
Q (L/hr)	0.28 (8.6)	10.0% (-)
V_2 (L)	0.14 (6.5)	11.4% (96.2)
V_{max} (mg/hr)	0.34 (8.1)	12.0% (42.4)
K_m (mg/L)	1.52 (17.5)	10.0% (-)
	Residual variability (SE%)	
Proportional error	2.9% (15.9)	

Note: Dashes indicate that the respective parameters tested during model building were fixed. % SE: percent standard error of the population parameter estimate.

Table 6-9. Unbound muscle voriconazole (5 mg/kg) individual noncompartmental pharmacokinetics analysis

Time (hr)	Concentration (mg/L)								
	51	52	53	54	55	56	Mean	SD	Median
0.33	1.39	1.40	1.70	1.43	1.54	1.48	1.49	0.12	1.45
0.67	1.16	1.24	1.50	1.17	1.28	1.17	1.25	0.13	1.21
1.00	1.12	1.19	1.34	0.90	1.27	1.10	1.15	0.15	1.15
1.33	1.02	1.14	1.13	0.86	1.17	0.89	1.03	0.13	1.07
1.67	0.90	1.06	1.07	0.80	1.07	0.82	0.95	0.13	0.98
2.00	0.83	0.94	1.05	0.79	0.98	0.80	0.90	0.11	0.88
2.33	0.77	0.86	1.00	0.71	0.92	0.71	0.83	0.12	0.82
2.67	0.74	0.84	0.93	0.67	0.90	0.69	0.80	0.11	0.79
3.00	0.71	0.80	0.86	0.67	0.88	0.67	0.77	0.09	0.75
3.33	0.68	0.78	0.82	0.63	0.87	0.65	0.74	0.10	0.73
3.67	0.65	0.76	0.77	0.58	0.87	0.63	0.71	0.11	0.71
4.00	0.63	0.74	0.76	0.56	0.83	0.61	0.69	0.10	0.68
4.33	0.61	0.71	0.70	0.55	0.74	0.58	0.65	0.08	0.65
4.67	0.59	0.67	0.65	0.49	0.72	0.56	0.61	0.08	0.62
5.00	0.57	0.65	0.64	0.49	0.69	0.54	0.59	0.08	0.60
5.33	0.56	0.61	0.60	0.43	0.66	0.54	0.57	0.08	0.58
5.67	0.55	0.60	0.58	0.42	0.64	0.51	0.55	0.08	0.57
6.00	0.54	0.57	0.57	0.40	0.62	0.47	0.53	0.08	0.55
6.33	0.53	0.54	0.55	0.37	0.60	0.45	0.51	0.08	0.54
6.67	0.51	0.54	0.49	0.35	0.57	0.43	0.48	0.08	0.50
7.00	0.50	0.51	0.45	0.32	0.55	0.40	0.45	0.09	0.47
7.33	0.46	0.49	0.42	0.30	0.51	0.38	0.43	0.08	0.44
7.67	0.41	0.45	0.38	0.27	0.48	0.36	0.39	0.07	0.40
8.00	0.39	0.41	0.36	0.25	0.44	0.31	0.36	0.07	0.37
K_e [hr^{-1}]	0.26	0.27	0.24	0.25	0.22	0.25	0.25	0.02	0.25
$t_{1/2}$ [hr]	2.69	2.61	2.94	2.74	3.17	2.83	2.83	0.20	2.78
AUC_∞[(mg/L)·hr]	7.33	7.90	8.22	6.04	8.85	6.77	7.52	1.02	7.62
$AUMC_\infty$ [(mg/L)·hr^2]	36.59	38.61	38.93	26.64	47.34	32.18	36.72	6.98	37.60
MRT_∞ [hr]	4.99	4.89	4.73	4.41	5.35	4.75	4.85	0.31	4.82
CL [mL/hr/g]	0.68	0.63	0.61	0.83	0.57	0.74	0.68	0.10	0.66

Table 6-10. Unbound muscle voriconazole (10 mg/kg) individual noncompartmental pharmacokinetics analysis

Time (hr)	Concentration (mg/L)								
	101	102	103	104	105	106	Mean	SD	Median
0.33	2.59	2.42	2.37	2.80	3.00	3.25	2.74	0.34	2.69
0.67	2.42	2.29	2.25	2.52	2.74	2.91	2.52	0.26	2.47
1.00	2.09	2.00	1.84	2.11	2.22	2.51	2.13	0.23	2.10
1.33	2.04	1.77	1.57	2.09	2.05	2.30	1.97	0.26	2.04
1.67	1.82	1.73	1.54	2.01	2.02	2.19	1.88	0.23	1.91
2.00	1.67	1.69	1.43	1.86	1.96	2.16	1.79	0.26	1.77
2.33	1.56	1.63	1.37	1.81	1.92	2.15	1.74	0.28	1.72
2.67	1.48	1.62	1.35	1.76	1.85	2.10	1.69	0.27	1.69
3.00	1.46	1.47	1.30	1.67	1.82	1.99	1.62	0.26	1.57
3.33	1.44	1.46	1.28	1.57	1.80	1.95	1.58	0.24	1.52
3.67	1.40	1.45	1.26	1.52	1.70	1.91	1.54	0.23	1.49
4.00	1.39	1.37	1.23	1.47	1.68	1.88	1.50	0.24	1.43
4.33	1.34	1.36	1.22	1.41	1.66	1.86	1.47	0.24	1.39
4.67	1.30	1.35	1.21	1.35	1.61	1.77	1.43	0.21	1.35
5.00	1.26	1.32	1.19	1.32	1.55	1.73	1.40	0.20	1.32
5.33	1.24	1.27	1.18	1.27	1.51	1.71	1.36	0.20	1.27
5.67	1.22	1.24	1.16	1.23	1.48	1.64	1.33	0.19	1.23
6.00	1.17	1.22	1.14	1.20	1.46	1.61	1.30	0.19	1.21
6.33	1.17	1.19	1.12	1.16	1.45	1.60	1.28	0.20	1.18
6.67	1.15	1.16	1.09	1.13	1.39	1.58	1.25	0.19	1.16
7.00	1.12	1.13	1.03	1.10	1.32	1.56	1.21	0.20	1.13
7.33	1.09	1.09	1.00	1.06	1.29	1.53	1.18	0.20	1.09
7.67	1.06	1.06	0.98	1.01	1.23	1.49	1.14	0.19	1.06
8.00	1.02	1.03	0.94	0.97	1.19	1.47	1.11	0.20	1.03
K_e [hr^{-1}]	0.12	0.09	0.13	0.13	0.12	0.06	0.11	0.03	0.12
$t_{1/2}$ [hr]	5.95	7.57	5.49	5.44	5.75	11.30	6.92	2.29	5.85
AUC_∞[(mg/L)·hr]	20.88	23.28	18.39	20.43	24.19	39.94	24.52	7.84	22.08
$AUMC_\infty$ [(mg/L)·hr^2]	186.06	254.35	156.14	162.96	210.20	638.19	267.98	184.84	198.13
MRT_∞ [hr]	8.91	10.93	8.49	7.98	8.69	15.98	10.16	3.02	8.80
CL [mL/hr/g]	0.48	0.42	0.58	0.46	0.40	0.25	0.43	0.11	0.44

Table 6-11. Rat total plasma and unbound muscle voriconazole PK analysis using two-compartment with non-linear elimination model

Parameter estimates	Population estimate (SE%)	Between subject variability (BSV) (SE%)
V_1 (L)	0.50 (1.6)	6.5% (23)
Q (L/hr)	0.28 (8.6)	10.0% (-)
V_2 (L)	0.14 (6.5)	18.7% (70.1)
V_{max} (mg/hr)	0.34 (8.1)	12.1% (24.6)
K_m (mg/L)	1.52 (17.5)	10.0% (-)
fu	0.38 (3.6)	13.0% (41.6)
	Residual variability	
	Total plasma concentration (SE%)	Unbound muscle concentration (SE%)
Proportional error	3.1% (21.6)	26.5% (13.5)
Additive error (mg/L)	-	0.032 (-)

Note: Dashes indicate that the respective parameters tested during model building were fixed. % SE: percent standard error of the population parameter estimate.

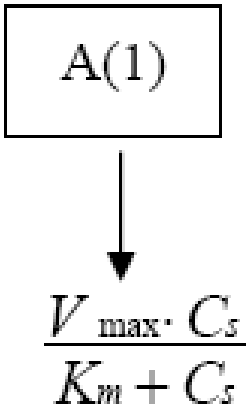

Figure 6-1. Cascade pharmacokinetic one-compartment model with non-linear elimination of voriconazole scheme

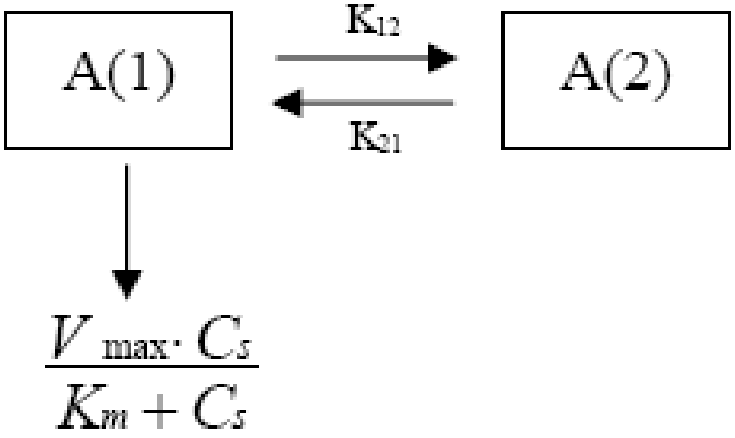

Figure 6-2. Cascade pharmacokinetic two-compartment model with non-linear elimination of voriconazole scheme

A

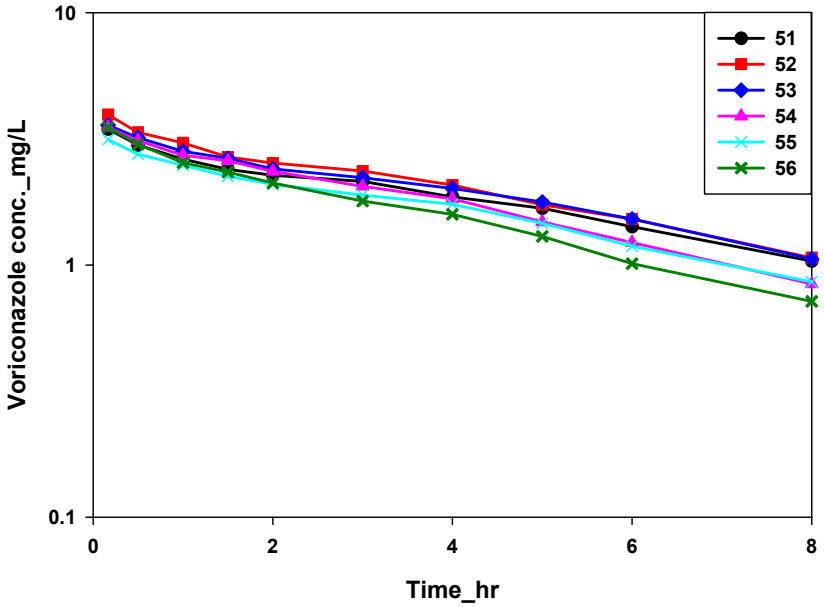

B

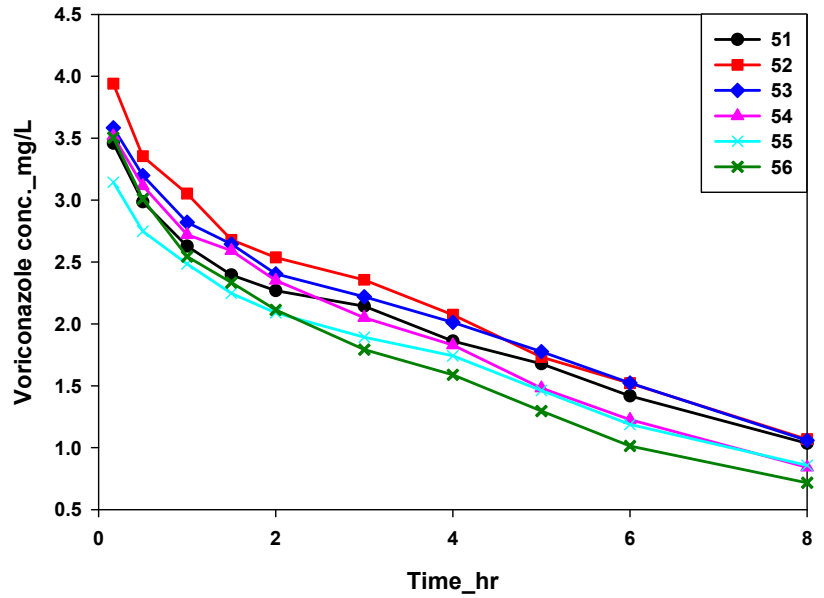

Figure 6-3. Dosage of 5 mg/kg *i.v.* bolus: total voriconazole concentration in rat plasma. A) Linear scale. B) Log scale.

A

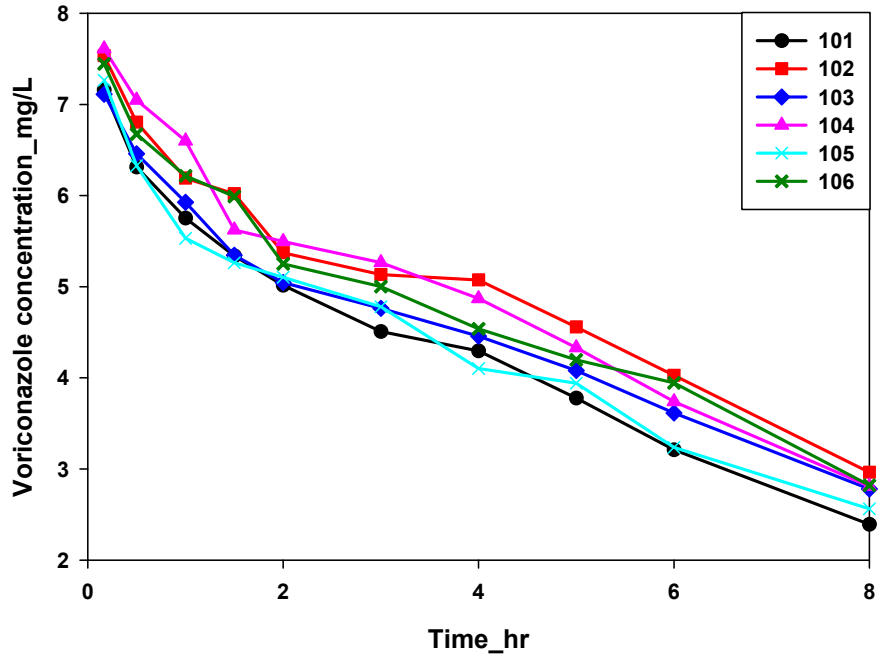

B

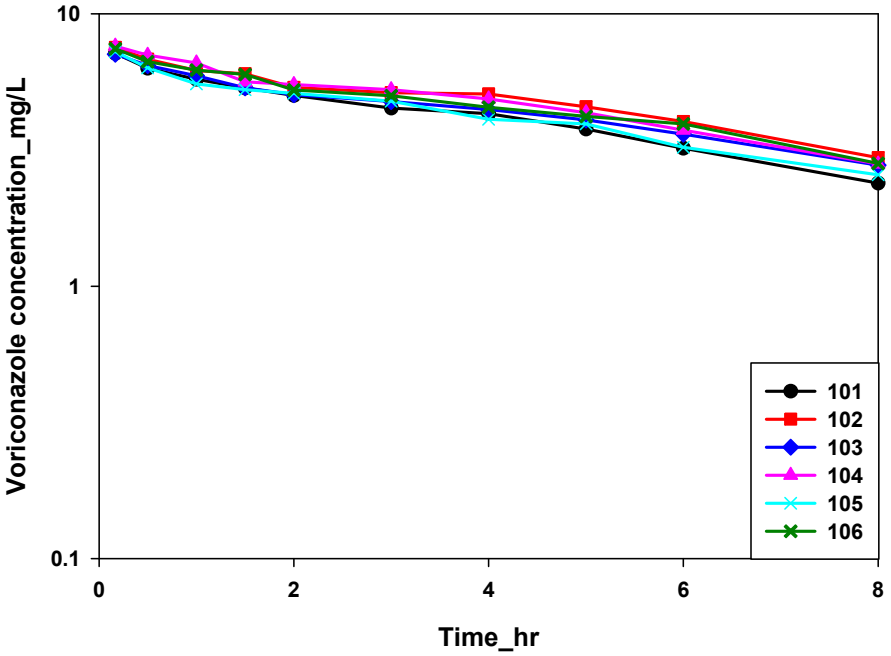

Figure 6-4. Dosage of 10 mg/kg *i.v.* bolus: total voriconazole concentration in rat plasma. A) Linear scale. B) Log scale.

A

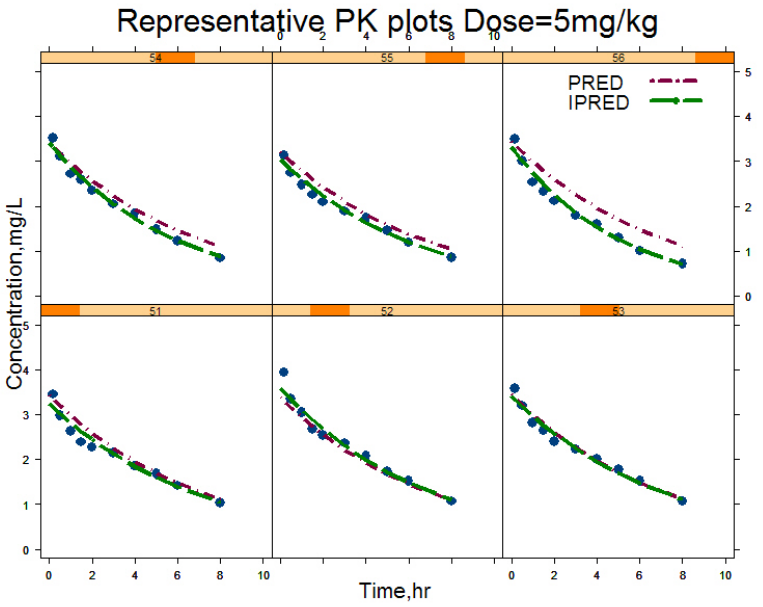

B

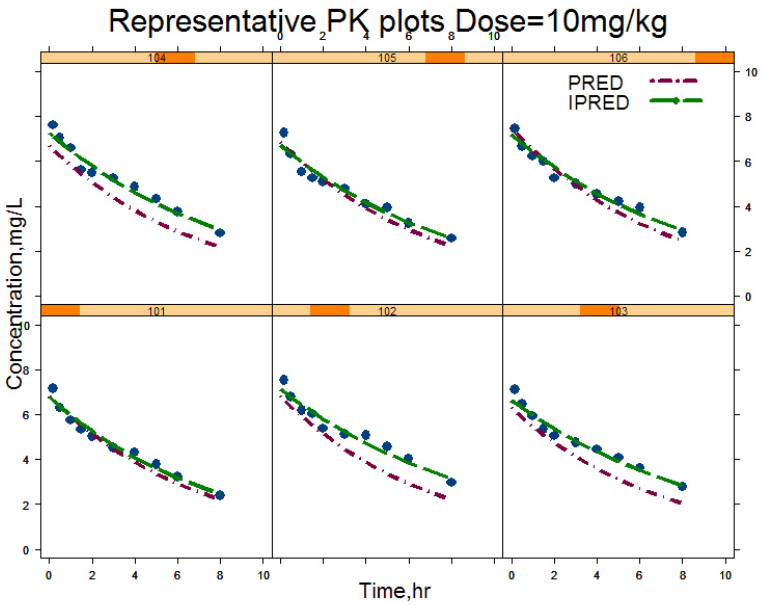

Figure 6-5. The PK plots using one-compartment with linear elimination model for PK analysis of rat total plasma voriconazole data: Plot of observed (•), individual predicted (IPRED) (---) and population predicted (PRED) (---) voriconazole concentration versus time. A) 5 mg/kg dose. B) 10 mg/kg dose.

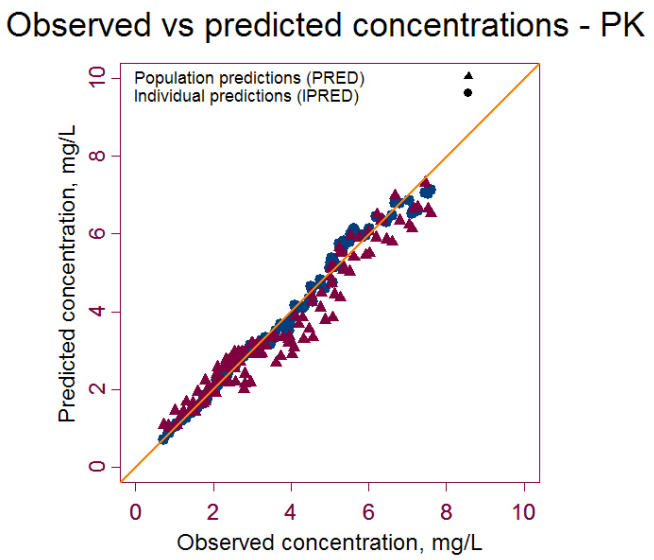

Figure 6-6. Goodness of fit plots for observed vs predicted concentrations (• - Observed vs individual predicted, ▲-Observed vs population predicted) using one-compartment with linear elimination model for PK analysis of rat total plasma voriconazole concentration data.

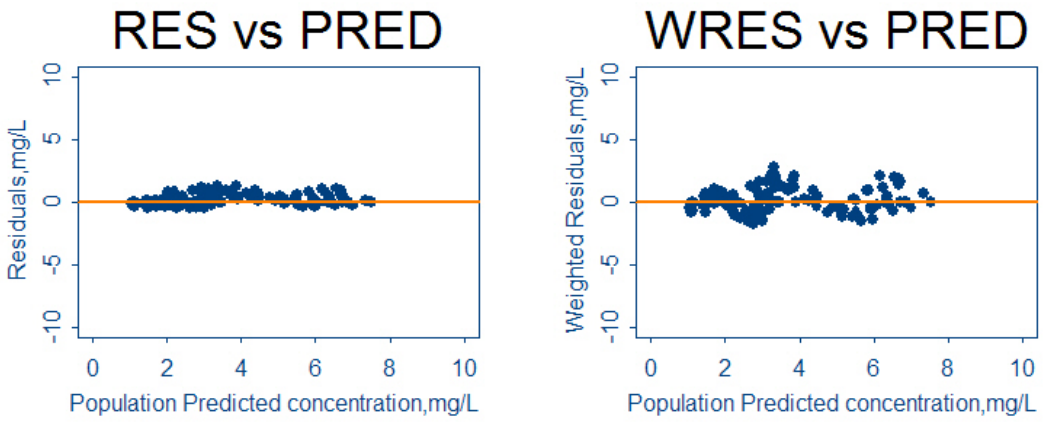

Figure 6-7. Goodness of fit plots for residuals using one-compartment with linear elimination model for PK analysis of rat total plasma voriconazole concentration data.

A

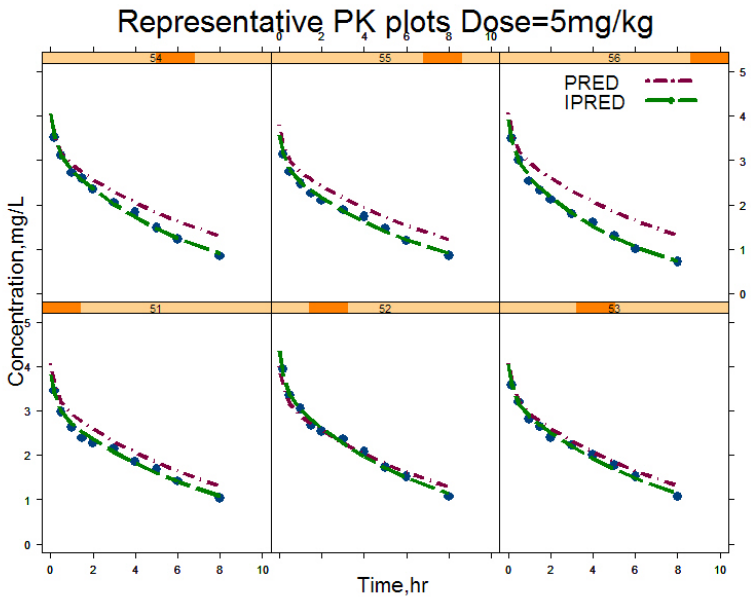

B

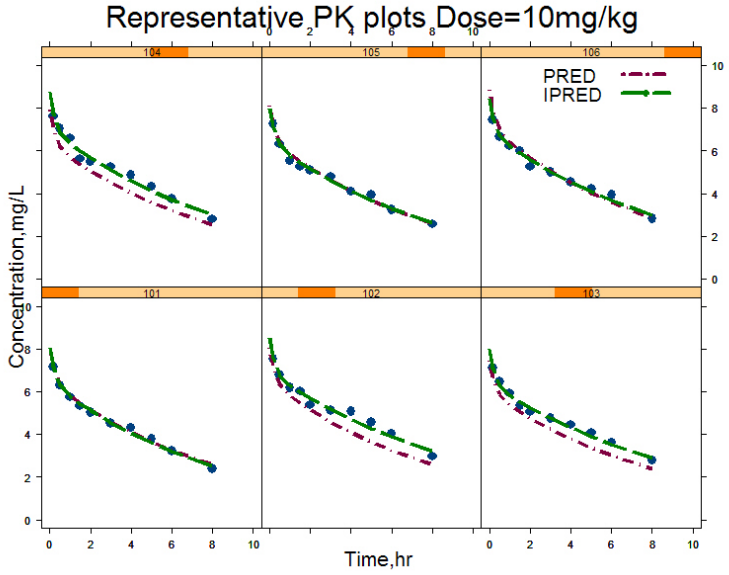

Figure 6-8. The PK plots using two-compartment with linear elimination model for PK analysis of rat total plasma voriconazole data: Plot of observed (•), individual predicted (IPRED) (---) and population predicted (PRED) (---) voriconazole concentration versus time. A) 5 mg/kg dose. B) 10 mg/kg dose.

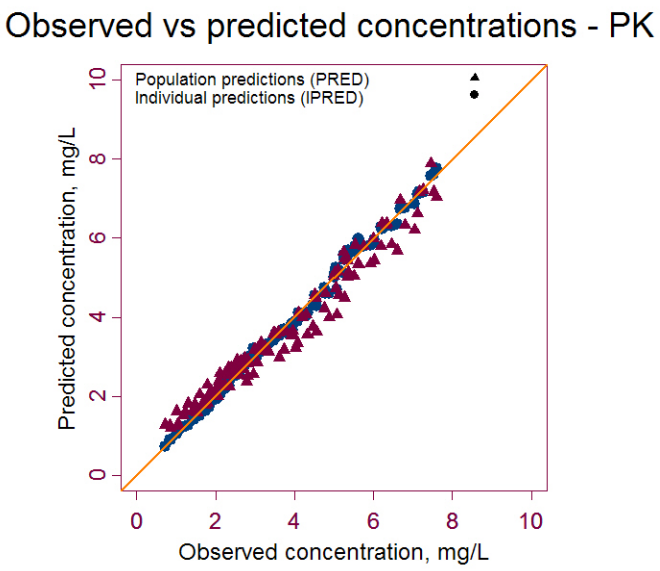

Figure 6-9. Goodness of fit plots for observed vs predicted concentrations (• - Observed vs individual predicted, ▲-Observed vs population predicted) using two -compartment with linear elimination model for PK analysis of rat total plasma voriconazole concentration data.

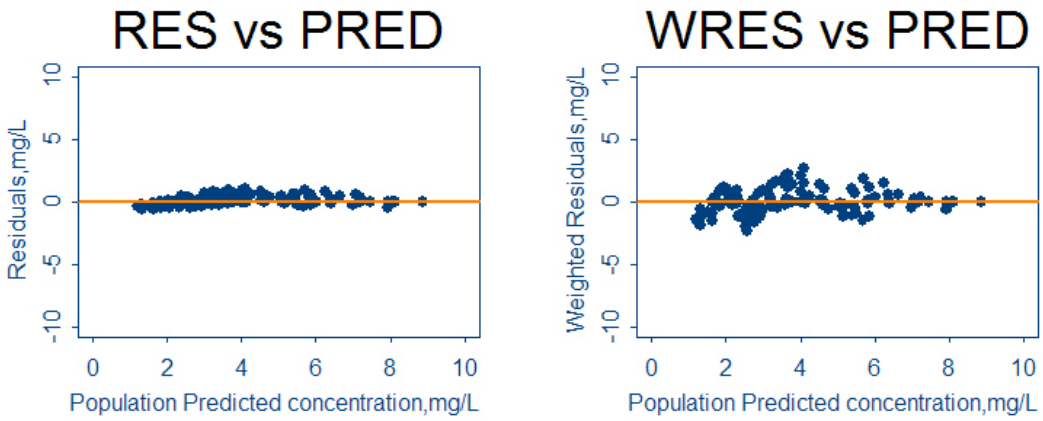

Figure 6-10. Goodness of fit plots for residuals using two-compartment with linear elimination model for PK analysis of rat total plasma voriconazole concentration data.

A

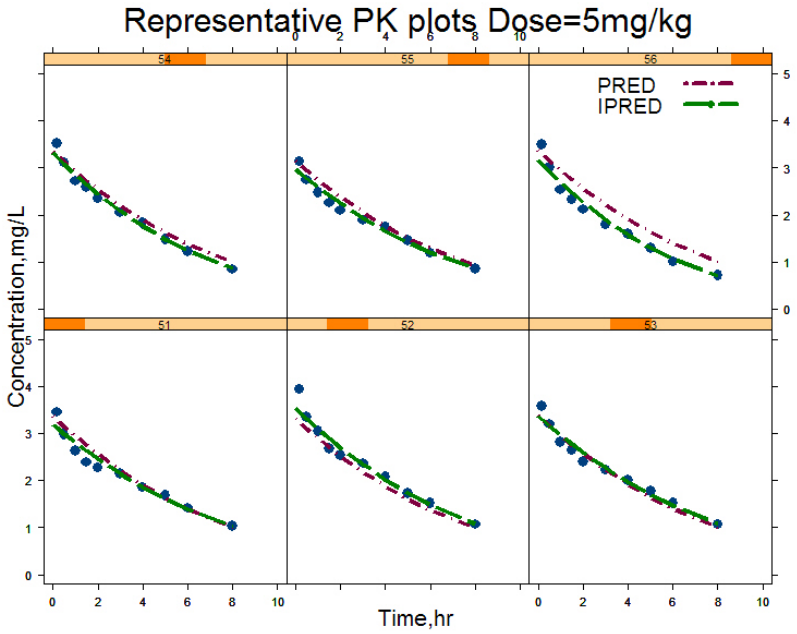

B

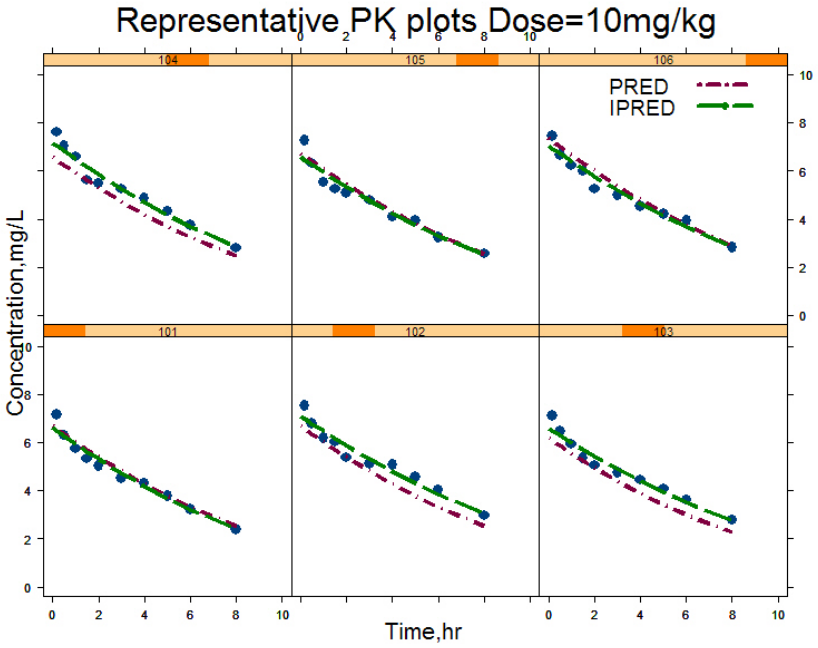

Figure 6-11. The PK plots using one-compartment with non-linear elimination model for PK analysis of rat total plasma voriconazole data: Plot of observed (•), individual predicted (IPRED) (---) and population predicted (PRED) (---) voriconazole concentration versus time. A) 5 mg/kg dose. B) 10 mg/kg dose.

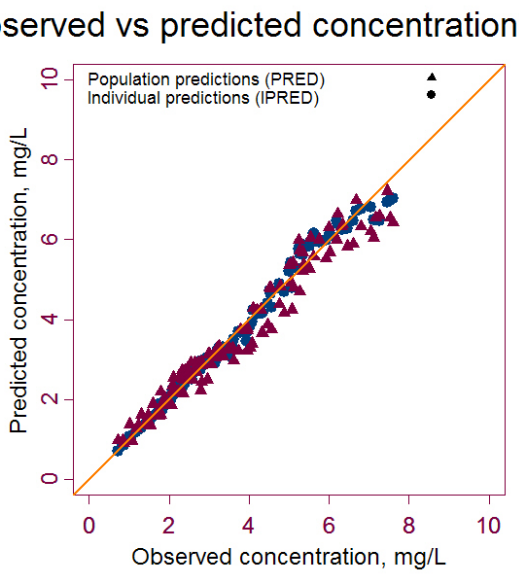

Figure 6-12. Goodness of fit plots for observed vs predicted concentrations (• - Observed vs individual predicted, ▲-Observed vs population predicted) using one-compartment with non-linear elimination model for PK analysis of rat total plasma voriconazole concentration data.

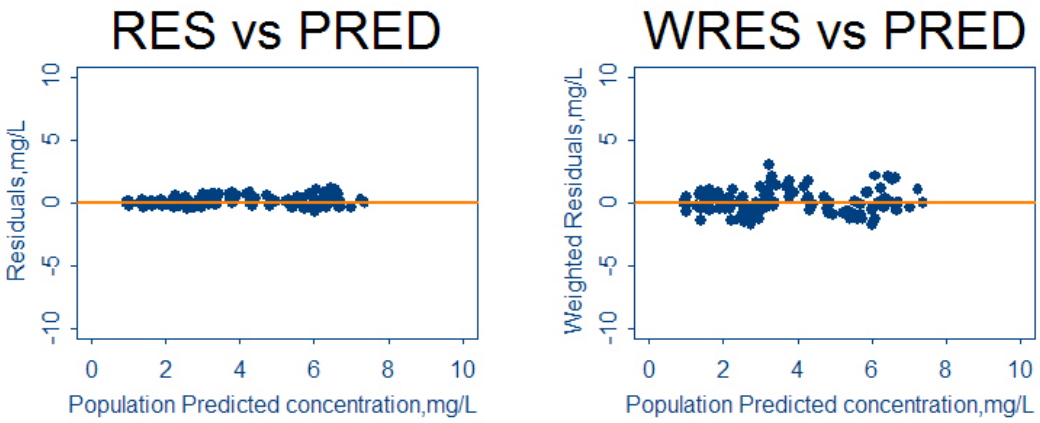

Figure 6-13. Goodness of fit plots for residuals using one-compartment with non-linear elimination model for PK analysis of rat total plasma voriconazole concentration data.

A

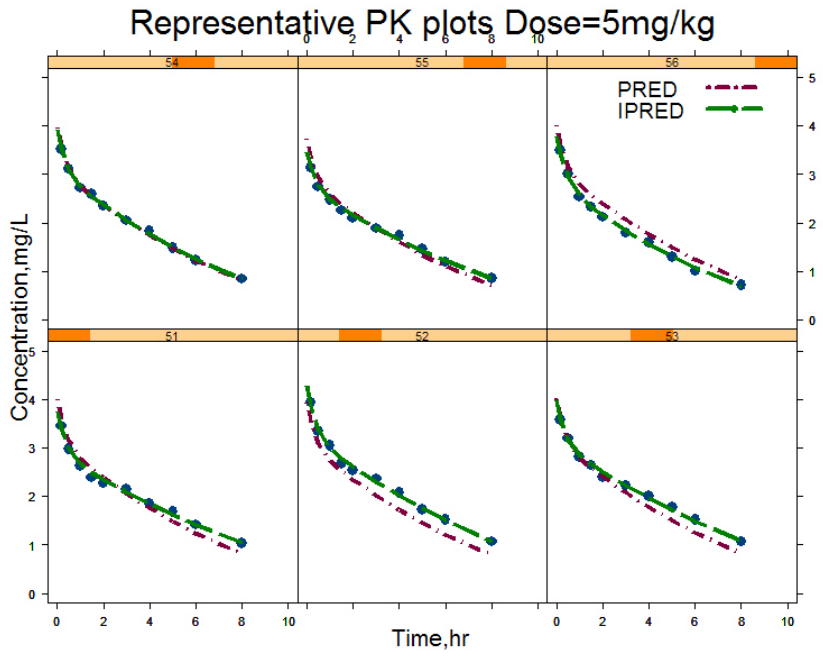

B

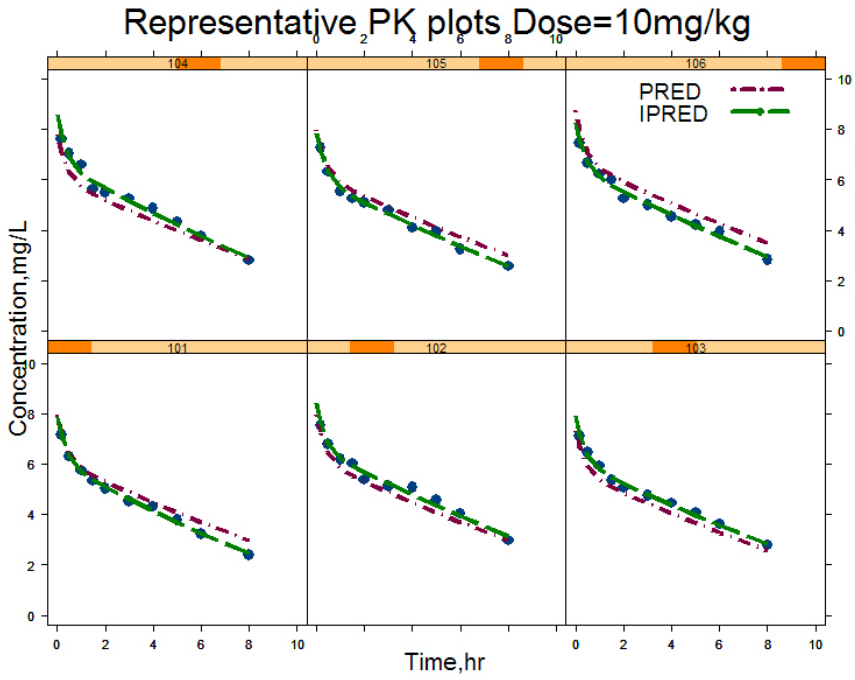

Figure 6-14. The PK plots using two-compartment with non-linear elimination model for PK analysis of rat total plasma voriconazole data: Plot of observed (•), individual predicted (IPRED) (---) and population predicted (PRED) (---) voriconazole concentration versus time. A) 5 mg/kg dose. B) 10 mg/kg dose.

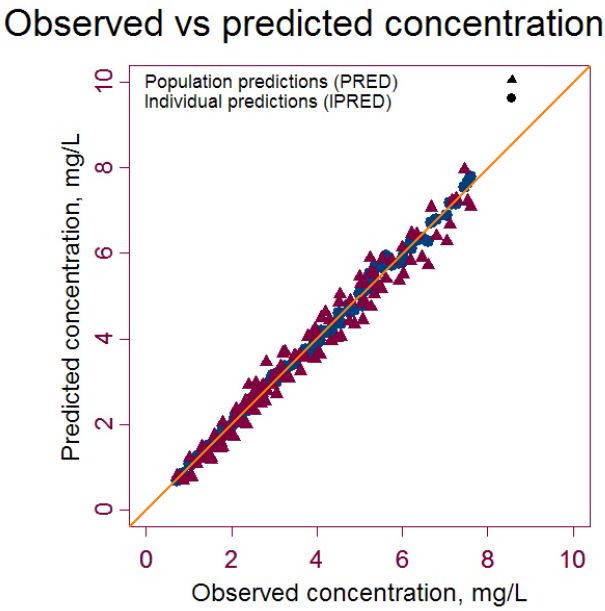

Figure 6-15. Goodness of fit plots for observed vs predicted concentrations (• - Observed vs individual predicted, ▲-Observed vs population predicted) using two-compartment with non-linear elimination model for PK analysis of rat total plasma voriconazole concentration data.

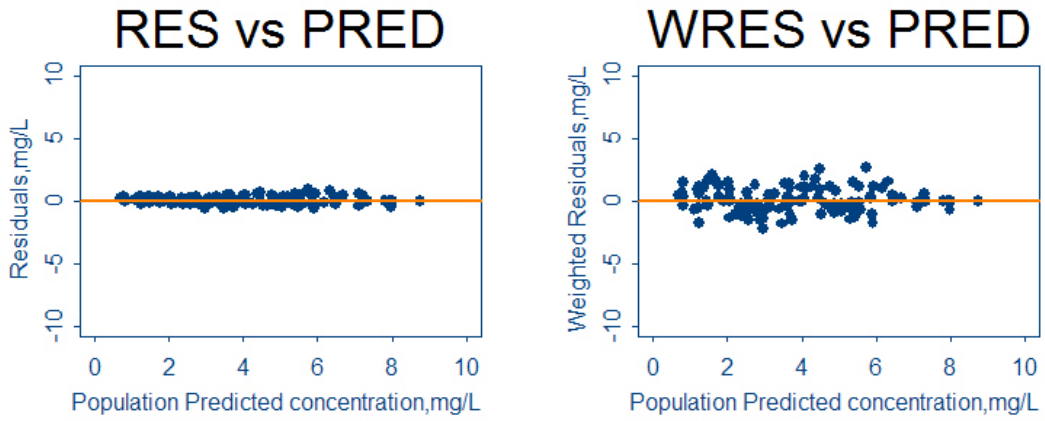

Figure 6-16. Goodness of fit plots for residuals using two-compartment with non-linear elimination model for PK analysis of rat total plasma voriconazole concentration data.

A

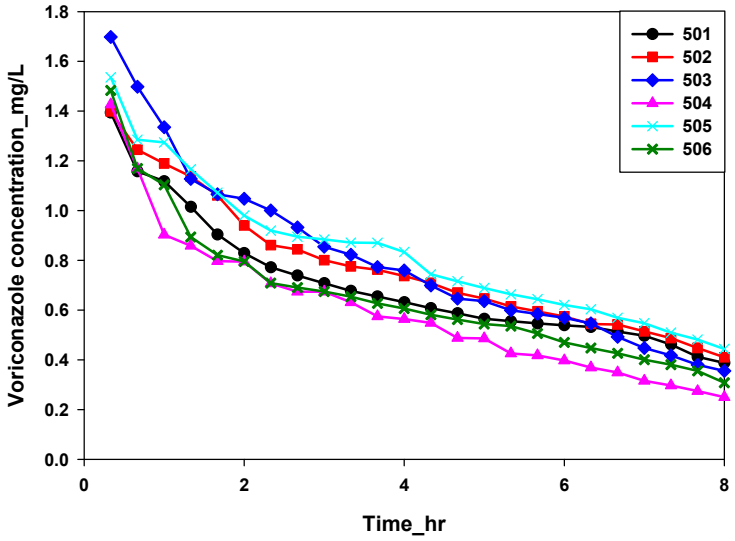

B

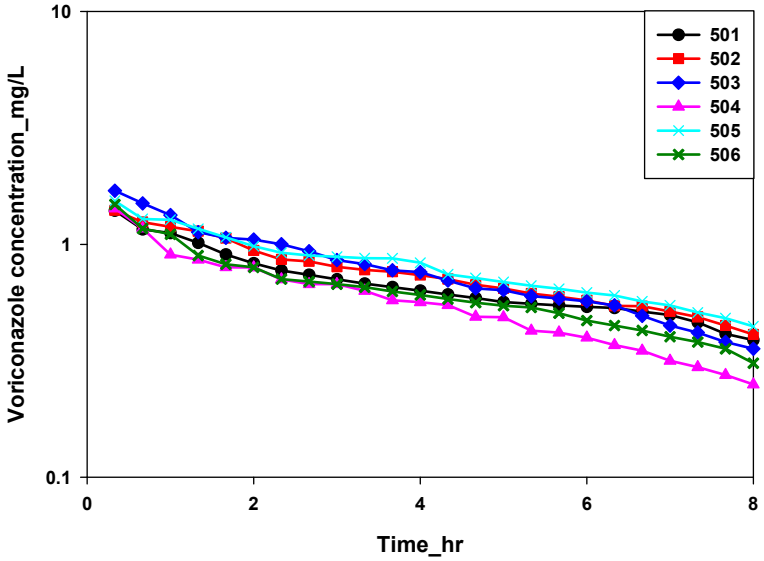

Figure 6-17. Dosage of 5 mg/kg *i.v.* bolus: unbound voriconazole concentration in rat muscle. A) Linear scale. B) Log scale.

A

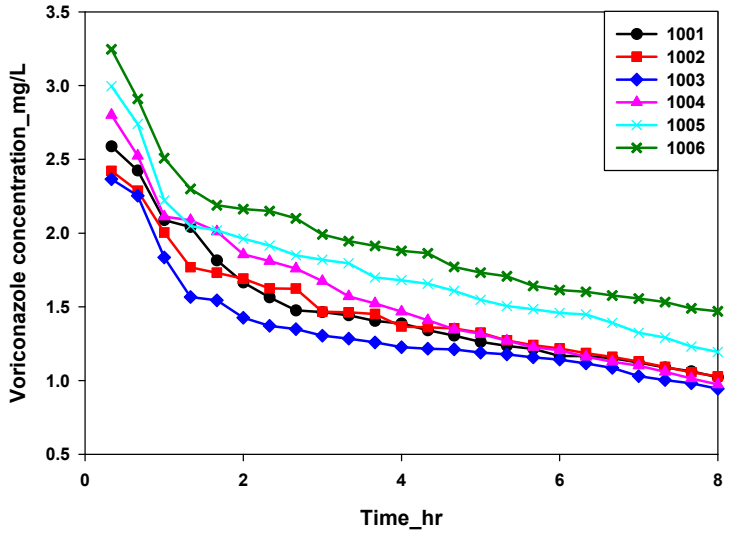

B

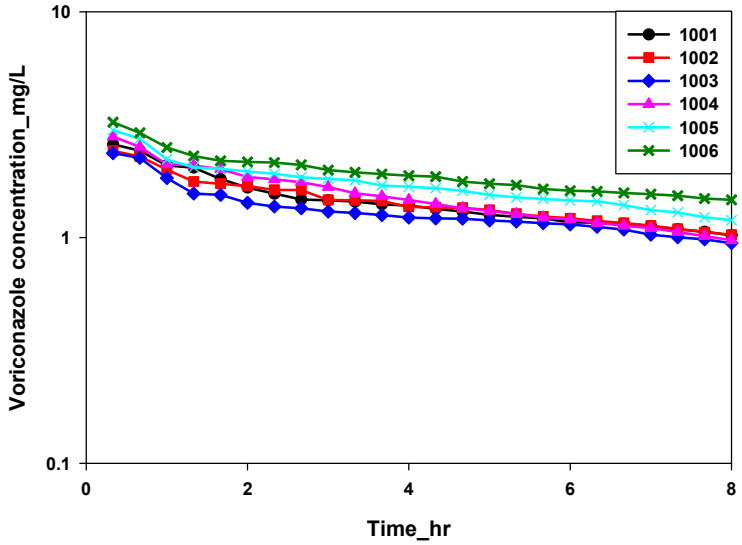

Figure 6-18. Dosage of 10 mg/kg *i.v.* bolus: unbound voriconazole concentration in rat muscle. A) Linear scale. B) Log scale.

A

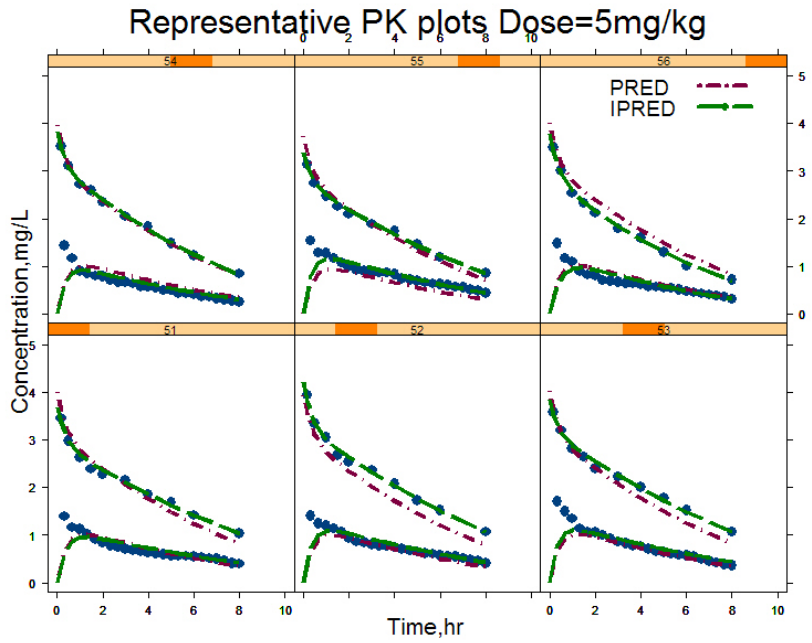

B

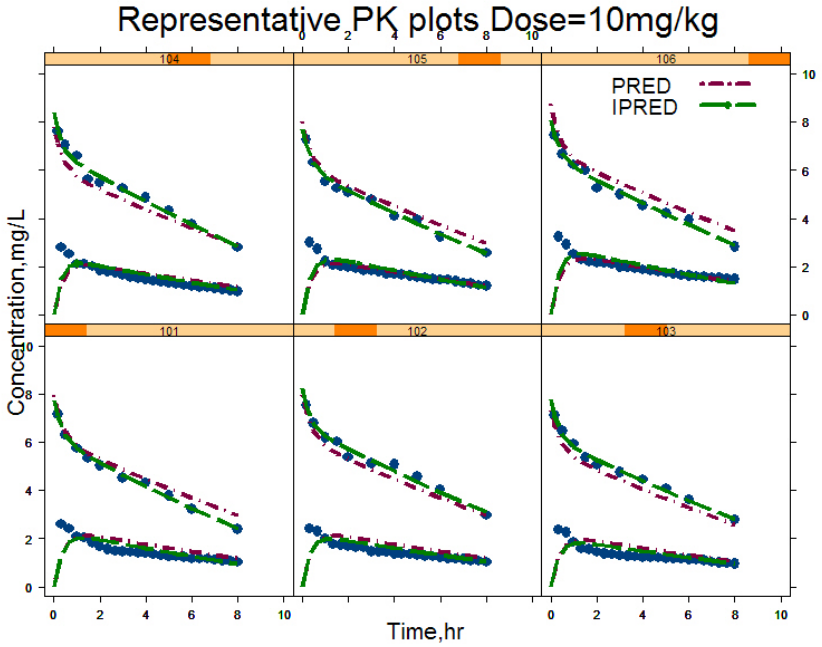

Figure 6-19. The PK plots using two-compartment with non-linear elimination model for analysis of rat total plasma (upper curves) and unbound muscle (lower curves) voriconazole data: Plot of observed (•), individual predicted (IPRED) (---) and population predicted (PRED) (---) voriconazole concentration versus time. A) 5 mg/kg dose. B) 10 mg/kg dose.

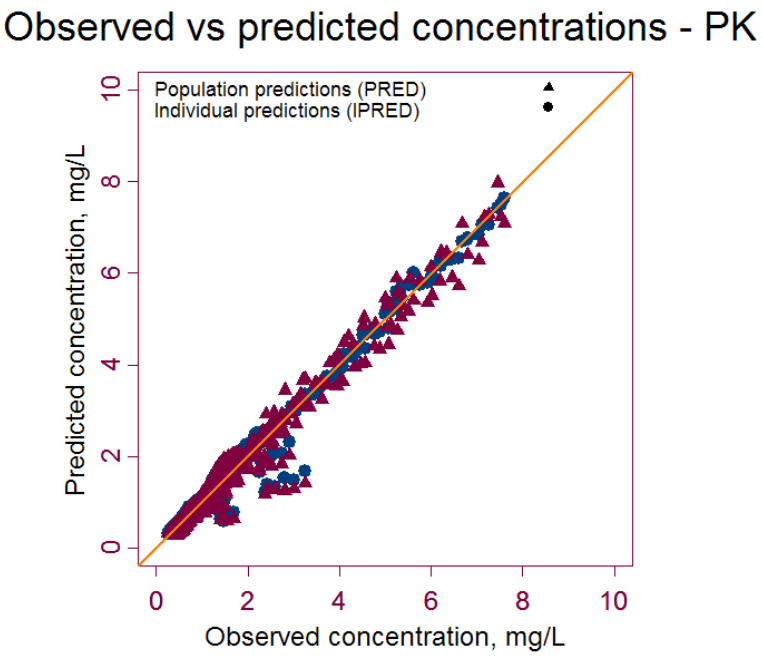

Figure 6-20. Goodness of fit plots for observed vs predicted concentrations (• - Observed vs individual predicted, ▲-Observed vs population predicted) using two-compartment with non-linear elimination model for PK analysis of rat total plasma and unbound muscle voriconazole concentration data.

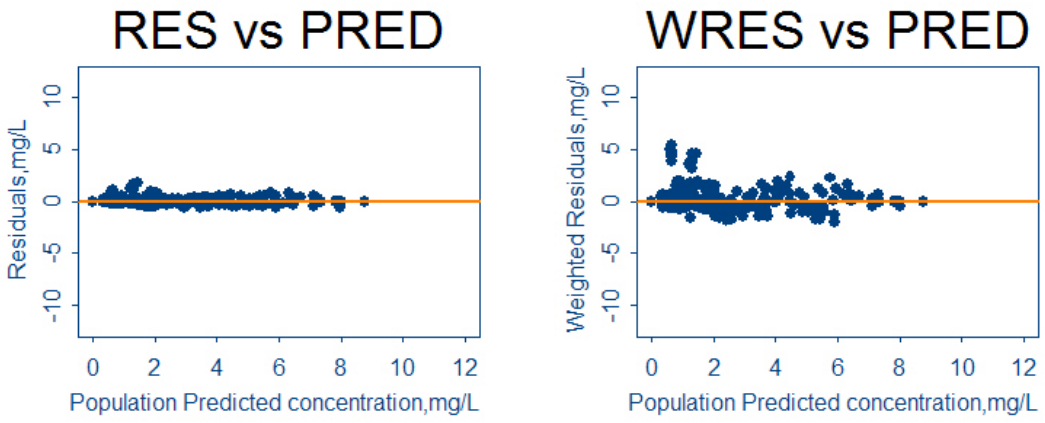

Figure 6-21. Goodness of fit plots for residuals using two-compartment with non-linear elimination model for PK analysis of rat total plasma and unbound muscle voriconazole concentration data.

A

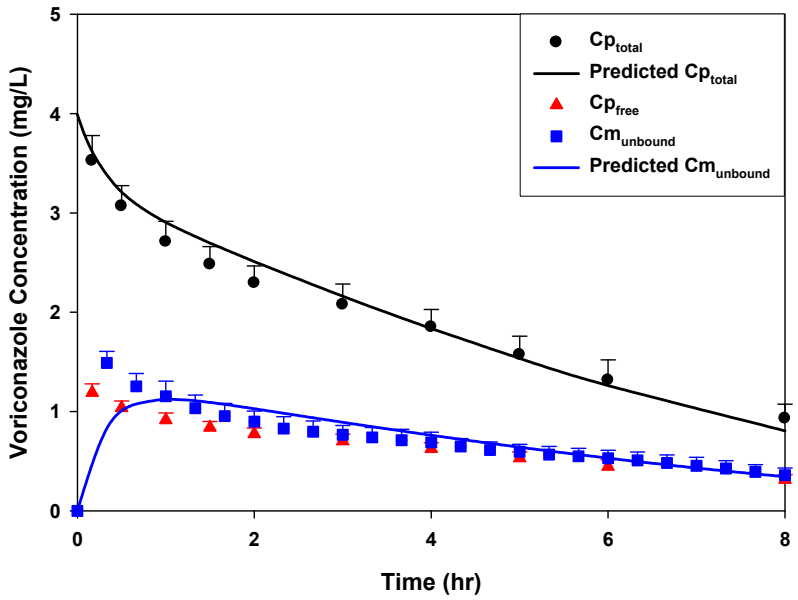

B

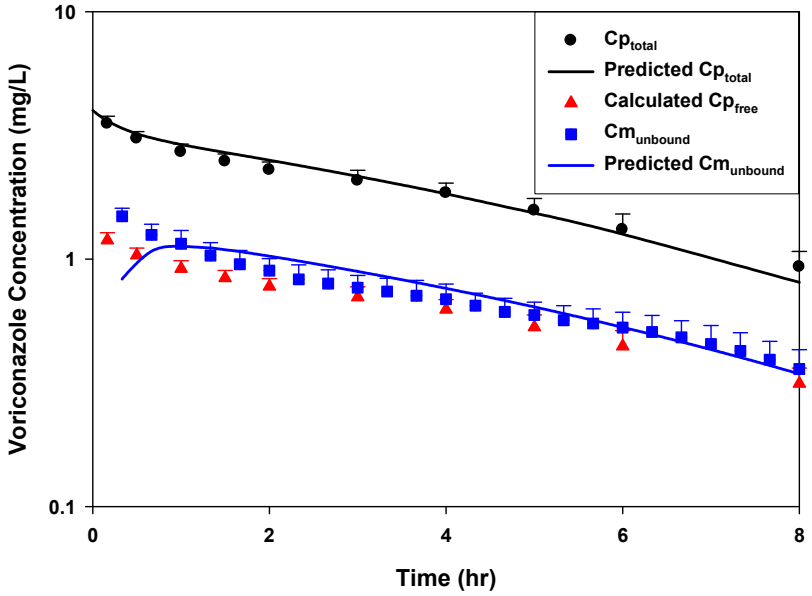

Figure 6-22. Dosage of 5 mg/kg *i.v.* bolus in rat: average plasma and muscle PK data analysis using two-compartment with non-linear elimination model. A) Linear scale. B) Log scale.

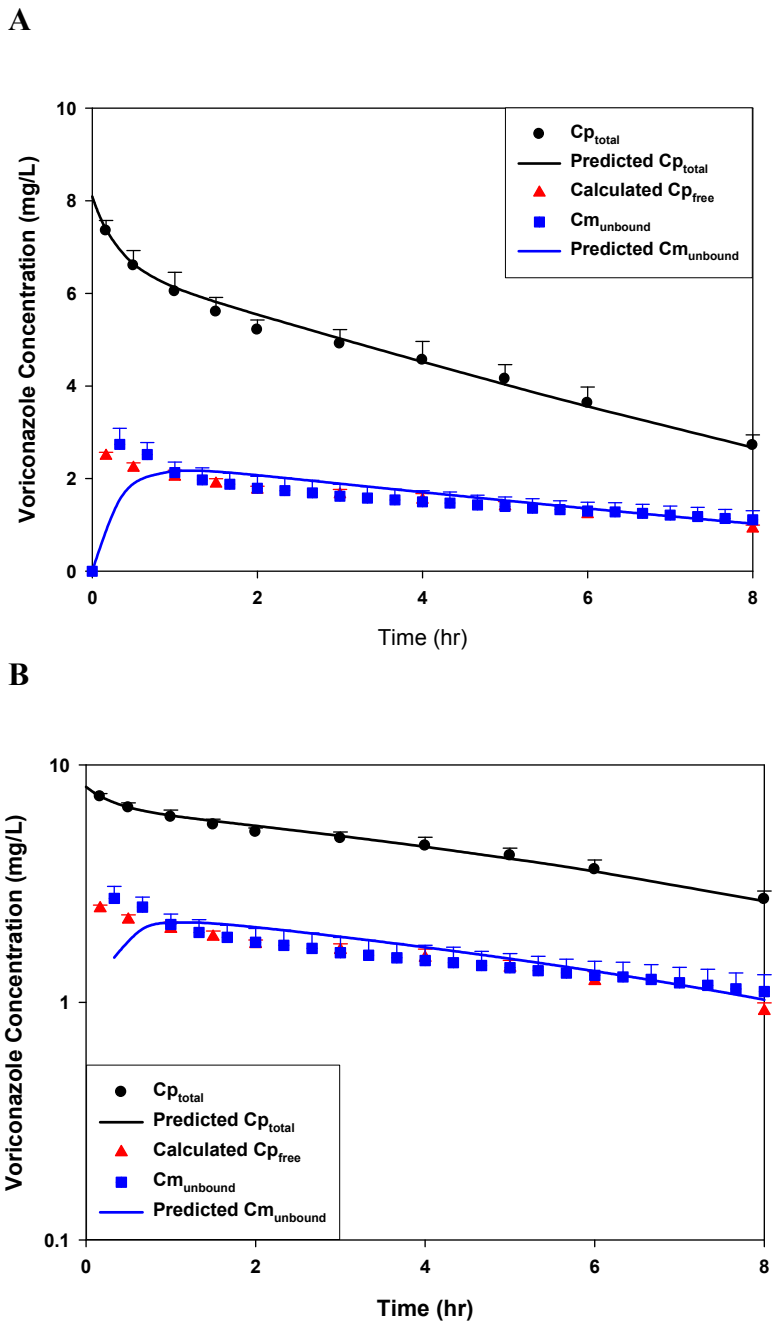

Figure 6-23. Dosage of 10 mg/kg *i.v.* bolus in rat: average plasma and muscle PK data analysis using two-compartment with non-linear elimination model. A) Linear scale. B) Log scale.

CHAPTER 7
CONCLUSIONS

The pharmacokinetic and pharmacodynamic characteristics of voriconazole have been reported in many publications. However, the correlation between *in vitro* activity and pharmacokinetic/pharmacodynamic parameters of voriconazole with its clinical outcome in fungal infections need to be further studied. There is need for mathematical models of this drug to guide its optimal use.

We did the time-kill and postantifungal- effect (PAFE) experiments for voriconazole against *Candida albicans*, *Candida glabrata*, and *Candida parapsilosis* isolates. Moreover, a high-performance liquid chromatography (HPLC) assay was developed to validate these experiments. Our findings demonstrated that voriconazole exerts prolonged fungistatic activity against *C. albicans*, *C. glabrata*, and *C. parapsilosis* but no PAFE at concentrations achievable in human sera with routine dosing. These findings are potentially relevant clinically with other antifungal agents, to which certain *Candida* isolates exhibit diminished susceptibility or develop resistance. HPLC confirmed that experiments were conducted at the desired steady-state voriconazole concentrations. To our knowledge, this is the first study to verify standard time-kill and PAFE methodologies by directly measuring drug concentrations. These HPLC methods were essential to the design of dynamic *in vitro* models to assess the pharmacodynamics of voriconazole and other agents prior to the achievement of steady-state conditions.

We developed a pharmacokinetic/pharmacodynamic (PK/PD) mathematical model that fits voriconazole time–kill data against *Candida* isolates *in vitro* and used the model to simulate the expected kill curves for typical intravenous and oral dosing regimens. A series of E_{max} mathematical models were used to fit time–kill data for two isolates each of *Candida albicans*, *Candida glabrata* and *Candida parapsilosis*. PK parameters extracted from human data sets

were used in the model to simulate kill curves for each isolate. Time–kill data were best fit by using an adapted sigmoidal E_{max} model that corrected for delays in candidal growth and the onset of voriconazole activity, saturation of the number of *Candida* and the steepness of the concentration–response curve. The rates of maximal killing by voriconazole (k_{max}) were highly correlated with the growth rates (k_s) of the isolates (Pearson's correlation coefficient = 0.9861). Simulations using PK parameters derived from the human data sets showed fungistatic effects against each of the isolates. The developed mathematical PK/PD model linked pharmacokinetic and pharmacodynamic of voriconazole to provide the basic understanding for defining optimal antifungal dosing regimens and predict antifungal treatment efficacy.

We established a dynamic system to mimic the *in vivo* conditions and the PK/PD relationship of voriconazole against Candida was accurately modeled. Modeling approaches that utilized human PK data were adapted to define the optimal use of voriconazole and other antifungal agents.

Microdialysis provided a simple, clean method for determining the free drug concentration *in vitro* and in *vivo*. In order to confirm that the performance of voriconazole microdialysis was feasible, we conducted the voriconazole protein binding with *in vitro* microdialysis method. The pharmacokinetics of voriconazole *in vivo* and modeling were further investigated. Plasma concentrations as well as unbound tissue concentrations in rat thigh muscle were measured. A two-compartment model with non-linear elimination was used to fit both the individual and the average plasma and muscle voriconazole concentrations and able to produce good curves. The results from animal study indicated that it is possible to use the free muscle concentrations as a surrogate marker for the free concentrations in plasma. The free fraction of voriconazole in tissue (fu) was predicted by PK analysis.

In the past, PK/PD approaches mainly based on the comparisons of pharmacokinetics of total plasma concentrations and *in vitro* MIC. Our PK/PD approach is a big improvement over the previously used. The developed PK/PD modeling approaches enables us to make rational antifungal agent dosing decisions by predicting the effect of various dosing regimens, taking into account the clinically effective free concentrations at the target site against candidiasis.

LIST OF REFERENCES

1. Gerzenshtein L, Patel SM, Scarsi KK, Postelnick MJ, Flaherty JP. Breakthrough Candida infections in patients receiving voriconazole. The Annals of pharmacotherapy. 2005 Jul-Aug;39(7-8):1342-5.

2. Fratti RA, Belanger PH, Sanati H, Ghannoum MA. The effect of the new triazole, voriconazole (UK-109,496), on the interactions of Candida albicans and Candida krusei with endothelial cells. Journal of chemotherapy (Florence, Italy). 1998 Feb;10(1):7-16.

3. Fukuoka T, Johnston DA, Winslow CA, de Groot MJ, Burt C, Hitchcock CA, et al. Genetic basis for differential activities of fluconazole and voriconazole against Candida krusei. Antimicrobial agents and chemotherapy. 2003 Apr;47(4):1213-9.

4. Pfizer Inc. Label: voriconazole for injection, tablets, oral suspension: LAB-0271-12. 2005 Mar.

5. Boucher HW, Groll AH, Chiou CC, Walsh TJ. Newer systemic antifungal agents : pharmacokinetics, safety and efficacy. Drugs. 2004;64(18):1997-2020.

6. Sheehan DJ, Hitchcock CA, Sibley CM. Current and emerging azole antifungal agents. Clin Microbiol Rev. 1999 Jan;12(1):40-79.

7. Craig WA. Pharmacokinetic/pharmacodynamic parameters: rationale for antibacterial dosing of mice and men. Clin Infect Dis. 1998 Jan;26(1):1-10.

8. Theuretzbacher U, Ihle F, Derendorf H. Pharmacokinetic/pharmacodynamic profile of voriconazole. Clin Pharmacokinet. 2006;45(7):649-63.

9. Pfizer Inc. Label: voriconazole for injection, tablets, oral suspension: LAB-0271-12. 2005 Mar.

10. Patterson TF. New agents for treatment of invasive aspergillosis. Clin Infect Dis. 2002 Aug 15;35(4):367-9.

11. Sambatakou H, Dupont B, Lode H, Denning DW. Voriconazole treatment for subacute invasive and chronic pulmonary aspergillosis. The American journal of medicine. 2006 Jun;119(6):527 e17-24.

12. Camuset J, Nunes H, Dombret MC, Bergeron A, Henno P, Philippe B, et al. Treatment of chronic pulmonary aspergillosis by voriconazole in nonimmunocompromised patients. Chest. 2007 May;131(5):1435-41.

13. Scott LJ, Simpson D. Voriconazole : a review of its use in the management of invasive fungal infections. Drugs. 2007;67(2):269-98.

14. Pearson MM, Rogers PD, Cleary JD, Chapman SW. Voriconazole: a new triazole antifungal agent. The Annals of pharmacotherapy. 2003 Mar;37(3):420-32.

15. Espinel-Ingroff A, Boyle K, Sheehan DJ. In vitro antifungal activities of voriconazole and reference agents as determined by NCCLS methods: review of the literature. Mycopathologia. 2001;150(3):101-15.

16. Manavathu EK, Ramesh MS, Baskaran I, Ganesan LT, Chandrasekar PH. A comparative study of the post-antifungal effect (PAFE) of amphotericin B, triazoles and echinocandins on Aspergillus fumigatus and Candida albicans. The Journal of antimicrobial chemotherapy. 2004 Feb;53(2):386-9.

17. Lyman CA, Walsh TJ. Systemically administered antifungal agents. A review of their clinical pharmacology and therapeutic applications. Drugs. 1992 Jul;44(1):9-35.

18. Odds FC, Cheesman SL, Abbott AB. Antifungal effects of fluconazole (UK 49858), a new triazole antifungal, in vitro. J Antimicrob Chemother. 1986 Oct;18(4):473-8.

19. Como JA, Dismukes WE. Oral azole drugs as systemic antifungal therapy. N Engl J Med. 1994 Jan 27;330(4):263-72.

20. Sanati H, Belanger P, Fratti R, Ghannoum M. A new triazole, voriconazole (UK-109,496), blocks sterol biosynthesis in Candida albicans and Candida krusei. Antimicrobial agents and chemotherapy. 1997 Nov;41(11):2492-6.

21. Belanger P, Nast CC, Fratti R, Sanati H, Ghannoum M. Voriconazole (UK-109,496) inhibits the growth and alters the morphology of fluconazole-susceptible and -resistant Candida species. Antimicrobial agents and chemotherapy. 1997 Aug;41(8):1840-2.

22. Li Y, Nguyen MH, Derendorf H, Cheng S, Clancy CJ. Measurement of voriconazole activity against Candida albicans, C. glabrata, and C. parapsilosis isolates using time-kill methods validated by high-performance liquid chromatography. Antimicrobial agents and chemotherapy. 2007 Aug;51(8):2985-7.

23. Espinel-Ingroff A. Mechanisms of resistance to antifungal agents: Yeasts and filamentous fungi. Rev Iberoam Micol. 2008 Jun;25(2):101-6.

24. Peman J, Salavert M, Canton E, Jarque I, Roma E, Zaragoza R, et al. Voriconazole in the management of nosocomial invasive fungal infections. Therapeutics and clinical risk management. 2006 Jun;2(2):129-58.

25. Quindos G, Carrillo-Munoz AJ, Eraso E, Canton E, Peman J. In vitro antifungal activity of voriconazole: New data after the first years of clinical experience. Rev Iberoam Micol. 2007 Sep 30;24(3):198-208.

26. Espinel-Ingroff A, Arthington-Skaggs B, Iqbal N, Ellis D, Pfaller MA, Messer S, et al. Multicenter evaluation of a new disk agar diffusion method for susceptibility testing of filamentous fungi with voriconazole, posaconazole, itraconazole, amphotericin B, and caspofungin. Journal of clinical microbiology. 2007 Jun;45(6):1811-20.

27. Borgers M. Mechanism of action of antifungal drugs, with special reference to the imidazole derivatives. Rev Infect Dis. 1980 Jul-Aug;2(4):520-34.

28. Muller FM, Weig M, Peter J, Walsh TJ. Azole cross-resistance to ketoconazole, fluconazole, itraconazole and voriconazole in clinical Candida albicans isolates from HIV-infected children with oropharyngeal candidosis. J Antimicrob Chemother. 2000 Aug;46(2):338-40.

29. Cadrobbi J, Hecq J, Lebrun C, Vanbeckbergen D, Jamart J, Galanti L. Long-term stability of voriconazole 4 mg/mL in dextrose 5% polyvinyl chloride bags at 4°C. The European Journal of Hospital Pharmacy Science. 2006;12 (3):57 - 9.

30. Langman LJ, Boakye-Agyeman F. Measurement of voriconazole in serum and plasma. Clin Biochem. 2007 Dec;40(18):1378-85.

31. Roffey SJ, Cole S, Comby P, Gibson D, Jezequel SG, Nedderman AN, et al. The disposition of voriconazole in mouse, rat, rabbit, guinea pig, dog, and human. Drug Metab Dispos. 2003 Jun;31(6):731-41.

32. Andes D, Marchillo K, Stamstad T, Conklin R. In vivo pharmacokinetics and pharmacodynamics of a new triazole, voriconazole, in a murine candidiasis model. Antimicrobial agents and chemotherapy. 2003 Oct;47(10):3165-9.

33. Sugar AM, Liu XP. Effect of grapefruit juice on serum voriconazole concentrations in the mouse. Med Mycol. 2000 Jun;38(3):209-12.

34. Saunte DM, Simmel F, Frimodt-Moller N, Stolle LB, Svejgaard EL, Haedersdal M, et al. In vivo efficacy and pharmacokinetics of voriconazole in an animal model of dermatophytosis. Antimicrobial agents and chemotherapy. 2007 Sep;51(9):3317-21.

35. Damle B, LaBadie R, Crownover P, Glue P. Pharmacokinetic interactions of efavirenz and voriconazole in healthy volunteers. British journal of clinical pharmacology. 2008 Apr;65(4):523-30.

36. Quintard H, Papy E, Massias L, Lasocki S, Arnaud P, Desmonts JM, et al. The pharmacokinetic profile of voriconazole during continuous high-volume venovenous hemofiltration in a critically ill patient. Therapeutic drug monitoring. 2008 Feb;30(1):117-9.

37. Jeu L, Piacenti FJ, Lyakhovetskiy AG, Fung HB. Voriconazole. Clin Ther. 2003 May;25(5):1321-81.

38. Sabo JA, Abdel-Rahman SM. Voriconazole: a new triazole antifungal. Ann Pharmacother. 2000 Sep;34(9):1032-43.

39. Purkins L, Wood N, Ghahramani P, Greenhalgh K, Allen MJ, Kleinermans D. Pharmacokinetics and safety of voriconazole following intravenous- to oral-dose escalation regimens. Antimicrobial agents and chemotherapy. 2002 Aug;46(8):2546-53.

40. Lazarus HM, Blumer JL, Yanovich S, Schlamm H, Romero A. Safety and pharmacokinetics of oral voriconazole in patients at risk of fungal infection: a dose escalation study. Journal of clinical pharmacology. 2002 Apr;42(4):395-402.

41. Arikan S, Lozano-Chiu M, Paetznick V, Nangia S, Rex JH. Microdilution susceptibility testing of amphotericin B, itraconazole, and voriconazole against clinical isolates of Aspergillus and Fusarium species. J Clin Microbiol. 1999 Dec;37(12):3946-51.

42. Espinel-Ingroff A. In vitro activity of the new triazole voriconazole (UK-109,496) against opportunistic filamentous and dimorphic fungi and common and emerging yeast pathogens. J Clin Microbiol. 1998 Jan;36(1):198-202.

43. McGinnis MR, Pasarell L, Sutton DA, Fothergill AW, Cooper CR, Jr., Rinaldi MG. In vitro activity of voriconazole against selected fungi. Med Mycol. 1998 Aug;36(4):239-42.

44. Clancy CJ, Nguyen MH. In vitro efficacy and fungicidal activity of voriconazole against Aspergillus and Fusarium species. Eur J Clin Microbiol Infect Dis. 1998 Aug;17(8):573-5.

45. Cordeiro RA, Brilhante RS, Rocha MF, Fechine MA, Costa AK, Camargo ZP, et al. In vitro activities of caspofungin, amphotericin B and azoles against Coccidioides posadasii strains from Northeast, Brazil. Mycopathologia. 2006 Jan;161(1):21-6.

46. Klepser ME, Malone D, Lewis RE, Ernst EJ, Pfaller MA. Evaluation of voriconazole pharmacodynamics using time-kill methodology. Antimicrobial agents and chemotherapy. 2000 Jul;44(7):1917-20.

47. Lignell A, Lowdin E, Cars O, Sjolin J. Characterization of the inhibitory effect of voriconazole on the fungicidal activity of amphotericin B against Candida albicans in an in vitro kinetic model. The Journal of antimicrobial chemotherapy. 2008 Apr 12.

48. Lozano-Chiu M, Arikan S, Paetznick VL, Anaissie EJ, Rex JH. Optimizing voriconazole susceptibility testing of Candida: effects of incubation time, endpoint rule, species of Candida, and level of fluconazole susceptibility. J Clin Microbiol. 1999 Sep;37(9):2755-9.

49. Nguyen MH, Yu CY. Voriconazole against fluconazole-susceptible and resistant candida isolates: in-vitro efficacy compared with that of itraconazole and ketoconazole. J Antimicrob Chemother. 1998 Aug;42(2):253-6.

50. Johnson EM, Szekely A, Warnock DW. In-vitro activity of voriconazole, itraconazole and amphotericin B against filamentous fungi. J Antimicrob Chemother. 1998 Dec;42(6):741-5.

51. Dannaoui E, Meletiadis J, Mouton JW, Meis JF, Verweij PE. In vitro susceptibilities of zygomycetes to conventional and new antifungals. J Antimicrob Chemother. 2003 Jan;51(1):45-52.

52. Varkey JB, Perfect JR. Rare and emerging fungal pulmonary infections. Seminars in respiratory and critical care medicine. 2008 Apr;29(2):121-31.

53. Alanio A, Brethon B, Feuilhade de Chauvin M, de Kerviler E, Leblanc T, Lacroix C, et al. Invasive pulmonary infection due to Trichoderma longibrachiatum mimicking invasive Aspergillosis in a neutropenic patient successfully treated with voriconazole combined with caspofungin. Clin Infect Dis. 2008 May 15;46(10):e116-8.

54. Martin MV, Yates J, Hitchcock CA. Comparison of voriconazole (UK-109,496) and itraconazole in prevention and treatment of Aspergillus fumigatus endocarditis in guinea pigs. Antimicrobial agents and chemotherapy. 1997 Jan;41(1):13-6.

55. Kirkpatrick WR, McAtee RK, Fothergill AW, Rinaldi MG, Patterson TF. Efficacy of voriconazole in a guinea pig model of disseminated invasive aspergillosis. Antimicrobial agents and chemotherapy. 2000 Oct;44(10):2865-8.

56. Capilla J, Guarro J. Correlation between in vitro susceptibility of Scedosporium apiospermum to voriconazole and in vivo outcome of scedosporiosis in guinea pigs. Antimicrobial agents and chemotherapy. 2004 Oct;48(10):4009-11.

57. Lionakis MS, Lewis RE, May GS, Wiederhold NP, Albert ND, Halder G, et al. Toll-deficient Drosophila flies as a fast, high-throughput model for the study of antifungal drug efficacy against invasive aspergillosis and Aspergillus virulence. J Infect Dis. 2005 Apr 1;191(7):1188-95.

58. Weerasuriya N, Snape J. Oesophageal candidiasis in elderly patients: risk factors, prevention and management. Drugs & aging. 2008;25(2):119-30.

59. Heinz WJ, Einsele H. Caspofungin for treatment of invasive aspergillus infections. Mycoses. 2008;51 Suppl 1:47-57.

60. Proia LA, Tenorio AR. Successful use of voriconazole for treatment of Coccidioides meningitis. Antimicrobial agents and chemotherapy. 2004 Jun;48(6):2341.

61. Stanzani M, Vianelli N, Bandini G, Paolini S, Arpinati M, Bonifazi F, et al. Successful treatment of disseminated Fusariosis after allogeneic hematopoietic stem cell transplantation with the combination of voriconazole and liposomal amphotericin B. The Journal of infection. 2006 Dec;53(6):e243-6.

62. Nesky MA, McDougal EC, Peacock Jr JE. Pseudallescheria boydii brain abscess successfully treated with voriconazole and surgical drainage: case report and literature review of central nervous system pseudallescheriasis. Clin Infect Dis. 2000 Sep;31(3):673-7.

63. Kappe R. Antifungal activity of the new azole UK-109, 496 (voriconazole). Mycoses. 1999;42 Suppl 2:83-6.

64. Ally R, Schurmann D, Kreisel W, Carosi G, Aguirrebengoa K, Dupont B, et al. A randomized, double-blind, double-dummy, multicenter trial of voriconazole and fluconazole in the treatment of esophageal candidiasis in immunocompromised patients. Clin Infect Dis. 2001 Nov 1;33(9):1447-54.

65. Kullberg BJ, Sobel JD, Ruhnke M, Pappas PG, Viscoli C, Rex JH, et al. Voriconazole versus a regimen of amphotericin B followed by fluconazole for candidaemia in non-neutropenic patients: a randomised non-inferiority trial. Lancet. 2005 Oct 22-28;366(9495):1435-42.

66. Hwang YK, Joo NH, Tee GY, Tan P, Tan L, Girija R. Clinical activity of the new triazole drug voriconazole (UK 109, 496) against disseminated hepatosplenic aspergillosis in a patient with relapsed leukemia. Haematologia (Budap). 2001;31(1):73-80.

67. Herbrecht R. Voriconazole: therapeutic review of a new azole antifungal. Expert review of anti-infective therapy. 2004 Aug;2(4):485-97.

68. Singh N, Limaye AP, Forrest G, Safdar N, Munoz P, Pursell K, et al. Combination of voriconazole and caspofungin as primary therapy for invasive aspergillosis in solid organ transplant recipients: a prospective, multicenter, observational study. Transplantation. 2006 Feb 15;81(3):320-6.

69. de la Pena A, Liu P, Derendorf H. Microdialysis in peripheral tissues. Adv Drug Deliv Rev. 2000 Dec 15;45(2-3):189-216.

70. Yokoyama M, Suzuki E, Sato T, Maruta S, Watanabe S, Miyaoka H. Amygdalic levels of dopamine and serotonin rise upon exposure to conditioned fear stress without elevation of glutamate. Neurosci Lett. 2005 Apr 29;379(1):37-41.

71. Humpel C, Ebendal T, Olson L. Microdialysis: a way to study in vivo release of neurotrophic bioactivity: a critical summary. J Mol Med. 1996 Sep;74(9):523-6.

72. Lee SC, Fung CP, Huang JS, Tsai CJ, Chen KS, Chen HY, et al. Clinical correlates of antifungal macrodilution susceptibility test results for non-AIDS patients with severe Candida infections treated with fluconazole. Antimicrobial agents and chemotherapy. 2000 Oct;44(10):2715-8.

73. Liu P, Fuhrherr R, Webb AI, Obermann B, Derendorf H. Tissue penetration of cefpodoxime into the skeletal muscle and lung in rats. Eur J Pharm Sci. 2005 Jul-Aug;25(4-5):439-44.

74. Liu P, Muller M, Grant M, Obermann B, Derendorf H. Tissue penetration of cefpodoxime and cefixime in healthy subjects. Journal of clinical pharmacology. 2005 May;45(5):564-9.

75. Traunmuller F, Zeitlinger M, Zeleny P, Muller M, Joukhadar C. Pharmacokinetics of single- and multiple-dose oral clarithromycin in soft tissues determined by microdialysis. Antimicrobial agents and chemotherapy. 2007 Sep;51(9):3185-9.

76. Hartings JA, Gugliotta M, Gilman C, Strong AJ, Tortella FC, Bullock MR. Repetitive cortical spreading depolarizations in a case of severe brain trauma. Neurological research. 2008 Jun 3.

77. Hutschala D, Skhirtladze K, Kinstner C, Mayer-Helm B, Muller M, Wolner E, et al. In vivo microdialysis to measure antibiotic penetration into soft tissue during cardiac surgery. The Annals of thoracic surgery. 2007 Nov;84(5):1605-10.

78. Tyvold SS, Solligard E, Lyng O, Steinshamn SL, Gunnes S, Aadahl P. Continuous monitoring of the bronchial epithelial lining fluid by microdialysis. Respiratory research. 2007;8:78.

79. Muller M, Brunner M, Schmid R, Mader RM, Bockenheimer J, Steger GG, et al. Interstitial methotrexate kinetics in primary breast cancer lesions. Cancer research. 1998 Jul 15;58(14):2982-5.

80. Hansen DK, Davies MI, Lunte SM, Lunte CE. Pharmacokinetic and metabolism studies using microdialysis sampling. J Pharm Sci. 1999 Jan;88(1):14-27.

81. de Lange, Elizabeth C. M., de Boer, A. G., Breimer DD. Methodological issues in microdialysis sampling for pharmacokinetic studies. Advanced Drug Delivery Reviews. 2000 2000/12/15;45(2-3):125-48.

82. Parent M, Bush D, Rauw G, Master S, Vaccarino F, Baker G. Analysis of Amino Acids and Catecholamines, 5-Hydroxytryptamine and Their Metabolites in Brain Areas in the Rat Using in Vivo Microdialysis. Methods. 2001 2001/1;23(1):11-20.

83. Day JC, Kornecook TJ, Quirion R. Application of in vivo microdialysis to the study of cholinergic systems. Methods. 2001 Jan;23(1):21-39.

84. Hows ME, Lacroix L, Heidbreder C, Organ AJ, Shah AJ. High-performance liquid chromatography/tandem mass spectrometric assay for the simultaneous measurement of dopamine, norepinephrine, 5-hydroxytryptamine and cocaine in biological samples. J Neurosci Methods. 2004 Sep 30;138(1-2):123-32.

85. Baseski HM, Watson CJ, Cellar NA, Shackman JG, Kennedy RT. Capillary liquid chromatography with MS3 for the determination of enkephalins in microdialysis samples from the striatum of anesthetized and freely-moving rats. J Mass Spectrom. 2005 Feb;40(2):146-53.

86. Bowser MT, Kennedy RT. In vivo monitoring of amine neurotransmitters using microdialysis with on-line capillary electrophoresis. Electrophoresis. 2001 Oct;22(17):3668-76.

87. Huynh BH, Fogarty BA, Martin RS, Lunte SM. On-line coupling of microdialysis sampling with microchip-based capillary electrophoresis. Anal Chem. 2004 Nov 1;76(21):6440-7.

88. Kanamori K, Ross BD. Suppression of glial glutamine release to the extracellular fluid studied in vivo by NMR and microdialysis in hyperammonemic rat brain. J Neurochem. 2005 Jul;94(1):74-85.

89. Lucas LH, Wilson SF, Lunte CE, Larive CK. Concentration profiling in rat tissue by high-resolution magic-angle spinning NMR spectroscopy: investigation of a model drug. Anal Chem. 2005 May 1;77(9):2978-84.

90. Mayer BX, Namiranian K, Dehghanyar P, Stroh R, Mascher H, Muller M. Comparison of UV and tandem mass spectrometric detection for the high-performance liquid chromatographic determination of diclofenac in microdialysis samples. J Pharm Biomed Anal. 2003 Nov 24;33(4):745-54.

91. Kanamori K, Kondrat RW, Ross BD. 13C enrichment of extracellular neurotransmitter glutamate in rat brain--combined mass spectrometry and NMR studies of neurotransmitter turnover and uptake into glia in vivo. Cell Mol Biol (Noisy-le-grand). 2003 Jul;49(5):819-36.

92. Lindon JC. HPLC-NMR-MS: past, present and future. Drug Discov Today. 2003 Nov 15;8(22):1021-2.

93. Lindon JC, Nicholson JK, Wilson ID. Directly coupled HPLC-NMR and HPLC-NMR-MS in pharmaceutical research and development. J Chromatogr B Biomed Sci Appl. 2000 Oct 1;748(1):233-58.

94. Lommen A, Godejohann M, Venema DP, Hollman PC, Spraul M. Application of directly coupled HPLC-NMR-MS to the identification and confirmation of quercetin glycosides and phloretin glycosides in apple peel. Anal Chem. 2000 Apr 15;72(8):1793-7.

95. Li Y, Peris J, Zhong L, Derendorf H. Microdialysis as a tool in local pharmacodynamics. The AAPS journal. 2006;8(2):E222-35.

96. Weikop P, Egestad B, Kehr J. Application of triple-probe microdialysis for fast pharmacokinetic/pharmacodynamic evaluation of dopamimetic activity of drug candidates in the rat brain. Journal of neuroscience methods. 2004 Dec 30;140(1-2):59-65.

97. Feng MR, Turluck D, Burleigh J, Lister R, Fan C, Middlebrook A, et al. Brain microdialysis and PK/PD correlation of pregabalin in rats. European journal of drug metabolism and pharmacokinetics. 2001 Jan-Jun;26(1-2):123-8.

98. Au-Yeung SC, Riggs KW, Gruber N, Rurak DW. The use of microdialysis for the study of drug kinetics: central nervous system pharmacokinetics of diphenhydramine in fetal,

newborn, and adult sheep. Drug metabolism and disposition: the biological fate of chemicals. 2007 Aug;35(8):1285-91.

99. Schuck VJ, Rinas I, Derendorf H. In vitro microdialysis sampling of docetaxel. Journal of pharmaceutical and biomedical analysis. 2004 Nov 19;36(4):807-13.

100. Derendorf H, Lesko LJ, Chaikin P, Colburn WA, Lee P, Miller R, et al. Pharmacokinetic/pharmacodynamic modeling in drug research and development. Journal of clinical pharmacology. 2000 Dec;40(12 Pt 2):1399-418.

101. Meibohm B, Derendorf H. Basic concepts of pharmacokinetic/pharmacodynamic (PK/PD) modelling. International journal of clinical pharmacology and therapeutics. 1997 Oct;35(10):401-13.

102. Li Y, Nguyen MH, Cheng S, Schmidt S, Zhong L, Derendorf H, et al. A pharmacokinetic/pharmacodynamic mathematical model accurately describes the activity of voriconazole against Candida spp. in vitro. International journal of antimicrobial agents. 2008 Apr;31(4):369-74.

103. Xu J, Winkler J, Derendorf H. A pharmacokinetic/pharmacodynamic approach to predict total prednisolone concentrations in human plasma. Journal of pharmacokinetics and pharmacodynamics. 2007 Jun;34(3):355-72.

104. Derendorf H, Hochhaus G, Krishnaswami S, Meibohm B, Mollmann H. Optimized therapeutic ratio of inhaled corticosteroids using retrometabolism. Die Pharmazie. 2000 Mar;55(3):223-7.

105. Derendorf H, Meibohm B. Modeling of pharmacokinetic/pharmacodynamic (PK/PD) relationships: concepts and perspectives. Pharmaceutical research. 1999 Feb;16(2):176-85.

106. Walsh TJ, Karlsson MO, Driscoll T, Arguedas AG, Adamson P, Saez-Llorens X, et al. Pharmacokinetics and safety of intravenous voriconazole in children after single- or multiple-dose administration. Antimicrobial agents and chemotherapy. 2004 Jun;48(6):2166-72.

107. Louie A, Liu QF, Drusano GL, Liu W, Mayers M, Anaissie E, et al. Pharmacokinetic studies of fluconazole in rabbits characterizing doses which achieve peak levels in serum and area under the concentration-time curve values which mimic those of high-dose fluconazole in humans. Antimicrobial agents and chemotherapy. 1998 Jun;42(6):1512-4.

108. Ohtani Y, Kotegawa T, Tsutsumi K, Morimoto T, Hirose Y, Nakano S. Effect of fluconazole on the pharmacokinetics and pharmacodynamics of oral and rectal bromazepam: an application of electroencephalography as the pharmacodynamic method. Journal of clinical pharmacology. 2002 Feb;42(2):183-91.

109. Louie A, Drusano GL, Banerjee P, Liu QF, Liu W, Kaw P, et al. Pharmacodynamics of fluconazole in a murine model of systemic candidiasis. Antimicrobial agents and chemotherapy. 1998 May;42(5):1105-9.

110. Katayama M, Igarashi H, Tani K, Nezu Y, Harada Y, Yogo T, et al. Effect of multiple oral dosing of fluconazole on the pharmacokinetics of cyclosporine in healthy beagles. The Journal of veterinary medical science / the Japanese Society of Veterinary Science. 2008 Jan;70(1):85-8.

111. Carrasco-Portugal Mdel C, Flores-Murrieta FJ. Gender differences in the oral pharmacokinetics of fluconazole. Clinical drug investigation. 2007;27(12):851-5.

112. Saari TI, Laine K, Neuvonen M, Neuvonen PJ, Olkkola KT. Effect of voriconazole and fluconazole on the pharmacokinetics of intravenous fentanyl. European journal of clinical pharmacology. 2008 Jan;64(1):25-30.

113. Andes D, Marchillo K, Stamstad T, Conklin R. In vivo pharmacodynamics of a new triazole, ravuconazole, in a murine candidiasis model. Antimicrobial agents and chemotherapy. 2003 Apr;47(4):1193-9.

114. Andes D, Marchillo K, Conklin R, Krishna G, Ezzet F, Cacciapuoti A, et al. Pharmacodynamics of a new triazole, posaconazole, in a murine model of disseminated candidiasis. Antimicrobial agents and chemotherapy. 2004 Jan;48(1):137-42.

115. Greer ND. Posaconazole (Noxafil): a new triazole antifungal agent. Proc (Bayl Univ Med Cent). 2007 Apr;20(2):188-96.

116. Courtney R, Pai S, Laughlin M, Lim J, Batra V. Pharmacokinetics, safety, and tolerability of oral posaconazole administered in single and multiple doses in healthy adults. Antimicrob Agents Chemother. 2003 Sep;47(9):2788-95.

117. Janssen-Pharmaceutica. Product information: SPORANOX® (ITRACONAZOLE) ORAL SUSPENSION: Hepatotoxicity Labeling –062602. 2002 June.

118. Pfizer. Product information: DIFLUCAN® (Fluconazole): LAB-0099 –6.1. 2004 August.

119. Clancy CJ, Huang H, Cheng S, Derendorf H, Nguyen MH. Characterizing the effects of caspofungin on Candida albicans, Candida parapsilosis, and Candida glabrata isolates by simultaneous time-kill and postantifungal-effect experiments. Antimicrobial agents and chemotherapy. 2006 Jul;50(7):2569-72.

120. Gage R, Stopher DA. A rapid HPLC assay for voriconazole in human plasma. J Pharm Biomed Anal. 1998 Sep;17(8):1449-53.

121. MacCallum DM, Whyte JA, Odds FC. Efficacy of caspofungin and voriconazole combinations in experimental aspergillosis. Antimicrob Agents Chemother. 2005 Sep;49(9):3697-701.

122. Pfaller MA, Diekema DJ, Rex JH, Espinel-Ingroff A, Johnson EM, Andes D, et al. Correlation of MIC with outcome for Candida species tested against voriconazole: analysis and proposal for interpretive breakpoints. Journal of clinical microbiology. 2006 Mar;44(3):819-26.

123. NCCLS. Reference method for broth dilution antifungal susceptibility testing of yeasts. Approved standard, 2nd ed. NCCLS document M27-A2. National Committee for Clinical Laboratory Standards, Wayne, PA.; 2002.

124. Smith J, Safdar N, Knasinski V, Simmons W, Bhavnani SM, Ambrose PG, et al. Voriconazole therapeutic drug monitoring. Antimicrobial agents and chemotherapy. 2006 Apr;50(4):1570-2.

125. Liu P, Rand KH, Obermann B, Derendorf H. Pharmacokinetic-pharmacodynamic modelling of antibacterial activity of cefpodoxime and cefixime in in vitro kinetic models. International journal of antimicrobial agents. 2005 Feb;25(2):120-9.

126. Schuck EL, Derendorf H. Pharmacokinetic/pharmacodynamic evaluation of anti-infective agents. Expert review of anti-infective therapy. 2005 Jun;3(3):361-73.

127. Treyaprasert W, Schmidt S, Rand KH, Suvanakoot U, Derendorf H. Pharmacokinetic/pharmacodynamic modeling of in vitro activity of azithromycin against four different bacterial strains. International journal of antimicrobial agents. 2007 Mar;29(3):263-70.

128. Canton E, Peman J, Gobernado M, Viudes A, Espinel-Ingroff A. Synergistic activities of fluconazole and voriconazole with terbinafine against four Candida species determined by checkerboard, time-kill, and Etest methods. Antimicrobial agents and chemotherapy. 2005 Apr;49(4):1593-6.

129. Manavathu EK, Cutright JL, Chandrasekar PH. Organism-dependent fungicidal activities of azoles. Antimicrobial agents and chemotherapy. 1998 Nov;42(11):3018-21.

130. Simonsen L, Jorgensen A, Benfeldt E, Groth L. Differentiated in vivo skin penetration of salicylic compounds in hairless rats measured by cutaneous microdialysis. Eur J Pharm Sci. 2004 Feb;21(2-3):379-88.

131. Sasongko L, Williams KM, Day RO, McLachlan AJ. Human subcutaneous tissue distribution of fluconazole: comparison of microdialysis and suction blister techniques. British journal of clinical pharmacology. 2003 Nov;56(5):551-61.

132. Fair W, Jr. An Algorithm for Weighted Linear Regression. Available from: http://www.codeproject.com/KB/recipes/LinReg.aspx

133. Araujo BV, Silva CF, Haas SE, Dalla Costa T. Microdialysis as a tool to determine free kidney levels of voriconazole in rodents: A model to study the technique feasibility for a moderately lipophilic drug. Journal of pharmaceutical and biomedical analysis. 2008 Feb 29.

134. Kusbeci T, Avci B, Cetinkaya Z, Ozturk F, Yavas G, Ermis SS, et al. The effects of caspofungin and voriconazole in experimental Candida endophthalmitis. Current eye research. 2007 Jan;32(1):57-64.

135. Breit SM, Hariprasad SM, Mieler WF, Shah GK, Mills MD, Grand MG. Management of endogenous fungal endophthalmitis with voriconazole and caspofungin. American journal of ophthalmology. 2005 Jan;139(1):135-40.

136. Verweij PE, de Pauw BE, Meis JF. Voriconazole (Pfizer ltd). IDrugs. 1999 Sep;2(9):925-37.

137. Yang H, Wang Q, Elmquist WF. The design and validation of a novel intravenous microdialysis probe: application to fluconazole pharmacokinetics in the freely-moving rat model. Pharmaceutical research. 1997 Oct;14(10):1455-60.

138. Tsai TH. Assaying protein unbound drugs using microdialysis techniques. Journal of chromatography. 2003 Nov 25;797(1-2):161-73.

139. Liu Z, Yang XG, Li X, Pan W, Li J. Study on the ocular pharmacokinetics of ion-activated in situ gelling ophthalmic delivery system for gatifloxacin by microdialysis. Drug development and industrial pharmacy. 2007 Dec;33(12):1327-31.

140. Uehara T, Sumiyoshi T, Itoh H, Kurata K. Lactate production and neurotransmitters; evidence from microdialysis studies. Pharmacology, biochemistry, and behavior. 2008 Aug;90(2):273-81.

141. Sumiyoshi T, Tsunoda M, Uehara T, Tanaka K, Itoh H, Sumiyoshi C, et al. Enhanced locomotor activity in rats with excitotoxic lesions of the entorhinal cortex, a neurodevelopmental animal model of schizophrenia: behavioral and in vivo microdialysis studies. Neuroscience letters. 2004 Jul 1;364(2):124-9.

142. Apparaju SK, Gudelsky GA, Desai PB. Pharmacokinetics of gemcitabine in tumor and non-tumor extracellular fluid of brain: an in vivo assessment in rats employing intracerebral microdialysis. Cancer chemotherapy and pharmacology. 2008 Feb;61(2):223-9.

143. Zhou Q, Gallo JM. In vivo microdialysis for PK and PD studies of anticancer drugs. The AAPS journal. 2005;7(3):E659-67.

144. Schwarz AJ, Zocchi A, Reese T, Gozzi A, Garzotti M, Varnier G, et al. Concurrent pharmacological MRI and in situ microdialysis of cocaine reveal a complex relationship between the central hemodynamic response and local dopamine concentration. NeuroImage. 2004 Sep;23(1):296-304.

145. Egashira N, Ishigami N, Mishima K, Iwasaki K, Oishi R, Fujiwara M. Delta9-Tetrahydrocannabinol-induced cognitive deficits are reversed by olanzapine but not haloperidol in rats. Progress in neuro-psychopharmacology & biological psychiatry. 2008 Feb 15;32(2):499-506.

146. van Duuren E, van der Plasse G, van der Blom R, Joosten RN, Mulder AB, Pennartz CM, et al. Pharmacological manipulation of neuronal ensemble activity by reverse microdialysis in freely moving rats: a comparative study of the effects of tetrodotoxin, lidocaine, and muscimol. The Journal of pharmacology and experimental therapeutics. 2007 Oct;323(1):61-9.

147. Nakashima K, Yamamoto K, Al-Dirbashi OY, Kaddoumi A, Nakashima MN. Semi-micro column HPLC of triazolam in rat plasma and brain microdialysate and its application to drug interaction study with itraconazole. Journal of pharmaceutical and biomedical analysis. 2003 Jan 15;30(6):1809-16.

148. Mathy FX, Ntivunwa D, Verbeeck RK, Preat V. Fluconazole distribution in rat dermis following intravenous and topical application: a microdialysis study. Journal of pharmaceutical sciences. 2005 Apr;94(4):770-80.

149. Kondoh S, Nagasawa S, Kawanishi M, Yamaguchi K, Kajimoto S, Ohta T. Effects of ebselen on cerebral ischemia and reperfusion evaluated by microdialysis. Neurological research. 1999 Oct;21(7):682-6.

150. Stimpfel TM, Gershey EL. Selecting anesthetic agents for human safety and animal recovery surgery. Faseb J. 1991 Apr;5(7):2099-104.

151. Martenson M, Houts J, Heinricher M, Ogden B. A simple device for humidification of inspired gases during volatile anesthesia in rats. Contemporary topics in laboratory animal science / American Association for Laboratory Animal Science. 2005 Mar;44(2):46-8.

152. Yang R, Tan X, Kenney RJ, Jr., Thomas A, Landis M, Qureshi N, et al. Hemorrhagic shock in the rat: comparison of carotid and femoral cannulation. The Journal of surgical research. 2008 Jan;144(1):124-6.

153. Beaumont DM, Mark TM, Jr., Hills R, Dixon P, Veit B, Garrett N. The effects of chrysin, a Passiflora incarnata extract, on natural killer cell activity in male Sprague-Dawley rats undergoing abdominal surgery. AANA journal. 2008 Apr;76(2):113-7.

154. Araujo BV, Conrado DJ, Palma EC, Dalla Costa T. Validation of rapid and simple LC-MS/MS method for determination of voriconazole in rat plasma. Journal of pharmaceutical and biomedical analysis. 2007 Aug 15;44(4):985-90.

155. Muller M, dela Pena A, Derendorf H. Issues in pharmacokinetics and pharmacodynamics of anti-infective agents: distribution in tissue. Antimicrobial agents and chemotherapy. 2004 May;48(5):1441-53.

156. Tegeder I, Lotsch J, Kinzig-Schippers M, Sorgel F, Kelm GR, Meller ST, et al. Comparison of tissue concentrations after intramuscular and topical administration of ketoprofen. Pharmaceutical research. 2001 Jul;18(7):980-6.

157. Muller M, Rohde B, Kovar A, Georgopoulos A, Eichler HG, Derendorf H. Relationship between serum and free interstitial concentrations of cefodizime and cefpirome in muscle and subcutaneous adipose tissue of healthy volunteers measured by microdialysis. Journal of clinical pharmacology. 1997 Dec;37(12):1108-13.

BIOGRAPHICAL SKETCH

Yanjun Li was born in 1974, in Hunan, China. She got her M.D. in Hunan Medical University (current name: Central South University Xiangya School of Medicine). She started her Ph.D. program in August 2004 in the Department of Pharmaceutics, College of Pharmacy, University of Florida, under the supervision of Dr. Hartmut Derendorf. Yanjun received her Ph.D. in pharmaceutics in August 2008.